STUDY OF DECOMPOSED METHANOL AS A LOW EMISSION FUEL

FINAL REPORT

Prepared For

OFFICE OF AIR PROGRAMS
ENVIRONMENTAL PROTECTION AGENCY

CONTRACT NO. EHS 70-118

APRIL 30, 1971

By

R. K. PEFLEY
M. A. SAAD
M. A. SWEENEY
J. D. KILGROE
R. E. FITCH

The University of Santa Clara • California

STUDY OF DECOMPOSED METHANOL AS A LOW EMISSION FUEL

FINAL REPORT

CONTRACT NO. EHS 70-118

APRIL 30, 1971

By

R. K. Pefley
M. A. Saad
M. A. Sweeney
J. D. Kilgroe
R. E. Fitch

Prepared For

Environmental Protection Agency
Office of Air Programs
Division of Emission Control Technology
Ann Arbor, Michigan 48103

Attention: Mr. Stephen Quick
Project Officer

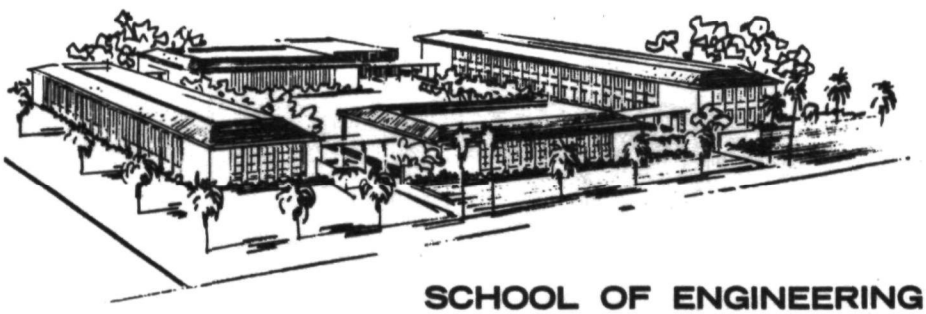

SCHOOL OF ENGINEERING

ENGINEERING AND APPLIED SCIENCE RESEARCH

UNIVERSITY OF SANTA CLARA

SANTA CLARA, CALIFORNIA AREA CODE 408-246-3200

CONTENTS

I. SUMMARY

Studies were conducted to evaluate blends of pure and decomposed methanol ($2H_2$ + CO) as fuels for reducing automotive IC engine air pollution. These investigations included laboratory IC engine tests and analysis, and a preliminary design study of possible methanol decomposition chambers with associated engine air-fuel (A/F) ratio controls.

Steady-state performance and emission tests were made on a variable compression ratio CFR engine operating at 900 RPM. A total of 191 tests were conducted. They included 184 tests with methanol blends and seven comparative gasoline fueled tests. Engine test variables were A/F ratio, per cent methanol dissociation*, compression ratio (CR), spark advance, and intake manifold temperature. Instrumentation consisted of apparatus for measuring air and fuel flow rates, engine load, engine emissions and various engine temperatures. Emissions instrumentation included CO, CO_2, O_2, and NO_X gas analyzers and a gas chromatograph (GC) using a flame ionization detector.

The engine operated easily on fuel blends from pure methanol to completely dissociated methanol on tests conducted over an A/F range of 5:1 to 9:1 and a CR range from 8.5:1 to 10.9:1. Little power difference was noted between the gasoline and pure methanol. Methanol blends of high dissociation percentage (70 and 100) indicated a slight to moderate reduction in power from the decrease in intake charge density. This power loss was partially offset by increases in the combustion efficiency and some recovery of fuel decomposition energy. The indicated thermal efficiency using pure methanol was essentially the same as that for gasoline.

For engine operation on methanol the number of different exhaust species were significantly fewer than for gasoline. Major unreacted emissions for the methanol fueled tests were carbon monoxide (CO), oxides of nitrogen (NO_X), methanol (CH_3OH),

*Dissociation and decomposition of methanol are used synonymously in this report.

methane (CH_4), formaldehyde (HCHO), and acetaldehyde (CH_3CHO). Low concentrations of ethane (C_2H_6), propane (C_3H_8), and an unknown hydrocarbon were also recorded.

Engine variables, particularly A/F ratio and spark advance, affected exhaust emissions in a manner similar to that noted for gasoline fueled engines. Near stoichiometric conditions (A/F = 6.48) all emission concentrations except for NO_X were low. Emissions for a typical test for 30% dissociated methanol at A/F = 6.5, CR = 8.5 and 10 degrees spark advance were: methanol, 51 ppm; hydrocarbons, 59 ppm; aldehydes, 169 ppm; CO, .08%; and NO_X, .322%. At low A/F ratio test points (5.0 and 5.5) CO, CH_3OH, and hydrocarbon emissions were higher and aldehyde and NO_X emissions were lower. As with gasoline, the NO_X concentrations for pure methanol peaked near the stoichiometric mixture. This peak was shifted to A/F = 7.5 for 100 per cent dissociation. Hydrocarbon and methanol exhaust emissions at A/F = 7.5 were reduced below stoichiometric values but aldehydes were at peak concentrations. At A/F = 9.0, all emissions except methanol were quantitatively low.

The use of dissociated methanol tended to reduce overall emissions (NO_X excepted) and resulted in shifts in the relative concentrations of the major species.

Decreasing the spark advance to between 0 and 10 degrees significantly reduced emissions at stoichiometric and lean A/F ratio without significantly affecting engine power. The effect of changing the spark advance at rich A/F ratios was not appreciable.

The effect of CR and intake manifold temperature on emissions was, except for special conditions, not significant.

Comparison of methanol and gasoline emission data was made for a limited number of tests near stoichiometric conditions. The total grams of carbon and CO per cent in the exhaust were in general an order of magnitude lower for methanol than for gasoline. NO_X emissions were equivalent for both fuels.

The preliminary study of the decomposition chamber and engine control methods defined several design constraints and indicated possible methods of solution. Major design constraints include requirements for methanol or catalyst bed heating to provide the endothermic heat of decomposition and catalyst bed condition-cycling with engine start up and shut-down. A constant decomposition flow rate with methanol augmentation for power demands was indicated as the easiest method of A/F ratio control.

Based upon the above results it is concluded that the use of pure or blended methanol can reduce IC engine hydrocarbon and CO emission levels significantly below that obtainable with gasoline. Nitrogen oxide levels will be similar to gasoline. Aldehyde emissions can be reasonably controlled through A/F and spark advance settings. These improvements are attainable without significant changes in engine power and thermal efficiency.

Use of a decomposition chamber with a methanol fueled engine operating under a steady speed and load condition is feasible. All of the fuel could be dissociated by the engine exhaust waste energy. However, reformer experiments would have to be made to ascertain the quality of the fuel decomposition. Assuming that steady-state experiments produced high quality decomposed products, it would then be possible to consider whether a reformer would be feasible for handling the intermittent performance requirements of an automotive engine.

Based upon these observations, it is recommended:

(1) That an automotive engine with carburetion modified for use of gasoline and methanol be tested on a dynamometer. That tests be conducted at constant speed and at speed-load variations equivalent to those specified in federal exhaust emission determination standards. That exhaust analyses be made using instrumentation equivalent to that used in the current test work.

(2) That a bench model reformer designed for steady flow operation be constructed and that the quality of dissociated products be evaluated.

SUMMARY SUPPLEMENT

A. Emission Evaluation Parameters:

It was found useful to rate the engine exhaust emissions in terms of gm/ihp-hr. This or its comparison-rating, gm/bhp-hr, are meaningful when comparing the pollution effects for different fuels or for different engine speeds and loads under laboratory conditions. With the rating base of ppm of engine exhaust for different speed, load, and/or fuels, it is possible to decrease the value of ppm and yet have an increase in pollution per unit energy delivered to the pistons (ihp-hr) or drive shaft (bhp-hr). This is avoided by using gm/ihp-hr or gm/bhp-hr. An alternative rating method using gm/vehicle-mile is not satisfactory for research comparisons, as an arbitrary conversion from engine power to mileage must be made. It is therefore recommended that the gm/ihp-hr or gm/bhp-hr ratings be standardized for laboratory-engine comparisons. It is noted that the 1973 heavy-duty vehicle standards for California utilize this form of evaluation.

Presuming that the recommended rating indices are attractive, there should be some work done in relating this value to the current standards in terms of gm/vehicle-mile. The work recommended in Section I would provide an opportunity for an equivalency investigation of the two rating parameters. For example, it may be found that gm/ihp-hr may be transposed to gm/vehicle-mile by assuming the vehicle is operating at 50 mph and developing 50 ihp. For such, the numerical value in gm/ihp-hr would be the same in gm/vehicle-mile.

B. GC Emissions Analysis:

Gas chromatographic analysis and sampling techniques for methanol fuel should be improved to minimize errors in data quantification. The possibility of sample degradation in the exhaust line should be tested and, if necessary, eliminated. The identify of the unknown peaks in the exhaust samples should be established--particularly, the peak eluted just before ethane. If it is an unsaturated C_2 hydrocarbon, it would contribute more to air pollution than a saturated hydrocarbon.

The feasibility of using the Porapak column for analysis of gasoline aldehyde emissions should be evaluated. Techniques for the gas chromatographic analysis of gasoline aldehyde exhaust emissions with Porapak columns have been developed.* However, these techniques do not determine formaldehyde, and they involve a complex backflushing procedure. In the program reported herein exploratory analyses of gasoline-fueled engine emissions with Porapak T columns were conducted. These analyses indicated that gasoline engine emissions could be resolved into many separate peaks without backflushing. While the laborious undertaking of identification of these peaks was not made, the columns were found to be capable of resolving formaldehyde. Based upon these results it is believed that a column that would identify individual peaks, including formaldehyde,with a less complex procedure can be developed.

---

*T. A. Bellar and J. E. Sigsby, Jr., Env. Sci. Tech. 4, 150 (1970).

II. INTRODUCTION

Atmospheric air pollution from gasoline powered IC engines poses an environmental crisis in many urban areas. Some net improvement in regional air quality has been experienced as a result of automotive engine design changes and incorporation of emission control devices, but growing car populations threaten to negate these advances unless stricter standards are met [1].* Since further reductions in emission controlled gasoline powered IC engines are difficult, other methods of reducing passenger car exhaust emissions have been sought. These methods have ranged from the use of alternative IC engine fuels to replacement of the IC engine with a different power plant. To date, no completely acceptable power plant replacement has been developed. An alternate fuel which has shown promise of reducing emissions below that obtainable with gasoline is methanol.

In previous work [2] a standard automobile modified to run on methanol fuel gave some evidence of reduced pollution in comparison with gasoline fuel. This evidence was not conclusive because of improper carburetion. Also included in this previous work was an exploratory investigation into the use of fuel blends of liquid methanol and dissociated methanol. A CFR engine was used for this phase of the work. The ultimate goal of this latter effort was to use waste thermal energy in the engine exhaust in conjunction with a catalytic surface to vaporize and dissociate the liquid methanol. The expected results were an improvement in methanol performance from exhaust energy recovery of the heat of decomposition, and a decrease in particulate and exhaust gas pollution resulting from combustion of a chemically simple fuel. These were to be achieved without major sacrifices in either vehicle performance, equipment or fuel costs.

It was found that within a broad band of A/F values and compression ratios (CR), the CFR engine could be operated on methanol fuel blends ranging from pure methanol to 100% dissociated methanol. It should be noted that the dissociated

---

*[1] refers to references.

methanol was simulated by a chemically correct mixture of CO and H_2 and intermediate fuel blends were achieved by mixing of pure methanol and dissociated methanol. The exploratory evidence from the CFR engine tests supported the thesis that methanol fuels might reduce exhaust pollution relative to gasoline fuels. The principal inadequacies in providing complete understanding from these tests were:

(1) A very limited test matrix in terms of engine variables.

(2) Limited emission instrumentation.

This exploratory evidence became the basis for the work herein reported. The objectives of this project were:

(1) Using the CFR engine, to assess engine operational control and steady-state, constant speed, power performance as functions of:
   (a) percentages of methanol and dissociated methanol,
   (b) air-fuel ratio,
   (c) compression ratio,
   (d) intake manifold temperature.

(2) To examine the exhaust emissions and relate the results to engine performance in meaningful ways.

(3) To carry out a preliminary design study which examines the feasibility of using engine waste exhaust energy as an energy source for dissociating methanol fuel.

III. DESCRIPTION OF EXPERIMENTAL APPARATUS

A. General:

Tests were conducted on a single cylinder, variable compression CFR engine manufactured by the Waukesha Company. Figure III-1 is a photograph of the experimental equipment and Fig. III-2 is a schematic of the engine test set-up. The engine carburetion and intake system were modified to allow injection and mixing of methanol and air, including provision for controlled heating of the fuel and/or fuel-air mixture. In order to hold the speed constant and provide the desired load, the engine was coupled to a synchronous motor running in parallel with the standard cradled DC dynamometer which was used primarily to start the engine. All tests were run at a speed of 900 RPM regardless of changes in the A/F ratio, spark advance, and CR.

The air flow to the engine was measured by a calibrated nozzle mounted on a plenum chamber. The flow of the liquid fuel and gaseous fuel was measured by rotameters. Both the air flow meter and the gaseous fuel meter were calibrated with positive displacement meters and readings are estimated to have a maximum uncertainty of $\pm$ 2%. During all tests the engine crankcase temperature was maintained at a constant value by a controllable electric heater.

A sampling line connected at the exhaust port of the engine fed exhaust gases to O_2, NO_X, CO and CO_2 meters and a gas chromatograph (GC)--see Fig. III-3. A second sampling line was provided for collection of aqueous samples. These samples were later subjected to post test GC analysis. A more detailed description of the emission instrumentation is presented in the following sections.

B. Gas Analysis Meters:

Continuous exhaust emission measurements were made using individual instruments for determination of O_2, NO_X, CO, and

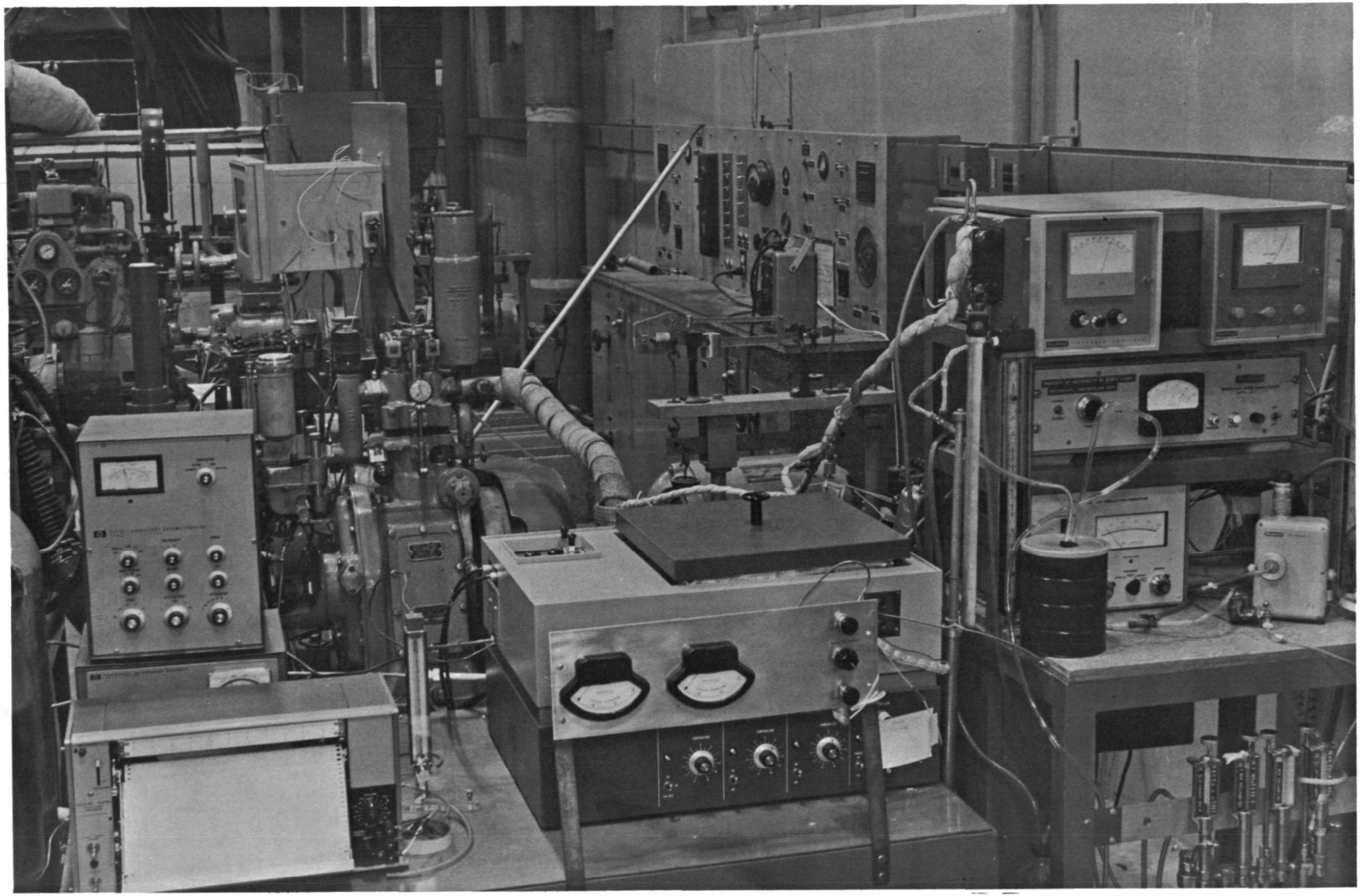

FIG.III-1: CFR ENGINE AND INSTRUMENTATION

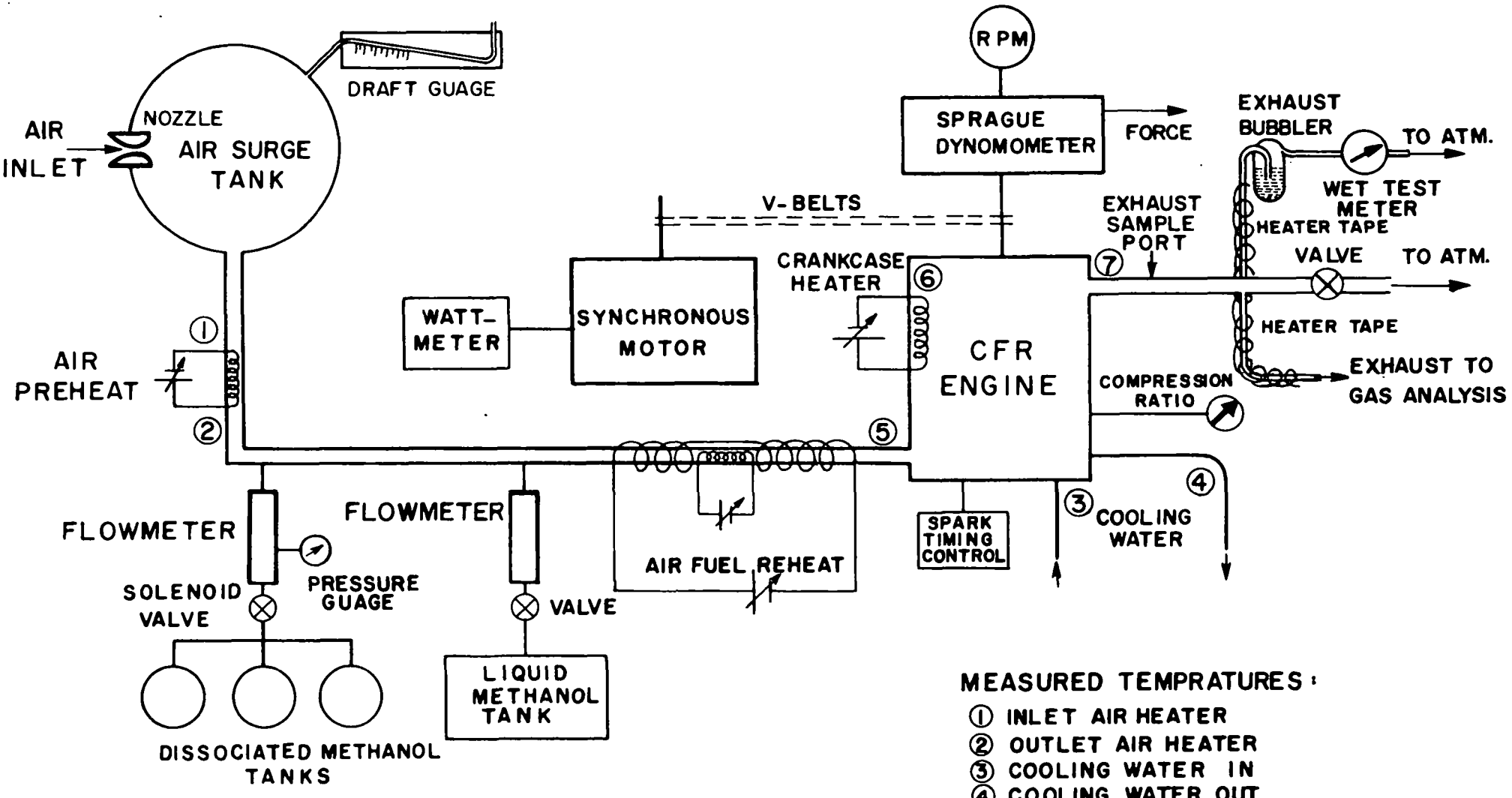

FIG.III-2: EQUIPMENT – SCHEMATIC METHANOL FUEL STUDY

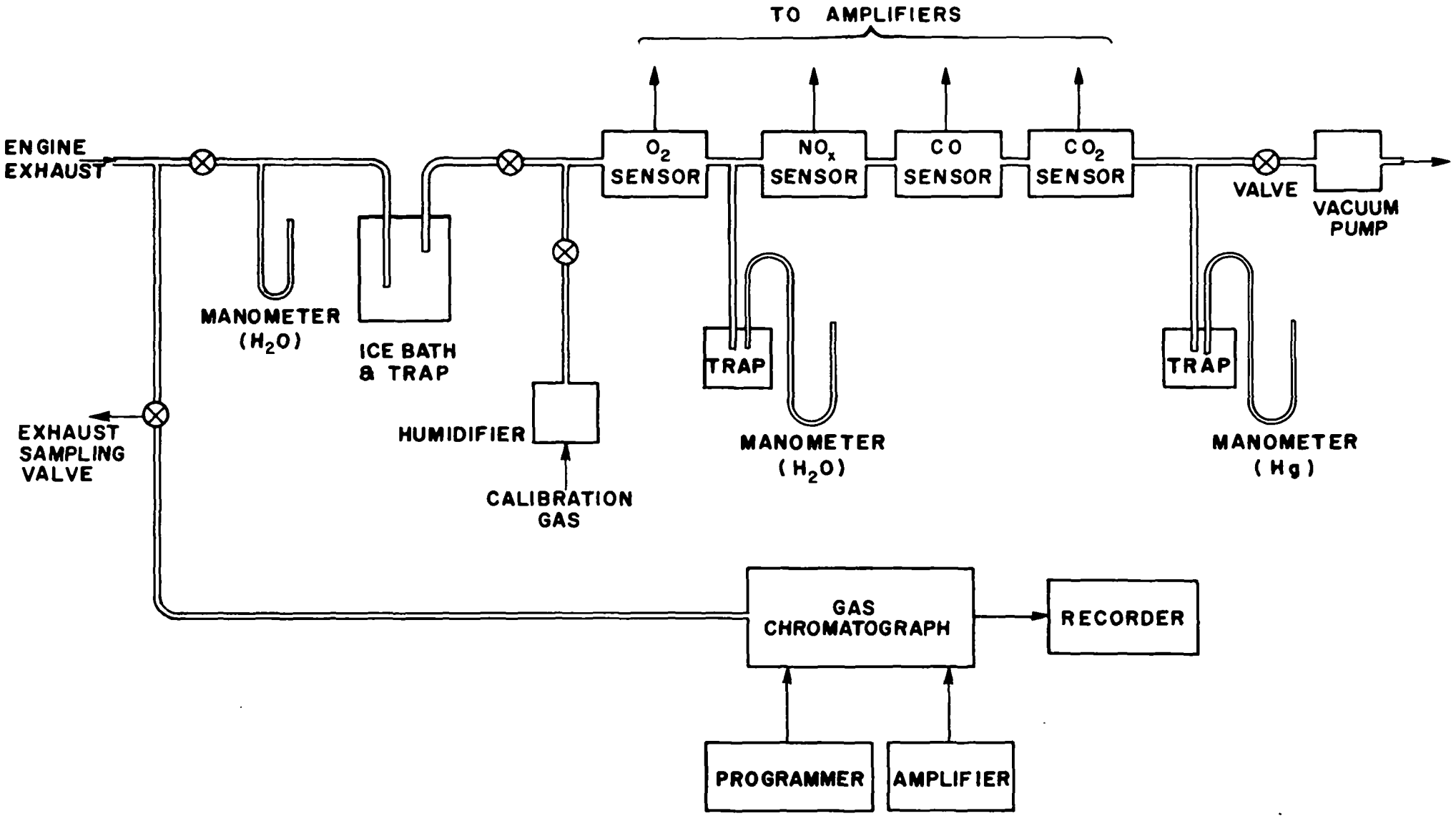

FIG. III-3: SCHEMATIC DIAGRAM OF GAS ANALYSIS INSTRUMENTATION

CO_2 exhaust concentrations. Carbon dioxide concentrations were measured with a Beckman LB-1 Medical Gas Analyzer and carbon monoxide with a Model 315a Beckman Infrared Analyzer. The oxygen content was measured with a Beckman Model 778 Process Oxygen Analyzer and the oxides of nitrogen were monitored by a Dynasciences Corporation Model NX 130 Air Pollution Monitor.

Pressure in the exhaust manifold was maintained at 10"H_2O by a valve at the exhaust pipe outlet. Pressures and flow rates in the sample line were adjusted and monitored by a series of valves, manometers and flow meters. A cold trap was provided upstream of the first instrument (see Fig. III-3) to prevent water condensation on the sensor elements. Heating tape was wrapped around the exhaust line between the exhaust manifold and first cold trap to prevent condensation in the sensor line. A pump was placed downstream of the last sensor to maintain a sufficient sample flow rate for optimum instrument response. It should be noted that all sensor pressures were slightly above atmospheric pressure to avoid exhaust dilution should there be any undetected leaks.

Premixed calibration gases from high pressure storage bottles could be fed into the sample line just upstream of the gas analyzers for instrumentation calibration. Valves in the exhaust sample and calibration gas lines permitted selection of gases from either of these sources. Calibration gas flow rates were adjustable by use of the bottle gas regulator and flow throttling valves by reference to manometers and flow meters in the sensor line. Calibrating gas flow rates and pressures were set to match the test pressures and flow rates.

C. Gas Chromatograph:

The GC (Hewlett-Packard Model 700, dual column, dual flame ionization detector) was fitted with two columns: one Porapak Q, the other Porapak T (manufactured by Waters Associates). Each column, made of 1/8-inch O.D. aluminum tubing, was six feet long and used 80/100 mesh packing.

Two different systems were provided for taking exhaust samples for the GC. In the first, a silicone septum was compressed in a port just downstream of the exhaust valve. A hypodermic needle of a heated gas syringe could be inserted through the septum and could sample the exhaust by filling the syringe. The second, more convenient system, consisted of a two-position valve (see Fig. III-4) connected to the exhaust gas sampling line. When the valve was closed, the exhaust sample passed continuously into the valve through a loop of known volume back into the valve, and then was vented to the atmosphere. Simultaneously, the carrier gas for the GC passed from the nitrogen cylinder through the valve, and into the columns. When the valve was opened, both flows were diverted. The exhaust stream passed directly through the valve to the vent, and the carrier gas passed through the loop, sweeping the exhaust sample in the loop into the column.

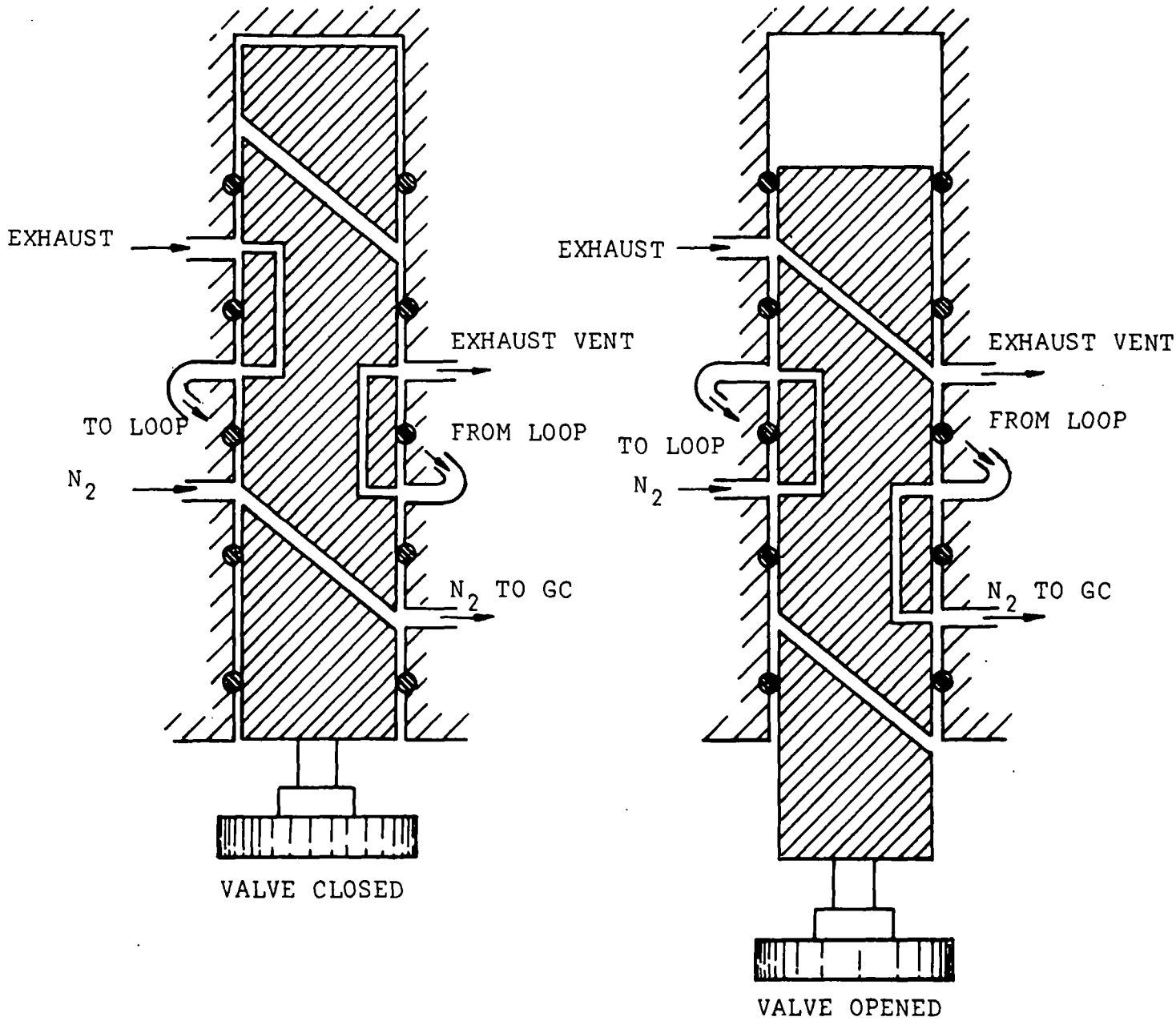

FIG. III-4: SAMPLING VALVE

IV. EXPERIMENTAL PROCEDURES

A. General:

Start up of the engine was accomplished by motoring with the dynamometer until combustion was sustained. The cradled dynamometer was then unloaded and allowed to rotate freely. The engine was set at a mid-range A/F ratio and allowed to warm up until the desired operating temperatures of the intake manifold and crankcase were stabilized.

Setting up a test run began by first stabilizing the crankcase temperature at 61-64°C. The desired compression ratio was then set at the required value with a hand crank and the cylinder head was clamped to prevent further movement. The barometric pressure, the ambient air temperature, and the pressure drop across the air intake nozzle were recorded and the air mass flow rate was calculated. The desired A/F ratio and per cent of fuel dissociation were then set using the calibration curves for the rotameters. If the air flow changed because of the fuel flow adjustments, the procedure was repeated until the proper setting was established.

The intake manifold temperature was set at the desired temperature by a variable resistance heater and the fuel flow rates were again checked and corrected, if necessary. The spark advance was either set at a desired point or optimized at the setting which produced the maximum power reading.

All of the above readings were then checked to insure that they were both correct and steady, and the test was begun. During the test run the readings were checked periodically. Some modes of operation required nearly continuous adjustments to offset drifting of the fuel flow rate or intake manifold temperature.

During the time of the test run, a portion of the exhaust was routed through the exhaust bubbler with the exhaust sample volume being measured by the wet test meter corrected for the temperature measured at the meter. Between tests the bubbled

sample was washed into another bottle and cataloged. The bubbler was then refilled with distilled water for the next test.

Another portion of the exhaust was routed to the gas analysis meters, where the CO, CO_2, O_2, and NO_X readings were regularly monitored. A gas chromatograph sample was taken once during each test run at a period of steady operation.

During each test, the following engine data were recorded:

Dynamometer Force
Spark Advance
Air Nozzle Pressure Difference
Barometric Pressure
Ambient Air Temperature
Fuel Rotameter (methanol and/or dissociated methanol)
Dissociated Fuel Pressure
Wattmeter Power*
Compression Ratio
Temperature
  (1) Intake Manifold
    (a) Heater Inlet
    (b) Heater Outlet
    (c) Engine Intake Port
  (2) Cooling Water In
  (3) Cooling Water Out
  (4) Crankcase Oil
  (5) Engine Exhaust

Test runs averaged about 22 minutes of steady-state operation, the approximate time necessary to cycle the GC. The time between runs was a function of the parameter being changed. Test runs were only begun after steady-state operation was established. All engine data were recorded at the beginning of the run and readings were checked at the middle and at the end of the runs. The average was recorded if a variation occurred. The gas analysis meters were monitored during the run and frequent data was recorded.

B. Instrumentation:

Calibration - Calibrations of the O_2, NO_X, CO, and CO_2 meters were made at the beginning and end of each test day

*The wattmeter power combined with the calibrated efficiency curve of the synchronous motor provided measurement of engine output to the synchronous motor.

and at intervals of approximately three hours throughout the day. The calibration duration was in each case long enough to insure that steady-state conditions had been established in the sensor line. These calibrations were accomplished by introducing premixed calibration gases into the instrumentation sampling line just upstream of the O_2 meter. The O_2, CO, and NO_X meters were calibrated using two reference gas concentrations, one of the references being zero. The CO_2 meter, which was not as linear, required three reference points. Zero concentration levels for the NO_X, CO, and CO_2 meters were obtained using air. A mixture of N_2 and CO_2 was used to zero the O_2 meter. The second calibration point was obtained using a reference gas mixture with concentrations of: CO_2, 12.0%; O_2, 4.0%; CO, 3.0%, NO_2, 0.15%; and N_2, 80.85%. The third calibration point for the CO_2 meter was established using a mixture of 5.0% CO_2 and 95.0% O_2.

Instrument gain settings were selected which gave good accuracy for all but the most extreme test conditions. The CO_2 meter was calibrated on a range from 0 to 16%, the CO meter on a range from 0 to 5%, the O_2 meter on either a range of 0 to 5% or a range from 0 to 25%, and the NO_X meter on one of the three ranges: 0 to 0.1%, 0 to 0.3%, 0 to 1.0%.

Three columns were used on the GC over the course of the test program. During initial check-out tests with the first column, the various methanol exhaust species, which were to be distinguished by the GC, were defined by their elution times as determined by authentic compounds. Subsequently, through the test program all columns were calibrated for elution time and peak sensitivity with pure reference samples of the primary exhaust emission contaminants. Periodic calibrations on each column were made with formaldehyde and methanol. For each column the elution time for a given constituent was constant until the effective lifetime of the column had been reached. At that time the column was replaced. Elution times and peak sensitivities were determined for methane on each of the three

columns and for ethane and propane on the first two columns. Complete calibration of all constituents on all three columns was not necessary since the elution times and peak sensitivities were constant for a given column and were in direct proportion to similar events on the other columns.

Testing - Exhaust sampling for the gas analysis meters was accomplished by shutting the valve to the calibration gas bottles and by opening the valve to the exhaust manifold. The valve downstream of the cold trap was then adjusted to give a positive pressure matching the calibrating gas pressure and guaranteeing a match of the exhaust and calibration flow rates through the sensors. Steady-state conditions were usually obtained in 5 to 8 minutes. An additional 10 to 12 minutes were then allowed to obtain average steady-state readings for all test instrumentation.

At the end of experimentation the instrumentation calibration was checked. If the calibration difference due to drift was greater than the reading error, then linear extrapolation in time was performed. If the drift was excessive, the experiments were repeated.

One or more gas chromatograms were taken during each test cycle. During early tests two or three were recorded. Later, after the test procedures became well established and it was determined that all the chromatograms obtained during a given run gave consistent data, only one was recorded per test. Exhaust samples were introduced into the GC column by cycling the gas sample valve, or for special tests by use of a heated syringe. Elution of the exhaust constituents from the column was accomplished by either one of two compound temperature programs. The primary program consisted of holding the column at 110°C for two minutes followed by a linear increasing temperature of 4°C per minute to a maximum temperature limit of 165°C. The second program, used to obtain more distinct separation of some peaks, consisted of holding the column at 60°C for four minutes with a subsequent linear temperature

increase of 4°C per minute to a limit of 165°C. Figures IV-1 and IV-2 show representative GC data for the two different temperature programs.

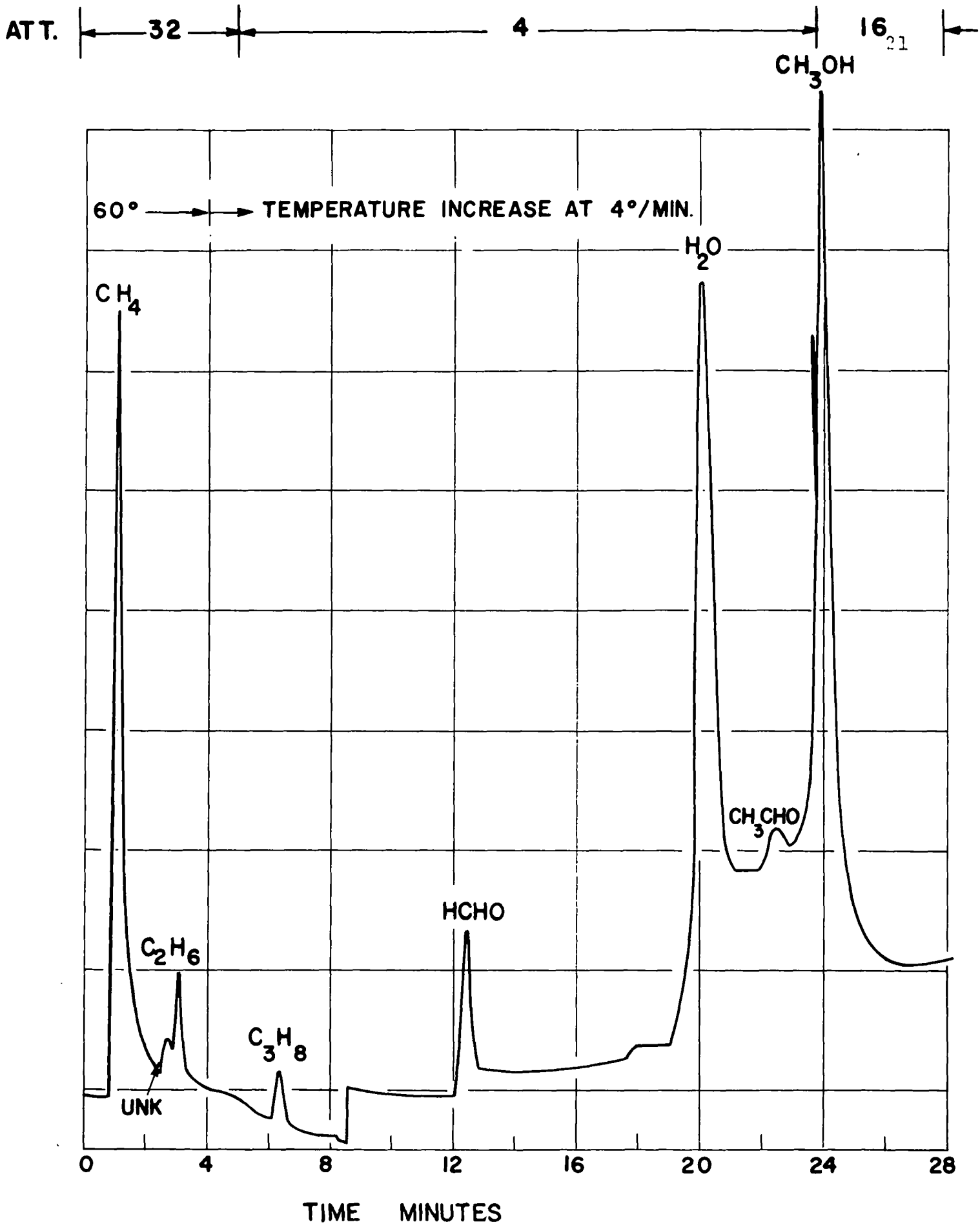

FIG IV-1: CHROMATOGRAM FOR 60°C TEMPERATURE PROGRAM
(TEST 46-2)

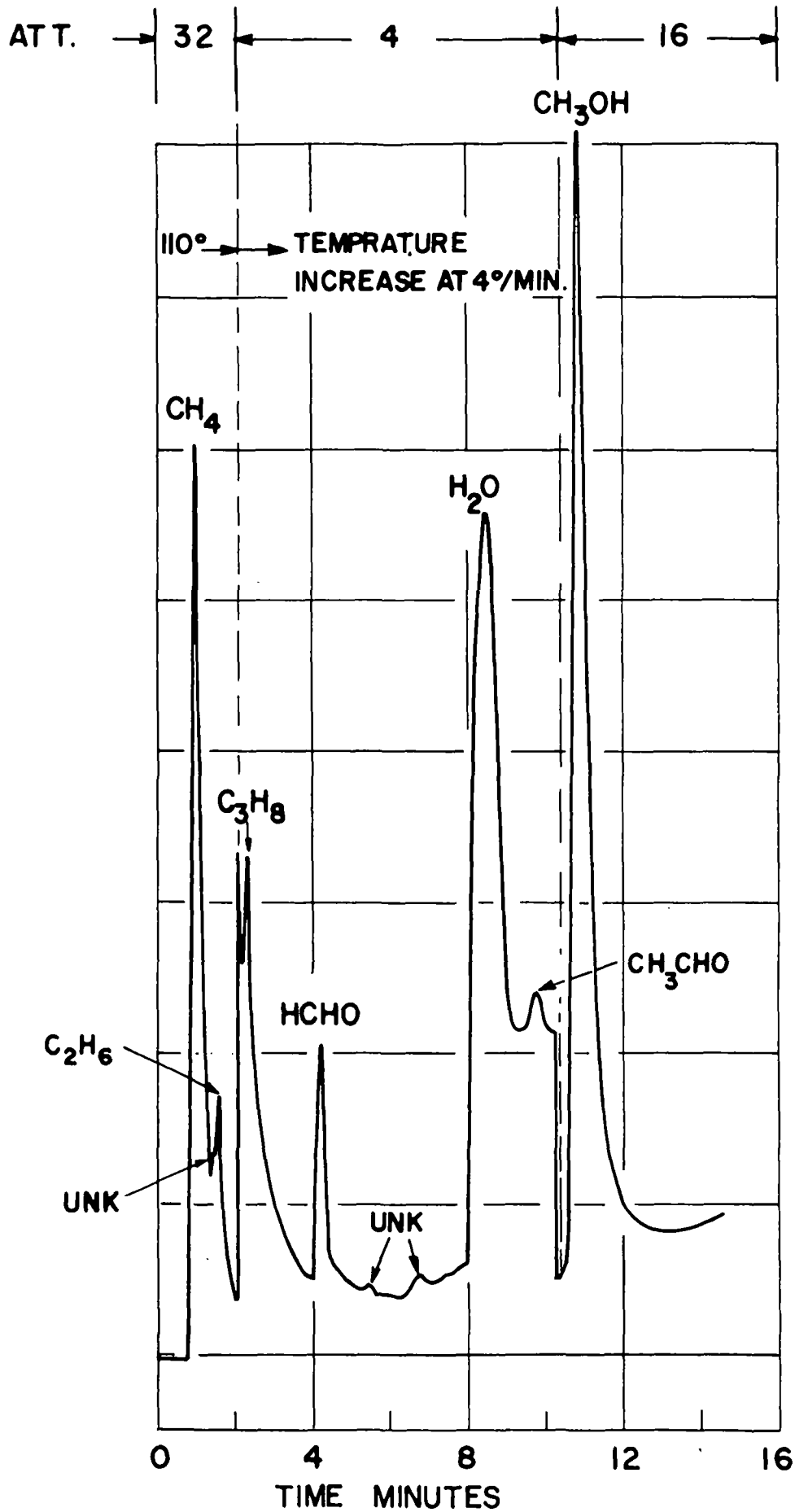

FIG. IV-2: CHROMATOGRAM FOR 110°C TEMPERATURE PROGRAM (TEST 65)

V. DATA REDUCTION

A. Engine Performance Data:

The determination of engine performance parameters of interest, apart from the exhaust gas constituent analysis, was by standard methods. (Sample engine performance data calculations are presented in Appendix A.)

The A/F values were determined from experimental air and fuel flow rate data.

The bhp and ihp determinations were complicated by simultaneous use of a synchronous motor as a means of loading the engine while holding its speed constant, and a cradle dynamometer for engine start. Engine brake power was used to drive the unloaded cradle dynamometer and the synchronous motor which was V-belt driven from the engine flywheel. The power to the cradled dynamometer could be directly determined. The power to the synchronous motor was determined by measuring its power output and dividing by the motor and belt efficiency. The synchronous motor efficiency was obtained by using the cradled dynamometer as a known power source and motoring the engine and synchronous motor at 900 RPM and at different load conditions. This same technique with the synchronous motor disconnected provided the engine friction horsepower at a nominal CR, which could be subtracted from the total motoring power to obtain the power supplied to the synchronous motor and V-belt drive.

Indicated horsepower was determined from the sum of brake horsepower and engine friction horsepower.

Indicated specific fuel consumption was determined by ratioing of the fuel flow rate and indicated horsepower.

B. Gas Analysis Meter Data:

The gas analysis meter data was reduced to determine the molar fractions of CO_2, CO, O_2, and NO_X in the exhaust sample of each test. Data reduction calculations were aided by use of a data reduction computer program. Input into the program

included steady-state or average test values and calibration data for each gas. Correction factors and assumptions used in reducing the data included:

(1) Oxygen meter electrode residual correction - instrument usually read 0.2% O_2 when nitrogen or carbon dioxide was purged under a slight positive pressure (1" H_2O).

(2) NO_X meter response to concentrations of CO according to the following expression:

$$\text{Indicated ppm } NO_X = 40 (\% \text{ CO})$$

(3) Assumptions that the oxides of nitrogen from the engine exhaust were primarily NO. The response of the NO_X meter to NO was approximately 10% less than to NO_2. The NO_X meter was calibrated with NO_2 and thus an additional correction factor was introduced to take this effect into account.

(4) Correction factor in the molar balance due to condensation of water in the cold trap. This correction factor assumed that the effect of ignoring the concentrations of NO_X and hydrocarbons in the exhaust was negligible.

The measurement accuracy of the O_2 content on the rich side of stoichiometric A/F was poor due to the almost complete lack of O_2. On the lean side of stoichiometric the CO measurement accuracy was likewise poor due to the almost negligible amount of the gas. At A/F values of 5, the CO content was greater than 5% and, therefore, could not be measured. For these cases it was necessary to assume a value in order to estimate a chemical balance and to express the emissions in terms of grams/ihp-hr. The CO and NO_X meters tended to be the most stable, while the CO_2 meter tended to baseline and sensitivity shifts. This was primarily a temperature phenomena due to lack of internal temperature compensation within the instruments. Maximum uncertainty in measurement, including errors in reading the meter values, extrapolating and reading from graphs (CO_2

and CO only), instrument sensitivity shift, baseline shift, and accuracy of calibration gas values are indicated below for nominal A/F values for tests using liquid methanol:

Maximum Uncertainty

	Rich A/F 5.5	Stoic A/F 6.5	Lean A/F 9.0
CO_2	6%	6.5%	7%
CO	10%	50%*	150%*
NO_X	11%	11%	18%
O_2	100%*	9%	13%

*High due to low-end scale reading on the instrument

C. Gas Chromatograph:

Quantitative analysis of emissions with the GC required identification of the peaks in the chromatograms and determination of constituent concentration corresponding to the area under the peak. Identification of the peaks was made by comparison of their elution times with those of authentic compounds. Since the elution time of many compounds displayed a small dependence on sample size, an extrapolation of the elution times with reference to standardization chromatograms made with different sample concentrations was required. Only one significant peak could not be unambiguously identified. In chromatograms with temperature programming starting at 110°C, this compound was eluted slightly before or during the peak for ethane (see Fig. IV-2). In chromatograms beginning at 60°C, this unknown component was clearly distinguished from ethane (see Fig. IV-1). When the two peaks could be resolved they were reported separately; otherwise, they were reported as a single number. Several other smaller peaks could not be identified but were sufficiently small as to represent an insignificant proportion of the exhaust concentrations.

Quantitative calibration and reduction of the chromatograms was done in several different ways. For gaseous compounds, such as methane, the pure gas was passed through the sampling valve, and the instrument response to the pure gas was measured. (The instrument response was defined as the peak area--height times the width at half maximum times the attentuation.) The volume fraction of that gas in the exhaust was then the ratio of the peak area in the chromatogram of the exhaust sample to the peak area for the pure gas. For liquids the sensitivity of the instrument was measured for small samples (usually one to two microliters). Knowing the peak area corresponding to a given volume, the peak area corresponding to a given mass was calculated from the density of the liquid. The volume of this mass in the vapor phase at 110°C, the usual temperature of the sampling valve, was calculated from the molecular weight of the compound and the ideal gas law. The volume fraction of the compound in the exhaust was then the ratio of this volume to 2.9 ml, the effective volume of the sampling valve. Calculations for the different compounds are described in Appendix A.

For some compounds it was inconvenient to measure the sensitivity directly (for example pentane, for the gasoline-fueled runs). For these cases the sensitivities of the GC to several C_6, C_7, and C_8 hydrocarbons were measured. Interpolation of these data with the information on CH_4, C_2H_6, and C_3H_8 was used to determine the GC sensitivity to other hydrocarbons.

Two runs were made with gasoline as fuel. A 2.9 ml sample of exhaust was injected into the gas chromatograph and over thirty separate components were resolved using the 60° program. The chromatograms from these two runs were reduced by measuring the total peak areas and by applying a standard hydrocarbon sensitivity factor to obtain the total hydrocarbon concentration in the exhaust.

The gas chromatograph appears to give data which at moderate to high concentrations is accurate to within about 10% of the actual constituent concentrations. This accuracy was

noted in the calibration tests with prepared samples. Repeatability was demonstrated on replicate chromatograms during continuous steady-state operation of the engine at specific test conditions (see Table V-1). Occasional wide variations of a constituent during a given run (for example methane during run 17) were noted but are attributed in most cases to variations in the instantaneous exhaust emissions. In analyzing the data, considerable scatter was noted for some species on tests at similar test conditions but conducted during different days. The data scatter is believed due to the inability to exactly reproduce given engine test conditions rather than significant data inaccuracies. This would seem to indicate that the reaction kinetics of some of the species are sensitive to small changes in engine operating variables. An example of this data scatter is seen by comparing runs 6, 12, and 83 (see Table 1 in Appendix B). Although engine operating variables were essentially the same the CO_2, CO, and CH_4 exhaust emissions varied systematically. In this case, the disagreement in GC methane emission data cannot be considered entirely spurious since the CO_2, CO, and CH_4 exhaust concentrations were measured independently.

D. Wet Chemistry:

Wet chemical techniques were used for formaldehyde determination as a comparison for the GC data. For each run the exhaust was passed through a heated line and through a glass bubbler filled with water. Formaldehyde and other water-soluble components were retained in the scrubber, while the rest of the exhaust was vented to the air. Formaldehyde absorption is nearly quantitative under these conditions [3].

Several techniques were tried but did not produce satisfactory data [4, 5, 6]. The most consistent data were data obtained with a colorimetric method using 2,4-dinitrophenyl hydrazine [7]. In this method, carbonyl-free methanol was made

TABLE V-1

RESULTS OF REPLICATE ANALYSES

Run No.	mg C/g Exhaust			ppm	
	CH_4	C_2H_6+ unknown	C_3H_8	HCHO	CH_3OH
5	.108	.008	.001	51	560
	.108	.009	.001	51	570
11	.083	.008	.001	32	783
	.083	.006	.001	34	689
12	.062	.008	.001	54	641
	.072	.008	.001	60	469
13	.008	.003	.0002	22	192
	.008	.003	.0003	27	142
15	.002	.002	.0001	13	394
	.002	.002	.0001	14	394
17	.074	.007	.0005	46	324
	.110	.007	--	50	--
	.172	.006	.0004	48	251
160	.406	.018	tr	25	457
	.427	.020	tr	69	391

by refluxing spectrograde methanol with a 2,4-dinitrophenyl hydrazine and by distilling. A 1 ml aliquot of scrubber liquid was mixed with 1 ml of saturated 2,4-dinitrophenyl hydrazine in carbonyl-free methanol. One drop of concentrated HCl was added and the mixture was heated at 60°C for about 20 minutes. After cooling, the sample was mixed with 5 ml of 10% KOH in 80% methanol. After the color developed for a few minutes, the optical density of the sample was measured at 4800 Å on a Beckman Model B spectrophotometer. Reproducibility and accuracy were good on standard samples, and the molar

extinction coefficient measured on standards agreed with published values [7].

This method does not measure formaldehyde, nor total aldehydes, but rather total carbonyl content of the sample. Since the exhaust should contain little ketone, the total carbonyl and total aldehyde concentration should not be too different. The method is reputed to be insensitive to interfering substances, but results on the scrubber samples gave poor reproducibility as compared to the GC data. It is believed that the gas chromatographic data are more reliable and that the wet chemistry results serve as a poor check on the total aldehydes in the exhaust samples. For this reason, only that data obtained from the GC are reported.

VI. EXPERIMENTAL PROBLEMS

The principal experimental problems encountered were in the calibration and reduction of exhaust emission data from the gas analysis meters and gas chromatograph. Reduction of data from the gas analysis meters was hampered for a considerable length of time because of difficulty in establishing the gas concentrations in the pre-mixed calibration gases. Analysis of the NO_2 content in the purchased gas mixture was originally given by the manufacturer as 1400 ppm and later amended to 1050 ppm. Final analysis of the original gas mixture by comparison with two properly analyzed bottles from separate sources showed that the real content was 780 ppm NO_2. Originally, it had been speculated by the manufacturer that the plain carbon steel bottle was absorbing some of the NO_2; however, identical runs over the course of experimentation could not produce any such evidence. In the data reduction program, as a result, correction factors were inserted depending upon which calibration gas bottle had been used.

The manufacturer of the NO_X meter stated in their manual that the instrument did not respond to CO. However, during experimentation the NO_X meter was found to respond to a bottled mixture of the H_2 and CO. After notifying the manufacturer on this point it was indicated that the instrument would respond to concentrations of CO as discussed previously--see Item 2, Page 24. Response of the sensor to hydrogen was found to be minimal.

Some experimentation was required in selection of the gas chromatograph columns and in determination of chromatographic techniques to be used with the selected columns. Additional problems were encountered in calibrating the volume of exhaust gas in the GC sample loop.

Extreme polar compounds, such as water and formaldehyde, are difficult to analyze on conventional packed columns, as they are irreversibly absorbed. This irreversible absorption causes broad, low, tailing, and non-reproducible peaks. In the

past this problem has usually been solved for aldehydes by forming volatile non-polar chemical derivatives of the aldehydes. This approach could not be used for the current analysis because of the low aldehyde concentrations. Consequently, a special column packing, unlike the usual solid support coated with a thin layer of absorbant was tried. Porapak (Waters Associates) is a porous polymer, principally polystyrene, fabricated into beads. When used as a column packing it does not irreversibly absorb polar compounds, and their peaks are sharp and reproducible. Several varieties of Porapak are available, modified to show different degrees of polarity. Evaluation of several of these indicated that one column, Porapak T, successfully resolved a mixture of formaldehyde, acetaldehyde, water, and methanol. An even more attractive feature of this column packing was that operating above room temperature it could resolve a mixture of methane, ethane, propane, and butane not only from one another but also from methanol and aldehydes. Thus, one analysis could furnish the concentrations of both the hydrocarbons and the aldehydes in an exhaust sample.

After selection of Porapak T as the best column packing material, the effect of column size, flow rates, operating temperatures and temperature programming on constituent elution times were investigated. It was found that the most effective Porapak T columns were made from 1/8" O.D. aluminum tubing, 6' long. The optimum flow rates were 18 ml/min for nitrogen carrier gas, 20 ml/min for hydrogen, and 120 ml/min for air. Column temperatures hot enough to elute methanol quickly were too hot to separate methane from other exhaust components. Two compound temperature programs were found to provide adequate resolution of data. In the primary program the columns were held at 110°C for two minutes, and then the temperature was automatically increased at 4°C/min to a maximum temperature of about 165°C. A second program was used to verify the elution times of some constituents. This program consisted of holding the column temperature constant at 60°C for four minutes

followed by an increase of 4°C/min to about 165°C. Figures IV-1 and IV-2 show typical runs under these conditions.

The GC exhaust samples used during the test program were collected using a Hewlett-Packard gas sampling valve. Special tests using a secondary sample collecting system were necessary to calibrate the volume within the gas sample valve loop. A port in the exhaust line about six inches downstream from the exhaust valves was fitted with an elastomer septum. A heating jacket was made for a gas syringe to keep it above 100°C. The needle of the heated syringe was inserted into the exhaust stream through the septum and the syringe was filled with exhaust gas. The needle was then withdrawn from the septum in the exhasut line, inserted into a similar septum in the gas chromatograph, and the contents of the syringe injected into the column. The volume of the syringe was verified to be 2 ml by water displacement (the nominal volume was correct within 2%). Comparative analysis of the calibrated syringe and sampling value data showed a sample value volume of 2.9 ml. This value was used for the value sample volume in all calculations involving this parameter (see Appendix A).

Another problem of concern which required some analysis was a shift in the chromatogram base line during temperature programming as shown in Figs. IV-1 and IV-2. This shift did not occur with a new column, and was not due to column bleeding because dual-column operation did not help. It is believed that unstable compounds, perhaps from the crankcase, were included in the exhaust samples and, hence, were loaded and retained on the columns during sampling of the exhaust. At low temperatures they were stable, but as column temperature rose they slowly decomposed, causing a flow of small amounts of decomposition products down the column and to the detector. This would cause the base line to rise, as observed. The base line shift did not interfere to a great extent with data analysis. At low temperatures the drift was not significant. At high temperatures the methanol and aldehyde peak areas

could be measured by interpolating the base line between the beginning and end of the peak. Although the area could not be measured so accurately as with a flat base line, inaccuracies, which are believed to be small, are restricted to the determination of acetaldehyde and methanol. Errors in distinguishing between these two species may account for some of the significant data scatter in methanol and acetaldehyde yield which were noted for similar test conditions.

VII. DISCUSSION OF RESULTS

A. General:

A total of 191 performance and emission tests were conducted on the CFR engine. Seven of these tests used gasoline as a fuel. The remainder used fuel blends ranging from pure methanol to 100% dissociated methanol. Table VII-1 represents a summary of engine test conditions used during these experiments. Complete engine test-variable, performance and exhaust emission data for each of the tests are presented in Appendix B.

All tests were carried out at steady-state conditions. No significant problems were encountered in starting or stopping nor while operating over a wide range of CR and A/F values. The ease of engine operation and the power performance using blends of methanol and dissociated methanol compared very well with gasoline performance. The peak power location and power variation of methanol and gasoline at identical fuel equivalence ratios (actual A/F/stoichiometric A/F) showed striking similarities. Indicated thermal efficiencies for equivalent conditions also produced nearly the same results. The differences observed in power between methanol and dissociated methanol were primarily due to differences in engine intake conditions. Under duplicate intake conditions, it is expected that the contrast would be slight.

The principal exhaust emissions analyzed were carbon monoxide, hydrocarbons, methanol, oxides of nitrogen, and aldehydes. In aggregate, the data indicated that the dissociated methanol is approximately equal to or superior to liquid methanol in reducing exhaust hydrocarbons and carbon monoxide for all A/F and CR values. The principal dissociated fuel disadvantage was higher NO_X emissions in the lean A/F range. Although a fuel comparison was not part of the study, limited data indicated that methanol is significantly superior to gasoline in reducing hydrocarbons and CO emissions.

TABLE VII-1

TEST MATRIX

Parametric Base Line Performance (maximum power spark advance--full throttle)

CR	A/F	% Diss.	T_{intake}
8.4	5.0	0	nominal (70°F)
9.2	5.5	30	
11.0	6.5	70	
	7.5	100	
	9.0		

Variable Intake Temperature (maximum power spark advance--full throttle)

CR	A/F	% Diss.	T_{intake}
8.4	6.5	0	40°F
11.0	7.5	30	110°F
		70	
		100	

Spark Timing (full throttle)

CR	A/F	% Diss.	Timing (°BTDC)
8.4	5.5	30	0
11.0	6.5		10
	7.5		20
	9.5		25

The following sections present an analysis of the CFR engine performance and emission data.

B. Engine Performance:

Before examining the details of the exhaust emissions it is of importance to obtain a general view of the engine's performance in terms of power and thermal efficiency using the methanol fuel blends. Thermal efficiency is adopted as a basis of comparison rather than specific fuel consumption because of the significant difference in heating values of the fuels to be compared.

(1) Dissociated Fuel Power Effects. The experimentally observed values of indicated horsepower (ihp) developed by the engine for pure methanol and 100% dissociated methanol as a function of A/F ratio are shown in Fig. VII-1 for various compression ratios. The increase in ihp with compression ratio approximately reflects that predicted by Otto cycle efficiency. However, all of the experimentally observed ihp values for pure methanol fuel as a function of A/F ratio are seen to be significantly higher than those for 100% dissociated methanol. This appears to be inconsistent with the fact that the dissociated methanol has 20% more energy per unit mass than the pure methanol by virtue of its recovery of decomposition energy. This apparent discrepancy is resolved by noting that the energy per unit volume of cylinder intake and not the specific fuel energy is the parameter which governs the engine power.

To consider changes in the intake charge energy with dissociated methanol, a volumetric energy parameter depending upon the degree of fuel dissociation was developed. This parameter, which is based upon a dimensionless energy per unit volume, is given by the equation:

$$\frac{E}{(LHV)\left(\frac{p_t M_a}{R_o T}\right)} = \frac{1 + 0.2x}{\frac{M_a}{M_{f,x}} + A/F}$$

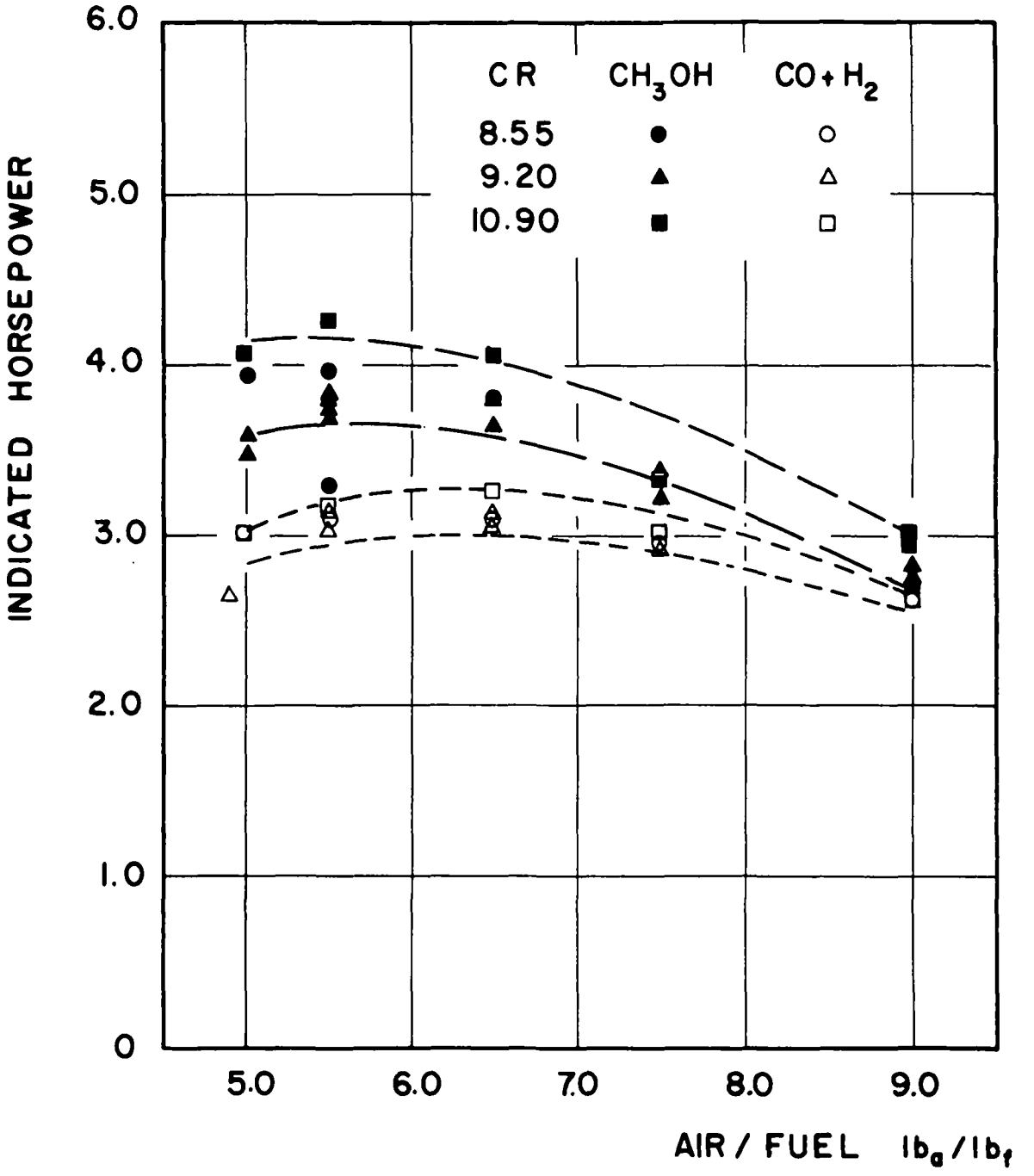

FIG VII-1 : FUEL DISSOCIATION & C R EFFECT ON IHP

E - energy per unit volume of change
(LHV) - lower heating value of pure methanol
p_T - total pressure in the intake manifold
M_a - molecular weight of air
$M_{f,x}$ - molecular weight of fuel blend
R_o - universal gas constant
T - absolute temperature
x - mass fraction of dissociated methanol

It was further assumed that the available fuel energy is restricted at a fuel rich mixture of 5.5:1, according to the reaction:

$$CH_3OH + 1.17\ [O_2] + 4.40\ N_2 \rightarrow 0.67\ CO + .33\ CO_2 + 2\ H_2O + 4.40\ N_2$$

Figure VII-2 shows the volumetric energy as determined from these equations as a function of the methanol dissociation for various A/F ratios.

Analysis of Fig. VII-2 indicates that if the intake pressure and temperature are held constant, the volumetric intake energy for a given A/F ratio decreases slightly with increased dissociation. This power reduction with dissociated fuel must have resulted primarily from changes in the intake charge density associated with charge temperature variations. This latter postulation was confirmed by showing that the experimental engine ihp performance with liquid and 100% dissociated methanol would be almost identical under equivalent intake energy conditions.

Figure VII-3 shows the results of correcting for intake charge effects. Factors accounted for included:

(a) Inlet manifold temperature differences between the liquid and dissociated fuel.
(b) Charge density increases through endothermic cooling from that portion of the fuel not previously vaporized at the saturated vapor conditions corresponding to the inlet manifold pressure and temperature (see Fig. VII-4).

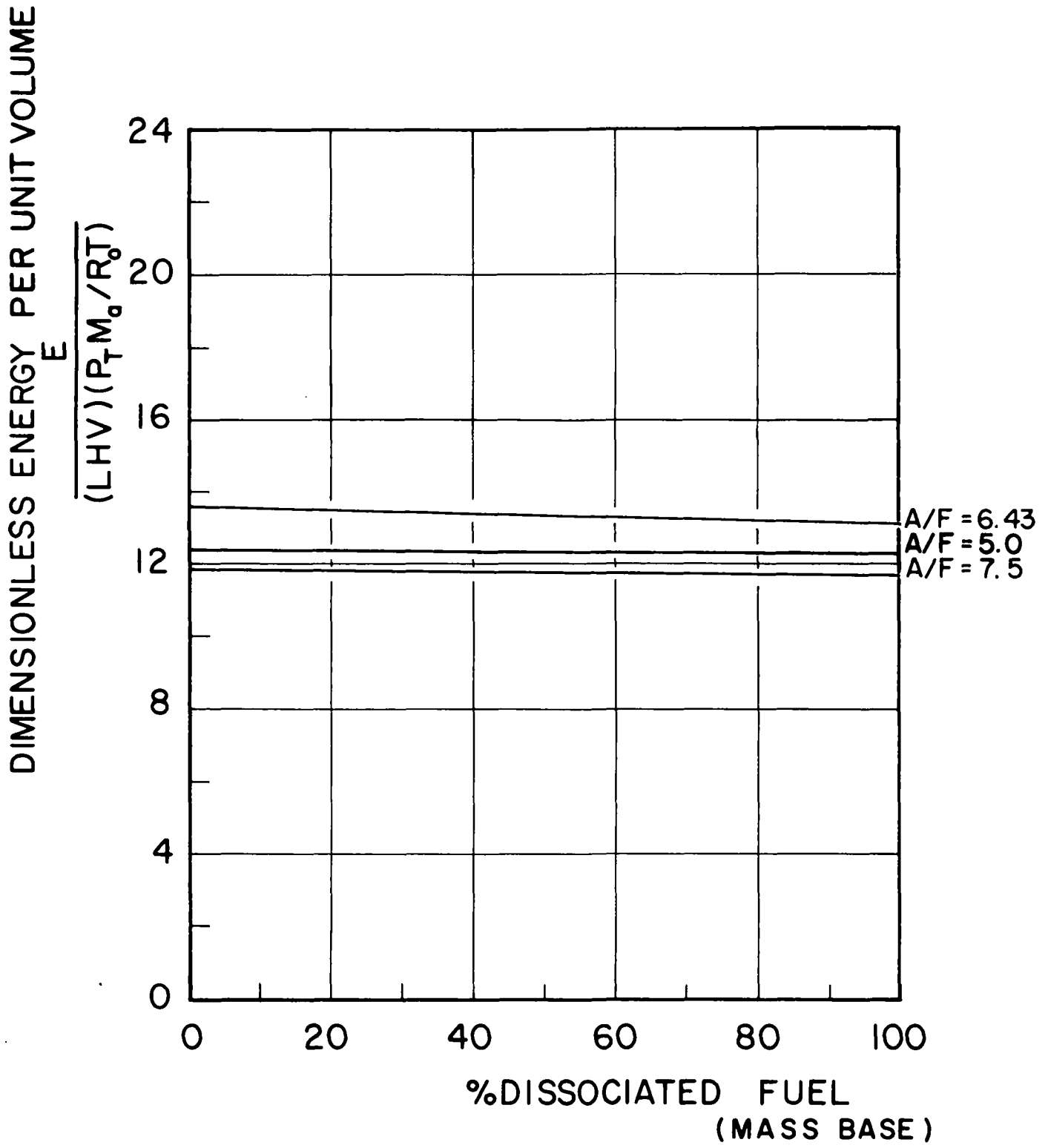

FIG. VII-2: DIMENSIONLESS ENERGY PER UNIT VOLUME OF INTAKE MIXTURE VS PERCENT DISSOCIATED METHANOL

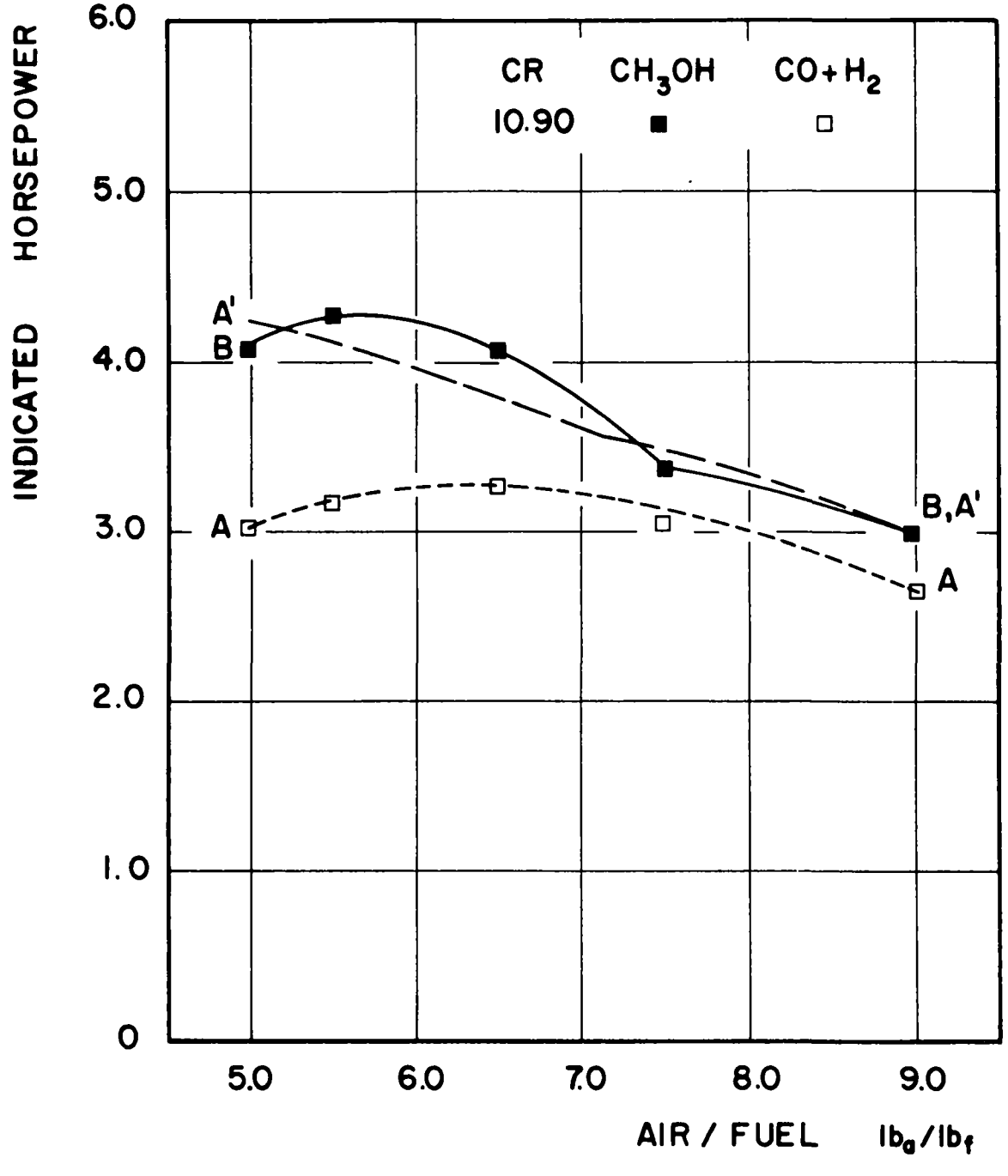

FIG. VII-3 : FUEL DISSOCIATION & C R EFFECT ON IHP

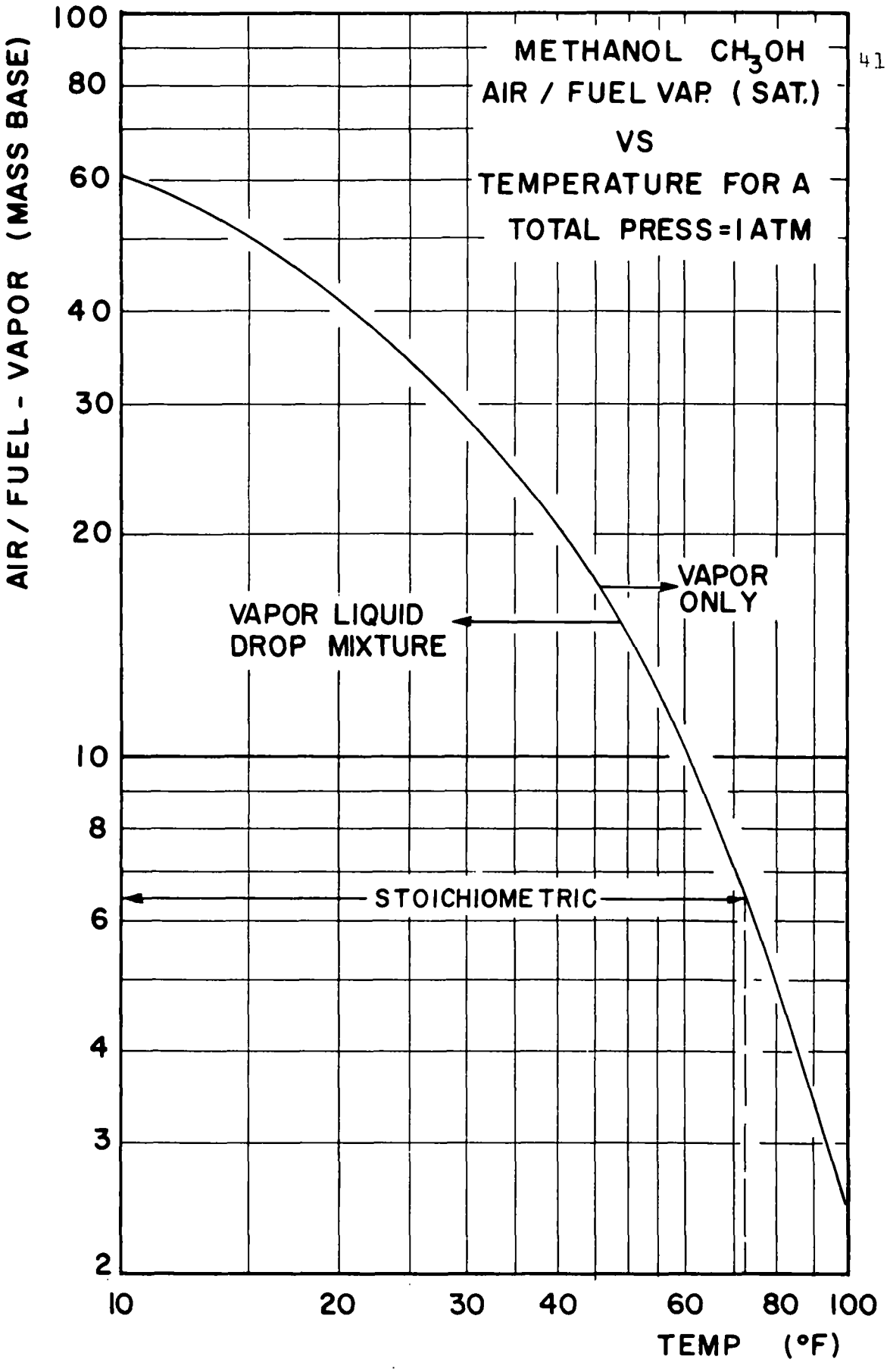

FIG. VII-4 : METHANOL A/F(VAPOR) VS TEMP.

In Fig. VII-3 curves A-A and B-B represent, respectively the experimental results for the liquid and dissociated methanol. Curve A' - A' is a correction for the dissociated methanol, curve A-A, taking charge density effects into account. Good agreement is indicated. It is thus seen that fuel vaporization effects and intake temperature differences existing in the test work exaggerated the differences in power performance of the pure methanol and the 100% dissociated methanol. Under identical intake manifold conditions the ihp contrast would be slight.

(2) Methanol and Gasoline Performance Comparison. The difference in power performance of the CFR engine operated on methanol and gasoline at equal equivalence ratios was found to be slight in terms of power and thermal efficiency. The maximum power the engine developed using methanol fuel at 900 RPM and a CR of 9.2 was 3.8 ihp. For gasoline at the same conditions it developed 3.9 ihp. These values agree quite well with what is expected when the fuels are compared on the dimensionless energy per unit volume base.

$$\frac{E}{LHV\ \left(\frac{P_T M_a}{R_o T}\right)_{stoich.}} = 0.136 \text{ for methanol}$$

$$= 0.137 \text{ for octane}$$

Figure VII-5 shows experimental comparisons using the equivalence ratio as a basis. The diminution of power from its peak shows very similar results for the gasoline and methanol. The indicated thermal efficiency of the two fuels are also quite similar. The dissociated methanol produced a somewhat lower thermal efficiency curve. An explanation for this reduced performance warrants further investigation. As indicated by the emission data, it is not due to incomplete combustion.

The general evidence thus indicates that there are no major disadvantages in engine power and efficiency performance when operated on methanol as compared to gasoline. These

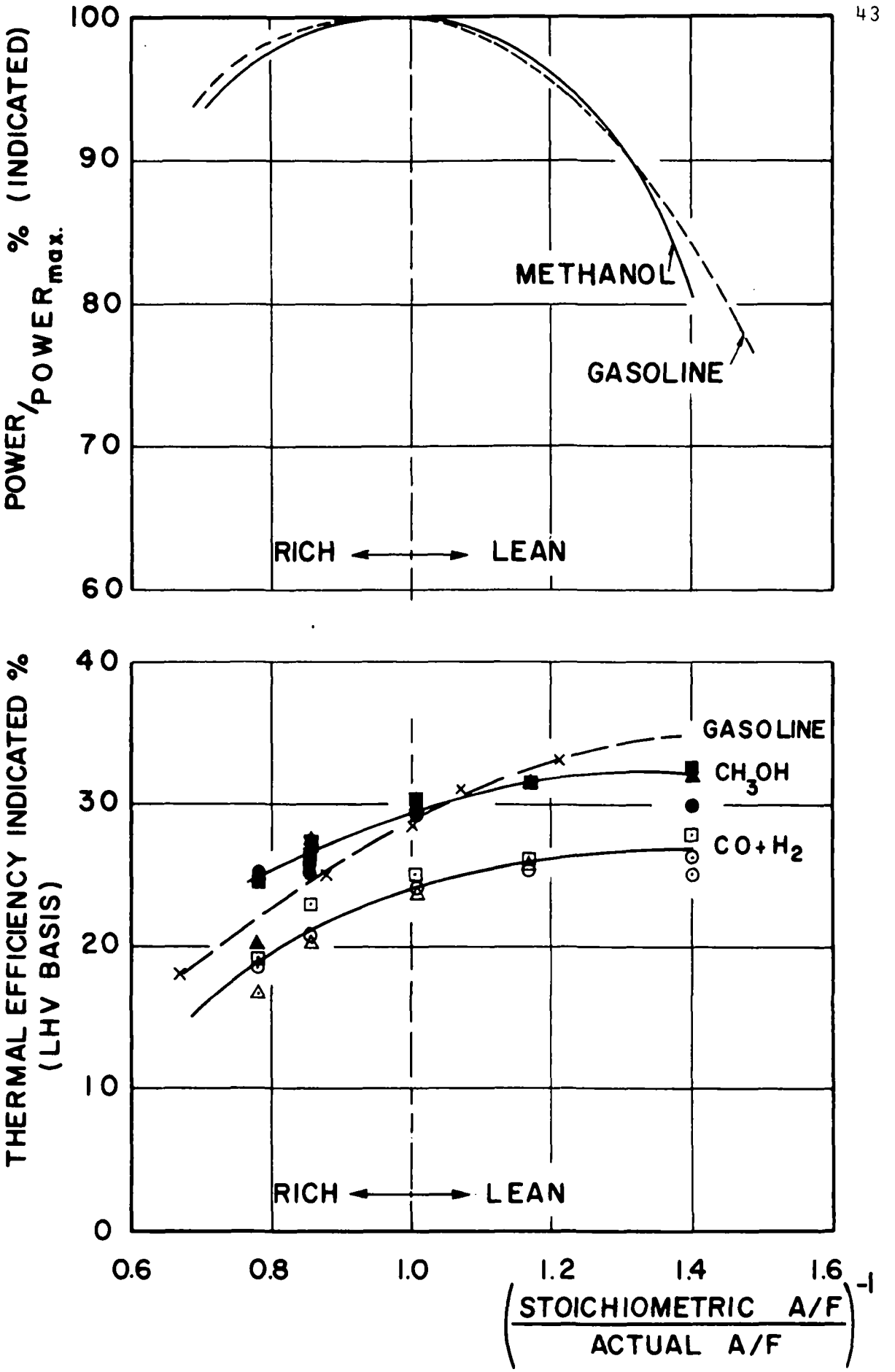

FIG. VII-5: GASOLINE & METHANOL PERFORMANCE COMPARISON

general observations are in agreement with others [8, 8a]. The relative performance merits of the two fuels must be established by the amounts and types of pollutants that each fuel produces.

C. Emission Data:

Engine emission data are normally presented in volume per cent of exhaust concentration or as parts per million (ppm) of exhaust concentration. In analysis of the data it was found to be desirable to use an additional parameter, grams of emission per indicated horsepower hour (gm/ihp-hr), as an evaluating criterion. This rating parameter indicates the emissions produced per unit of work delivered to the piston face. It is analogous to the "grams of pollutant per mile" used as a vehicle rating. However, the latter rating is not particularly meaningful for a laboratory engine operation at constant speed and load. In contrast the gm/ihp-hr rating was found to be particularly valuable in this investigation since the engine power output varied with percentage of fuel decomposition. Its use is encouraged as a generally useful parameter in comparing performance of different fuels, engine sizes, and loadings.

A selected amount of the total data is graphically presented for analysis. The three principal variables used for evaluation of the test results were the A/F ratio, the compression ratio (CR) and per cent of fuel in dissociated form. In a majority of cases the A/F ratio was used as the independent variable and CR or per cent of dissociation were used as parameters. Cross-plotting with per cent dissociation or CR as the independent variable was made as necessary to illustrate the effects of these variables. In some tests the effect of the per cent dissociation on the independent variable was not large and the data for intermediate dissociation percentages were bounded by the zero and 100 per cent extremes. In these cases, only the data for the extreme blends were plotted.

Analysis of portions of the emission data was hindered because of significant data scatter and the large number of interacting engine variables involved. For some emissions, particularly the aldehydes, the data scatter made graphical

interpretation of the results difficult. In these cases tabular data were analyzed for identifiable trends.

The effect of engine test variables upon emissions was qualitatively similar to that reported for gasoline. Hydrocarbon and unburned methanol emissions were high at low and very high A/F ratios and were reduced near stoichiometric conditions (see Fig. VII-6). Total aldehyde emissions were low at low A/F and increased for lean A/F ratios.

Increased spark advance tended to increase hydrocarbon, aldehyde and NO_X emissions at stoichiometric and lean A/F ratios (see Table VII-2). For these cases, maximum power spark advance occurred between 10° and 15° before top dead center (BTDC). Emissions improved appreciably below 10° with small loss in power. At rich A/F ratios the effect of spark advance was not as pronounced.

The percentage of fuel dissociation had varying effects upon the different emission species (see Fig. VII-7). As one would expect, unburned methanol concentrations were decreased for increasing fuel dissociation at all A/F ratios. At high dissociation percentages the decrease in methanol concentrations appeared to be at the expense of increased hydrocarbon and aldehyde emissions. For these cases the reaction kinetics appeared to favor methane production at low A/F ratios and acetaldehyde production at high A/F ratios. NO_X emissions were increased with increasing dissociation at both high and low A/F ratios.

Comparison of methanol and gasoline emission data was made for a limited number of test conditions. Near stoichiometric the total grams of carbon and per cent of CO in the exhaust were in general an order of magnitude lower for methanol than for gasoline. NO_X emissions were equivalent for both fuels.

A further discussion of the effect of engine operating variables on major emission species and comparison of gasoline and methanol emission data are presented in the following paragraphs.

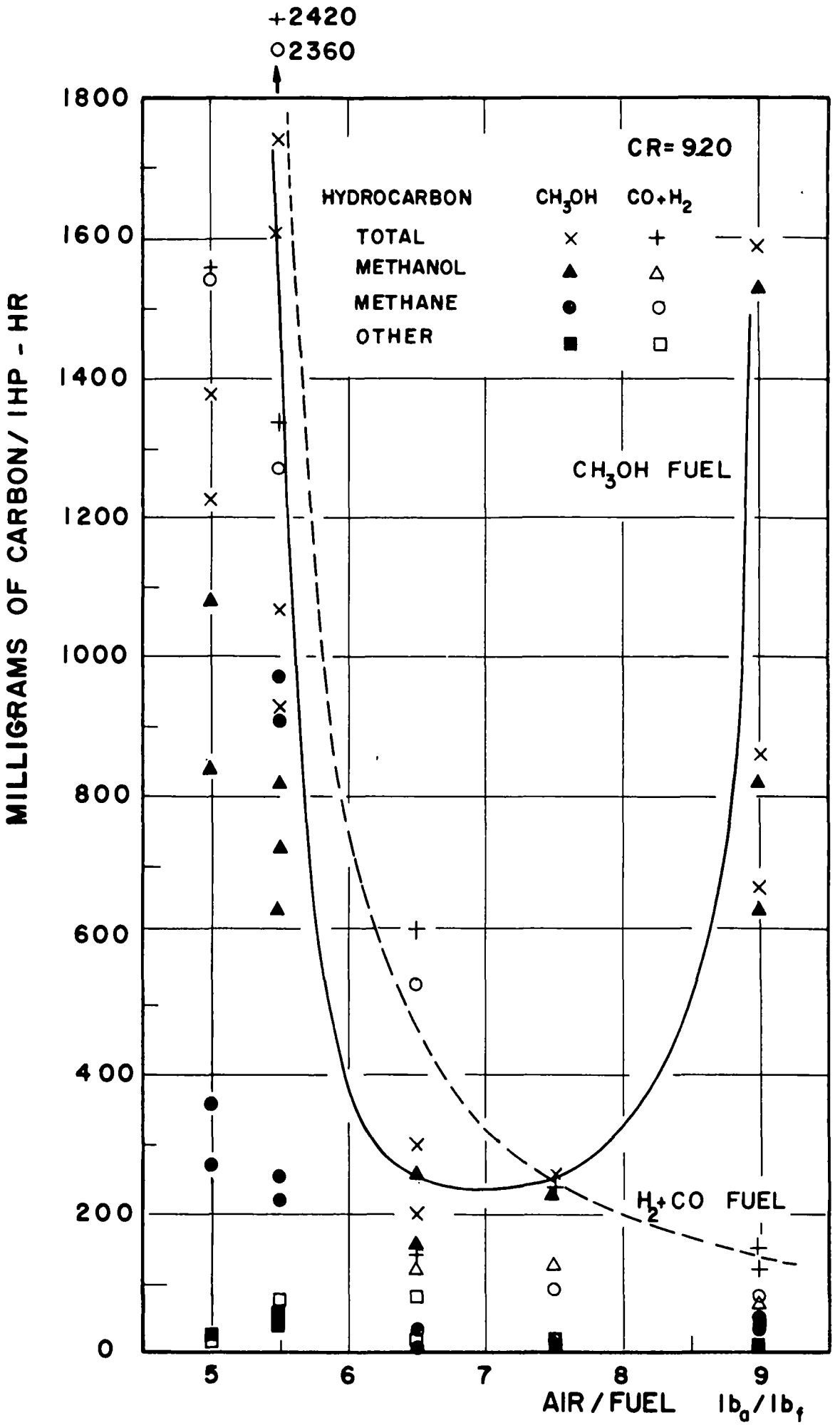

FIG. VII-6: EXHAUST HYDROCARBON DISTRIBUTION

TABLE VII-2
SPARK ADVANCE EFFECT ON EXHAUST EMISSIONS

Test	A/F	CR	% Diss	SA	T_{im}	ihp	isfc	CO_2 (%)	O_2 (%)	CO (%)	NO_X (%)	CH_3OH (ppm)	CH_4 (ppm)	C_2H_6+U (ppm)	C_3H_6 (ppm)	HCOH (ppm)	CH_3CHO (ppm)
142	6.5	10.9	30	2	70	3.52	.985	10.82	1.24	0.08	0.299	40	47	16	1	37	127
141	6.5	10.9	30	10	70	3.58	.97	10.93	1.04	0.08	0.347	83	47	17	1	44	138
138	6.5	10.9	30	20	70	3.55	.98	10.93	1.03	0.09	0.404	115	50	17	Tr	52	139
137	6.5	10.9	30	23	70	3.49	.98	10.97	0.95	0.09	0.406	114	48	17	Tr	60	139
161	7.5	10.9	30	1	70	3.10	1.005	9.54	3.55	0.08	0.142	59	12	9	Tr	26	4
162	7.5	10.9	30	10	70	3.27	.455	9.55	3.53	0.08	0.252	114	16	10	-	47	55
163	7.5	10.9	30	15	70	3.31	.94	9.53	3.56	0.09	0.295	159	24	12	Tr	53	221
164	7.5	10.9	30	20	70	3.26	.955	9.53	3.57	0.09	0.357	134	21	11	Tr	46	374
165	7.5	10.9	30	23	70	3.22	.97	9.61	3.42	0.09	0.407	133	21	11	Tr	36	237
61	5.4	8.5	30	2	73	3.80	1.07	9.87	0.07	2.12	0.142	237	483	11	1	62	12
62	5.5	8.5	30	10	72	3.73	1.04	9.97	0.09	1.97	0.173	227	476	16	Tr	71	8
63	5.5	8.5	30	12	71	3.77	1.07	10.06	0.09	1.85	0.187	207	431	16	Tr	77	17
64	5.5	8.5	30	20	71	3.61	1.12	9.79	0.11	2.18	0.167	249	654	17	Tr	64	12
65	5.5	8.5	30	23	72	3.57	1.14	9.74	0.11	2.26	0.166	223	548	16	1	61	15
71	7.5	8.5	30	2	70	3.01	1.01	9.02	4.49	0.08	0.101	101	9	4	Tr	68	10
72	7.5	8.5	30	10	70	3.14	0.96	9.02	4.49	0.08	0.206	130	18	8	Tr	47	36
73	7.5	8.5	30	14	70	3.25	0.93	9.18	4.20	0.08	ND	162	35	10	Tr	68	128
74	7.4	8.5	30	20	70	3.22	0.94	9.22	4.14	0.08	ND	106	40	12	Tr	62	384
75	7.4	8.5	30	23	70	3.11	0.97	9.19	4.19	0.08	ND	--	40	11	Tr	61	487

A/F - air-fuel ratio
CR - compression ratio
% Diss - per cent of methanol in dissociated form
SA - spark advance
T_{im} - intake manifold temperature
ihp - indicated horsepower
isfc - indicated specific fuel consumption, lb/hp-hr
-- - no data
Tr - trace of specie less than .5 ppm

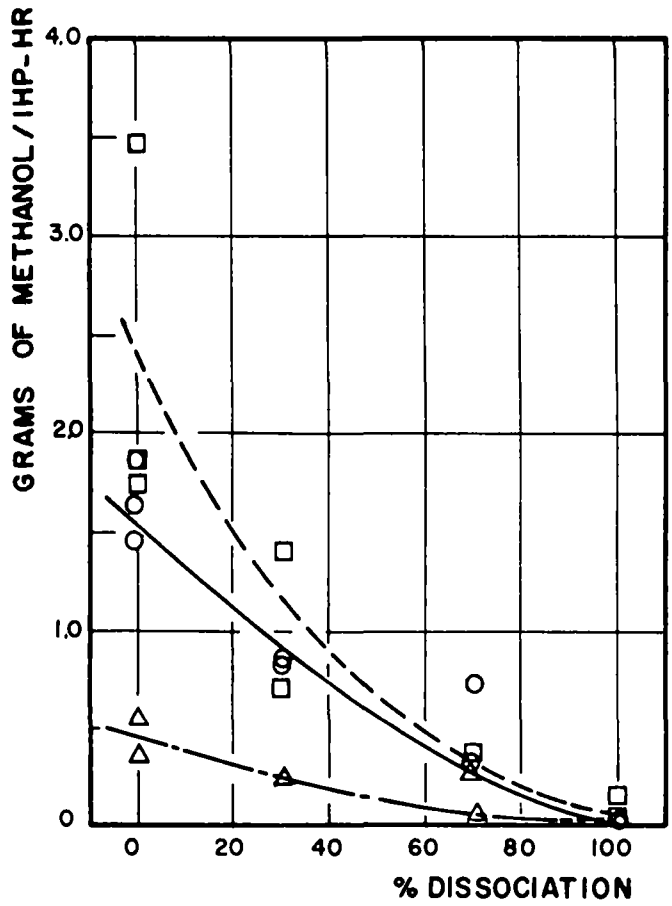

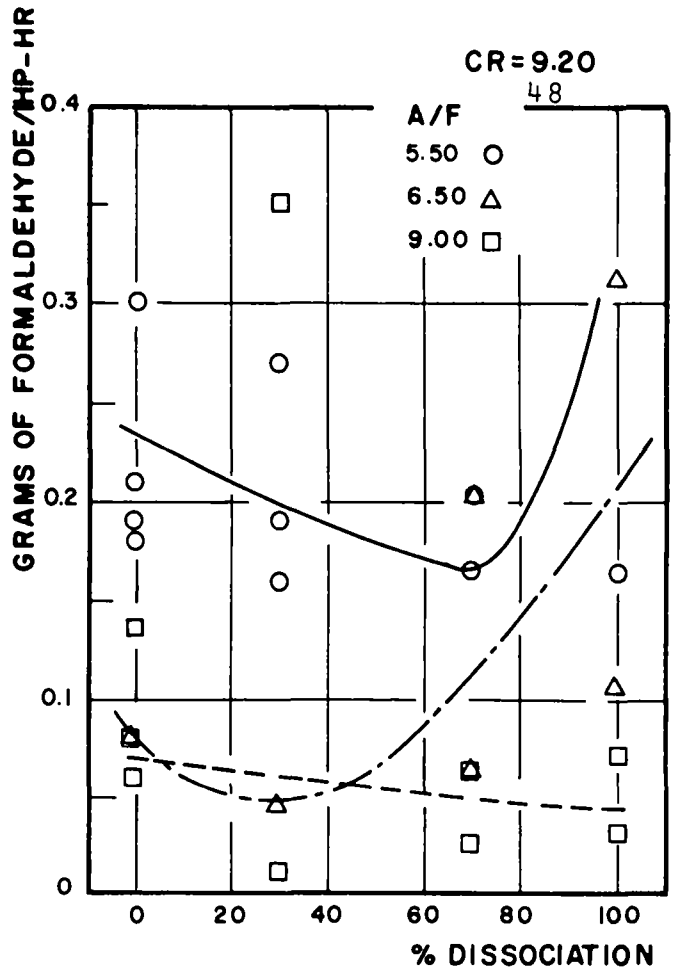

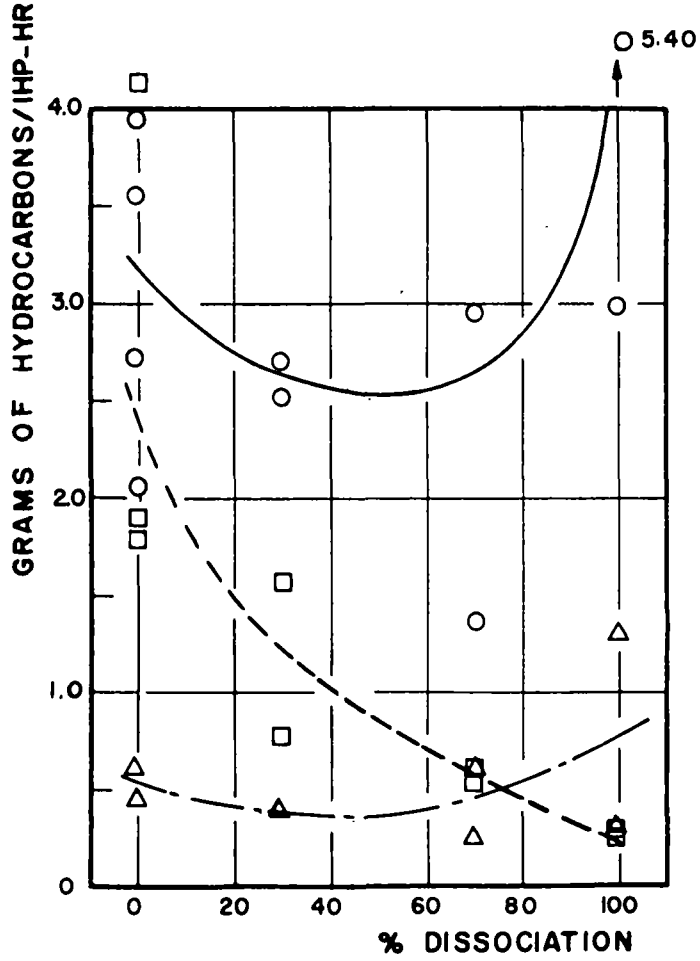

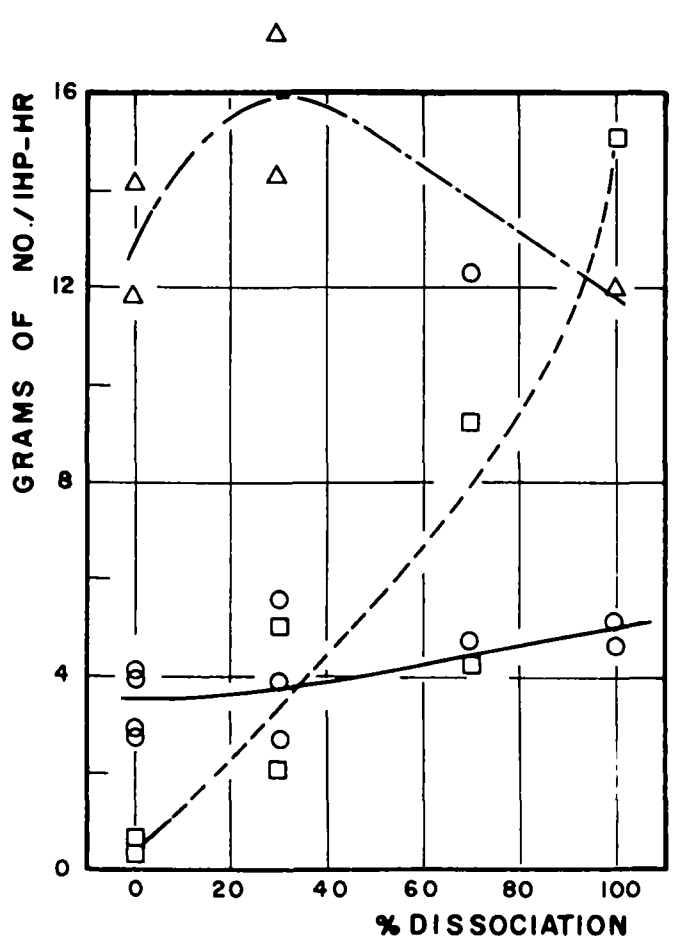

FIG. VII-7 : EXHAUST EMISSIONS VS METHANOL DISSOCIATION

(1) Carbon Monoxide. Consistent with the behavior of hydrocarbon fuels the methanol and dissociated methanol exhibit a rapid increase in CO as the A/F ratio moved into the fuel rich region. Similarly, they were at trace levels at A/F ratios in excess of stoichiometric (see Fig. VII-8a,b). The most significant contrast between the pure methanol and the dissociated methanol was found at the stoichiometric condition. At this condition the dissociated methanol shows a threefold higher percentage of CO in the exhaust than does the pure methanol. It is postulated that this results from the probability that any unburned fuel in the 100 per cent dissociated methanol would preferentially show up as unreacted CO, while in the case of liquid methanol the unburned fuel would more probably be unburned methanol or hydrocarbons. If this is true, then the CO exhaust concentrations at all fuel rich mixtures should be higher for dissociated than undissociated methanol. This is seen to be confirmed by the data in Fig. VII-8a, b.

(2) Hydrocarbons. The major unburned fuel species in the exhaust were methanol and methane.* The amount of methanol and methane were highly dependent upon A/F and per cent dissociation and to a lesser extent on CR. Other hydrocarbons, including C_2H_6 and C_3H_8 were also present but were in small concentrations relative to the combined amounts of CH_3OH and CH_4 components.

Large methanol exhaust concentrations were noted at low and high A/F ratios for engine operation on liquid methanol (see Fig. VII-9). These high concentrations are attributed to insufficient oxidizer for rich mixtures and poor combustion efficiency for lean mixtures. The advantage of combusting dissociated methanol was most pronounced for very rich mixtures and lean A/F ratios. As expected, methanol exhaust concentrations decreased proportionally with increased per cent dissociation until only trace concentrations were present for completely dissociated fuel.

---

*Although methanol is an alcohol rather than a hydrocarbon it is grouped with the latter for ease of reporting.

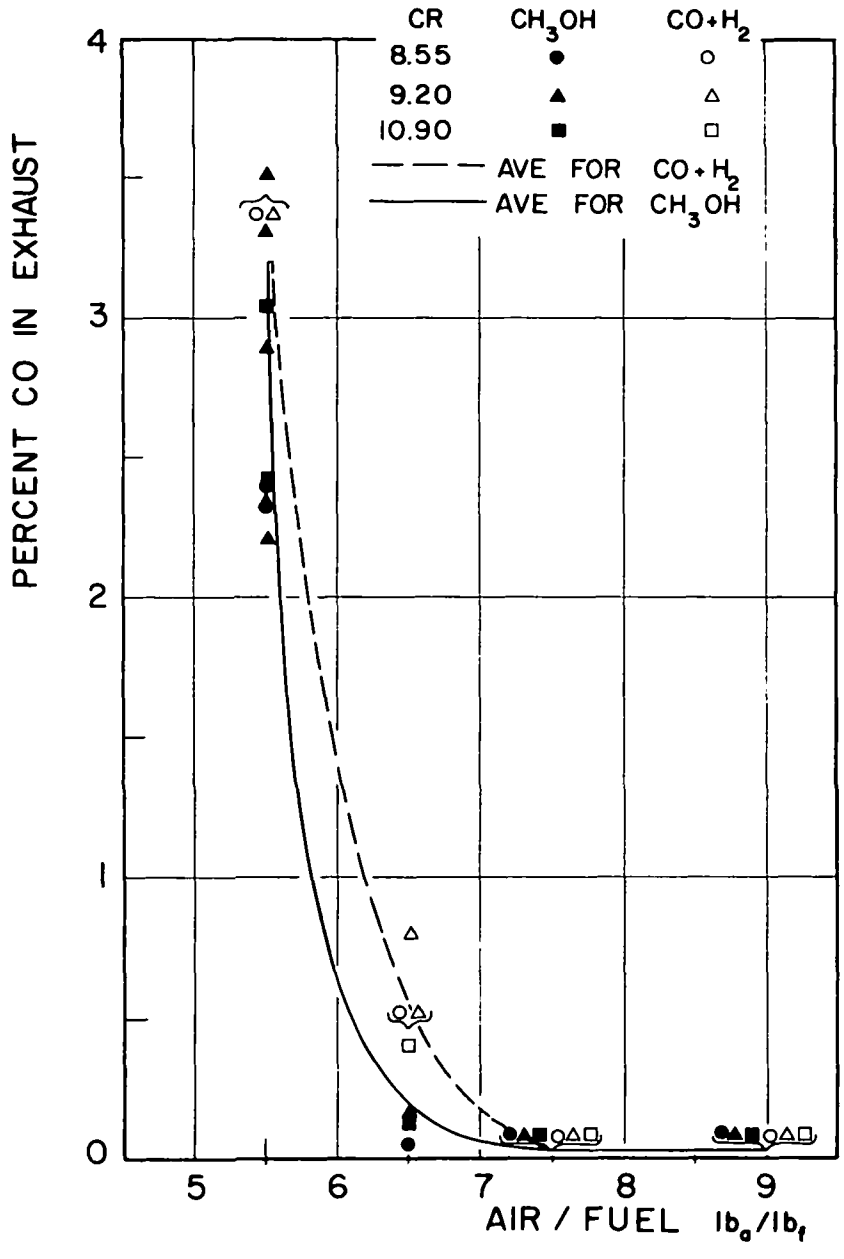

FIG. VII-8a: CARBON MONOXIDE EMISSIONS, %

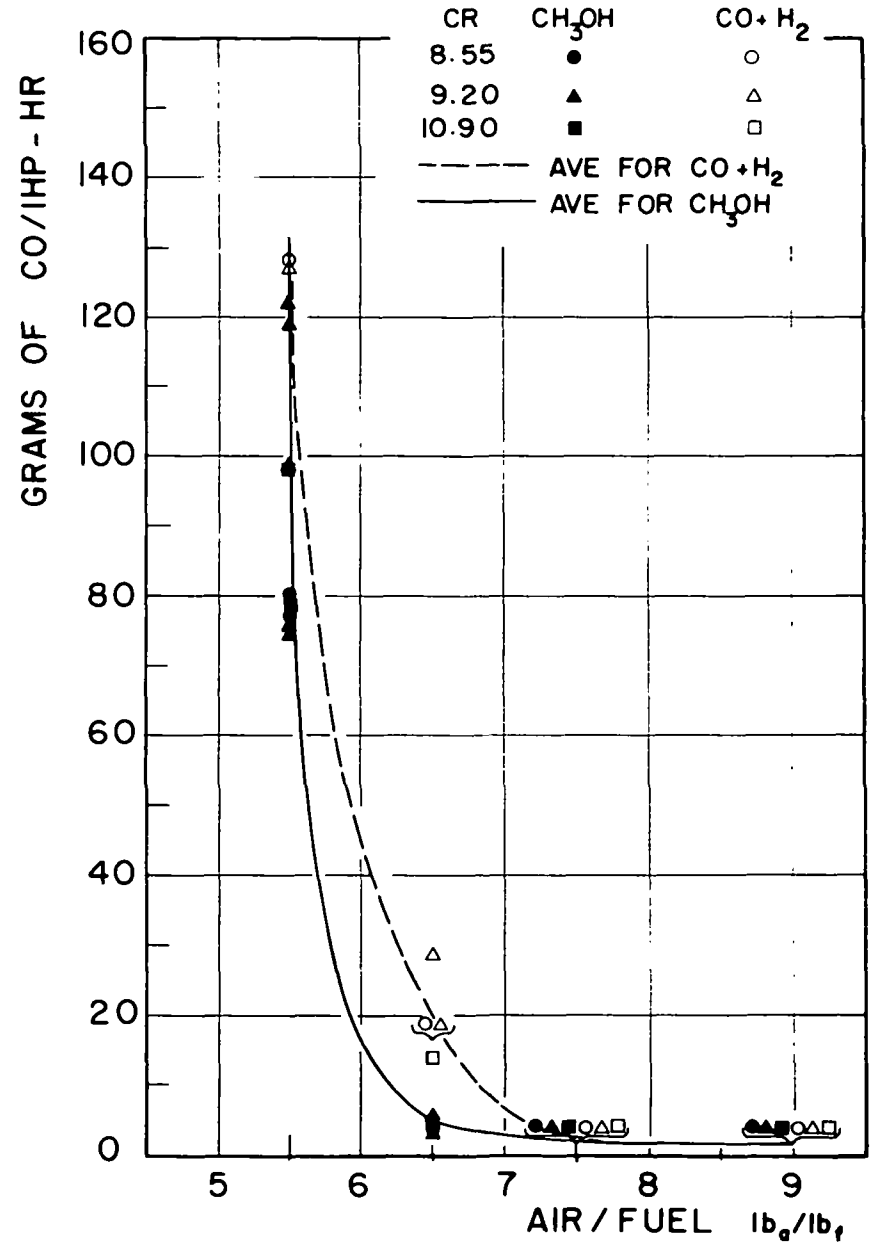

FIG. VII-8b: CARBON MONOXIDE EMISSIONS, GRAM/IHP-HR

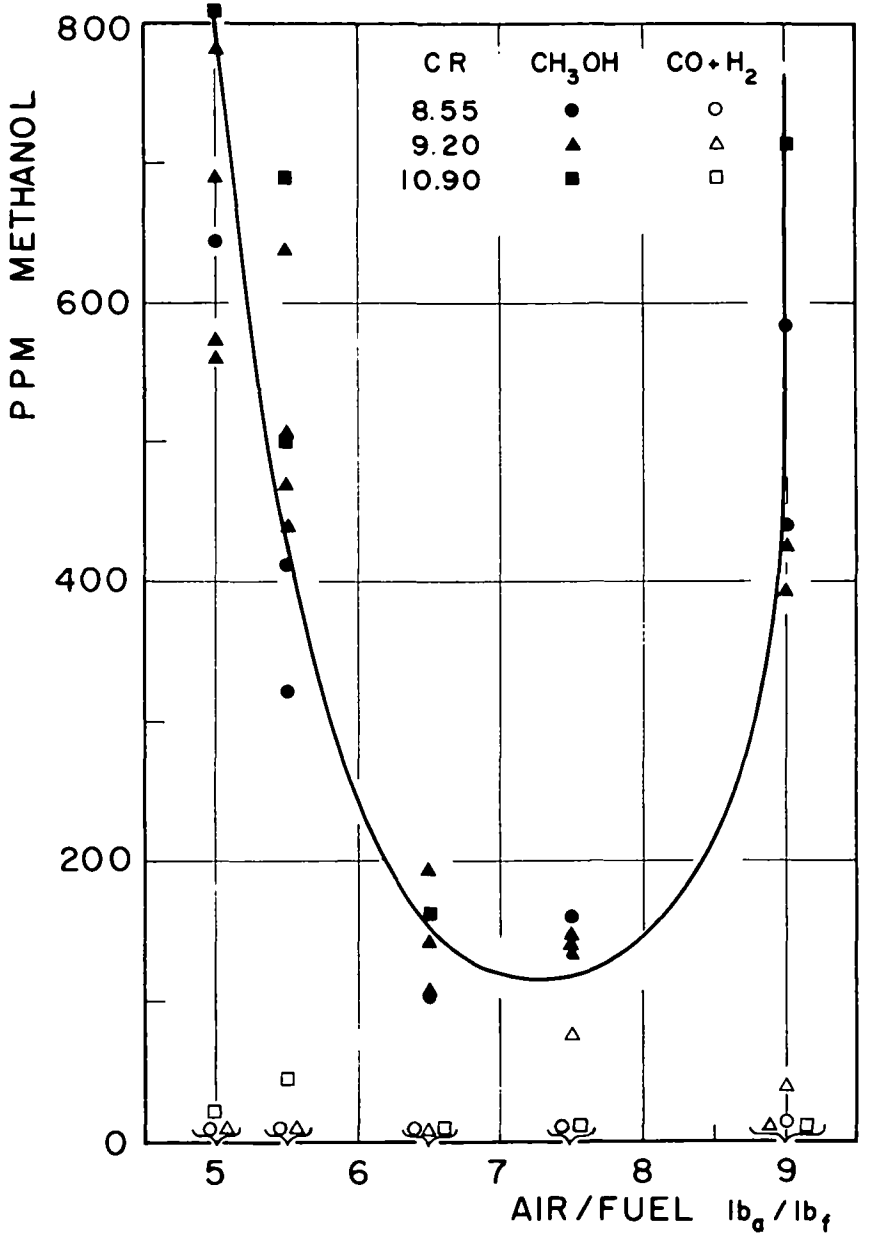

FIG. VII-9a: METHANOL EMISSIONS, PPM

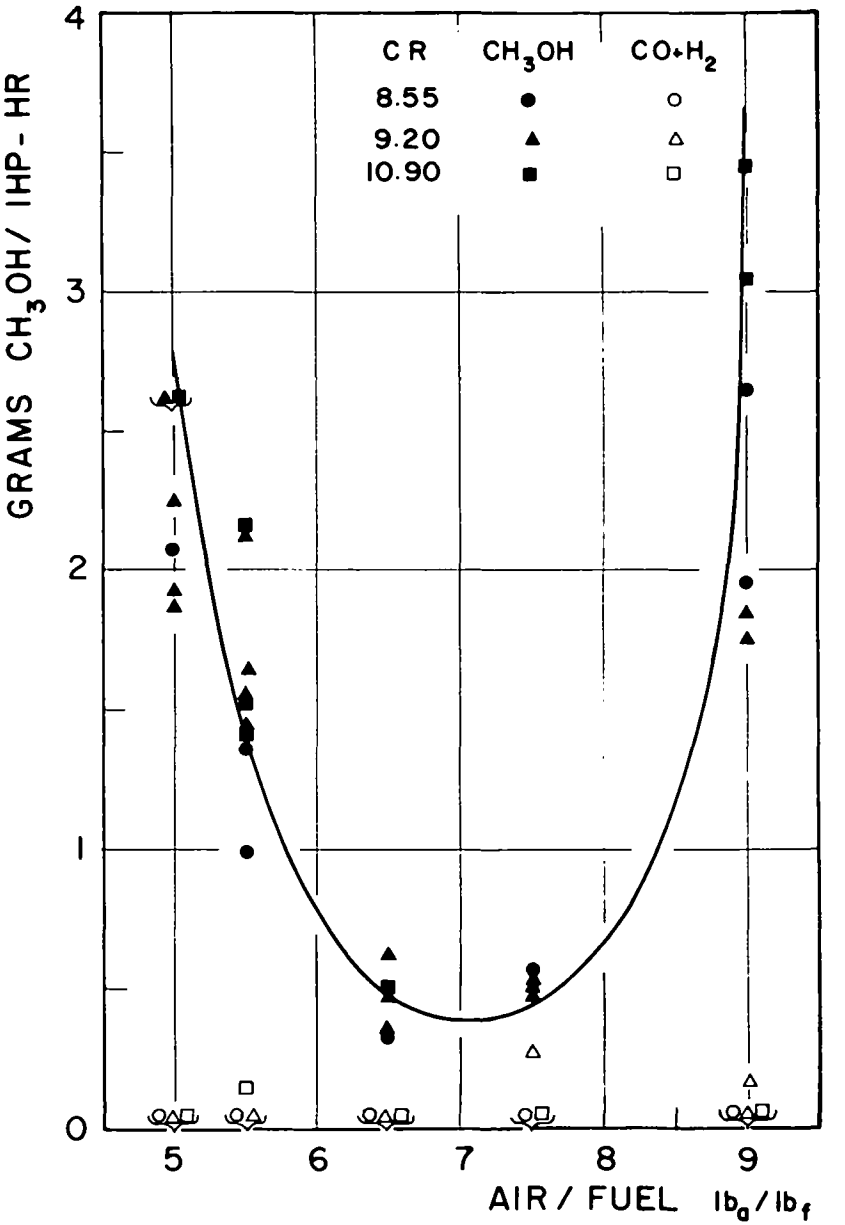

FIG. VII-9b: METHANOL EMISSIONS, GRAMS/IHP-HR

Significant concentrations of methane were found in the engine exhaust when it was operating at rich A/F ratios (see Fig. VII-10a,b). It was also noted that dissociated methanol produced a higher yield of CH_4 than the pure methanol in this region. The source of this methane is probably in part from recombination of the CO and H_2 according to the reaction:

$$CO + 3H_2 \rightarrow CH_4 + H_2O$$

This process was shown by Sabatier to proceed readily at temperatures above 200°C in the presence of iron [9]. A related reaction may also be the source of the ethane found in the exhaust. The relative absence of methane at higher A/F ratios probably results from the higher oxygen concentrations which enable oxidation of methane.

The total carbon exclusive of methanol in the hydrocarbon exhaust components given as microgram carbon/gram exhaust and as gram carbon/ihp-hr are shown in Fig. VII-11a, b. Hydrocarbons exclusive of methanol and methane were found only in small concentrations (compare Fig. VII-6 with Fig. VII-11a). With one exception, the maximum concentration for all these species was less than 40 ppm for all conditions (see Table I, Appendix B). As expected, these hydrocarbon concentrations were highest at low A/F ratios. As in the case of methane, the concentrations for dissociated fuel were generally higher than for liquid methanol. This would indicate that the H_2 and O_2 react more readily to form hydrocarbons than does methanol.

It was difficult to assess the exact effect of CR on the methanol, methane and other hydrocarbon emissions. Sometimes they appeared to increase then decrease with increasing compression ratio. For other conditions no appreciable changes were noted.

(3) Oxides of Nitrogen. Changes in A/F ratio and the per cent fuel dissociation were shown to have a pronounced effect on the level of NO_X emissions (see Fig. VII-12a). As with gasoline, liquid methanol was shown to exhibit a large NO_X peak near stoichiometric conditions. At fuel rich conditions there

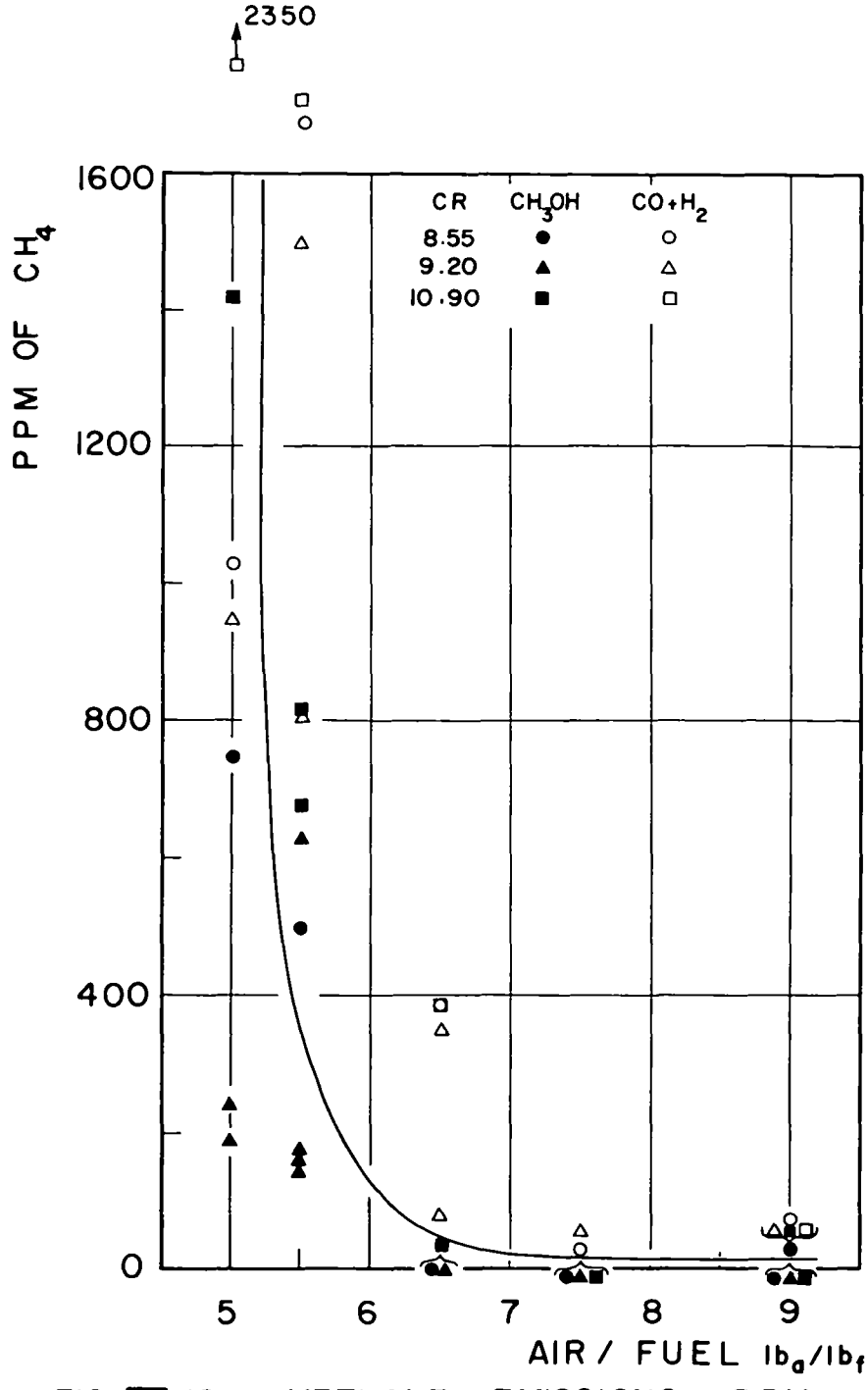

FIG. VII-10 a : METHANE EMISSIONS , PPM

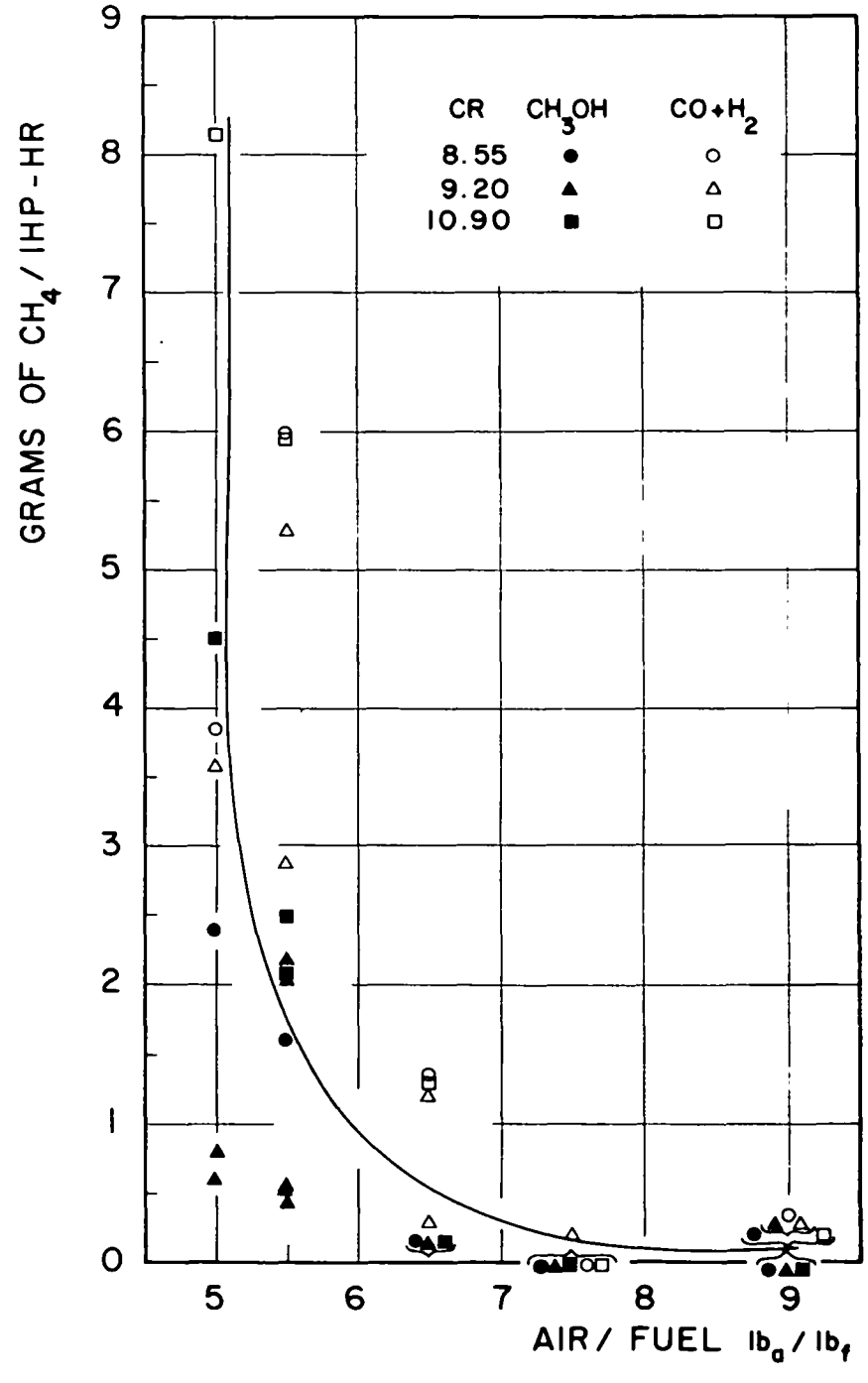

FIG. VII-10b : METHANE EMISSIONS, GRAMS/ IHP-HR

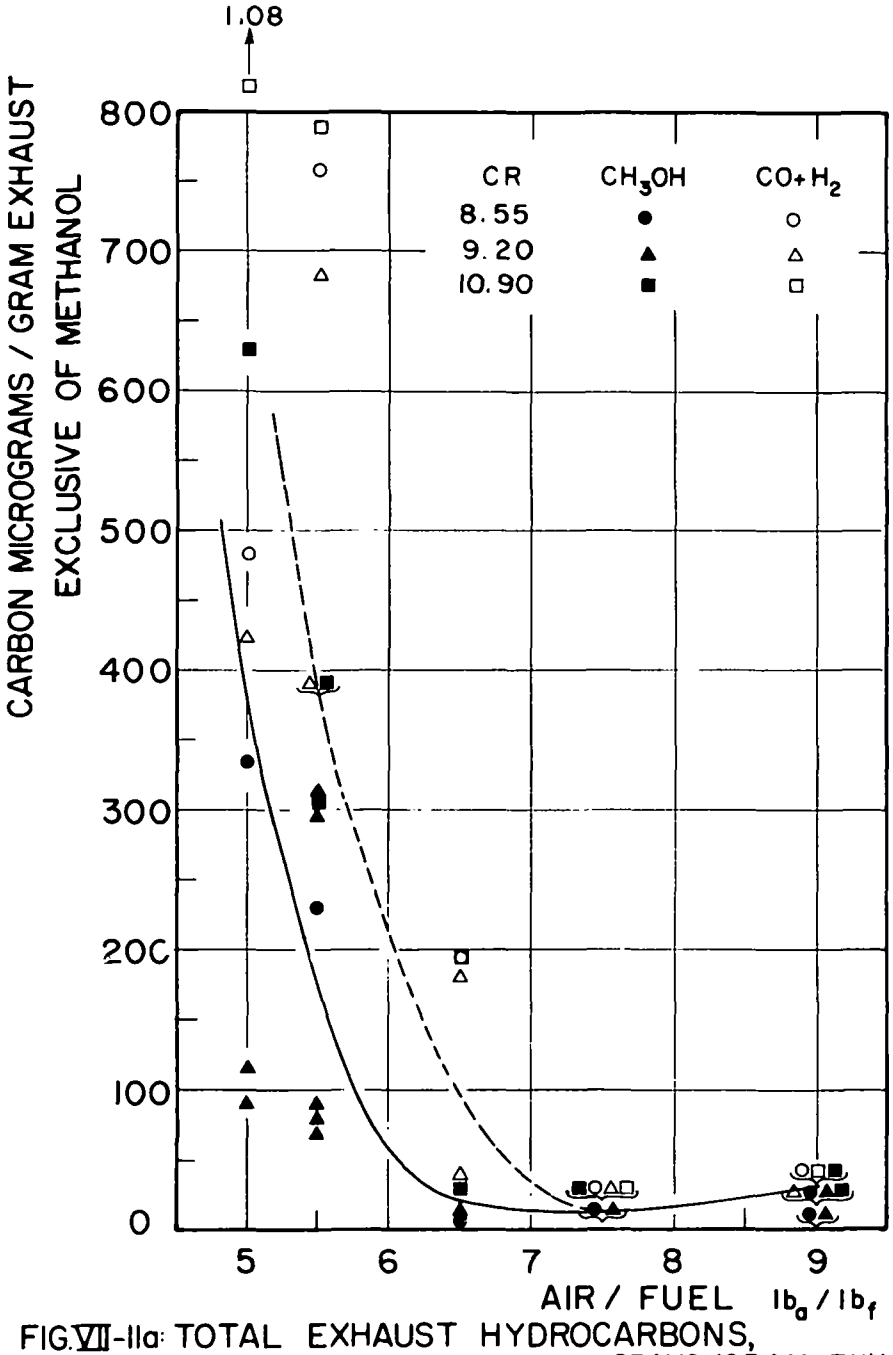

FIG. VII-11a: TOTAL EXHAUST HYDROCARBONS, MICROGRAMS/GRAM EXHAUST

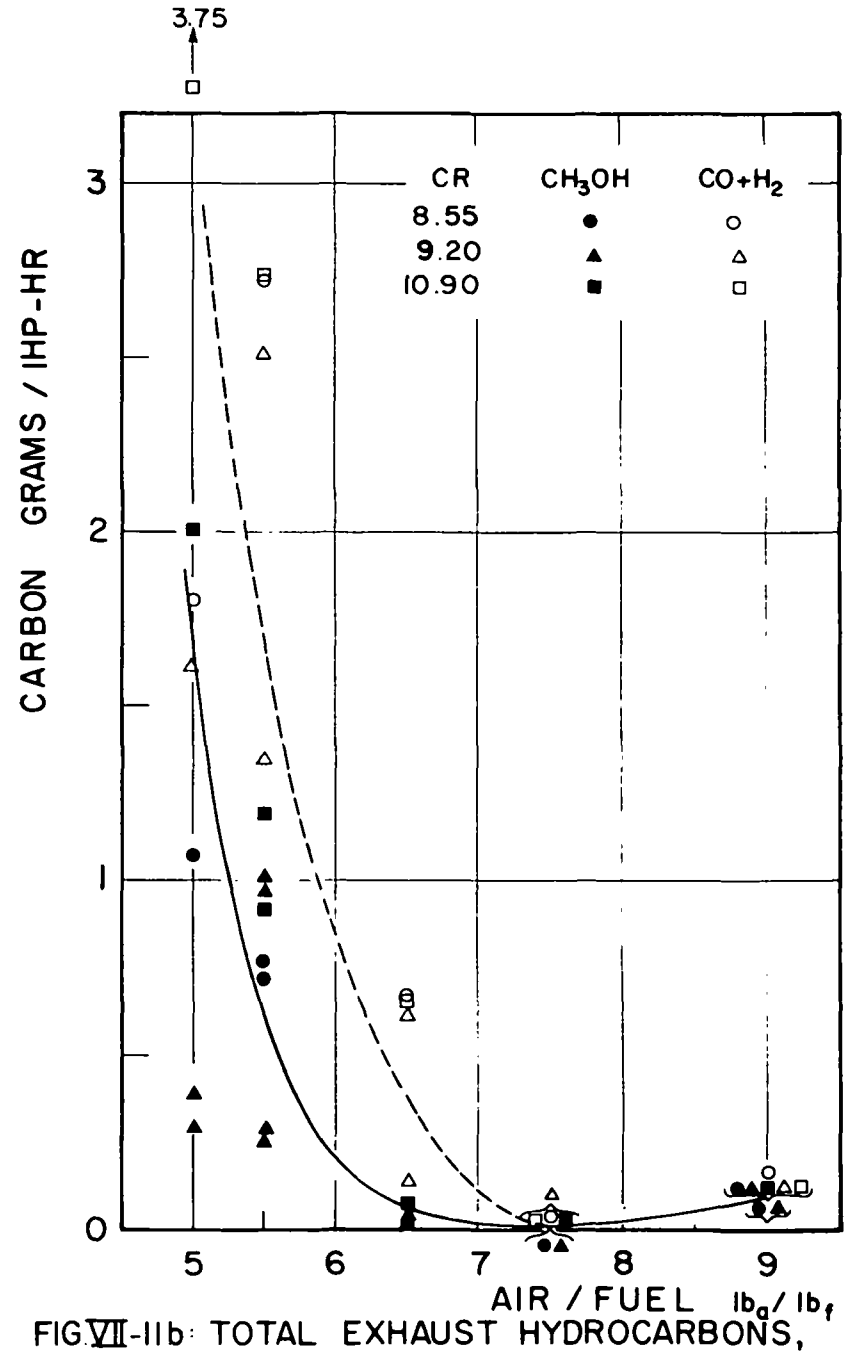

FIG. VII-11b: TOTAL EXHAUST HYDROCARBONS, GRAMS/IHP-HR

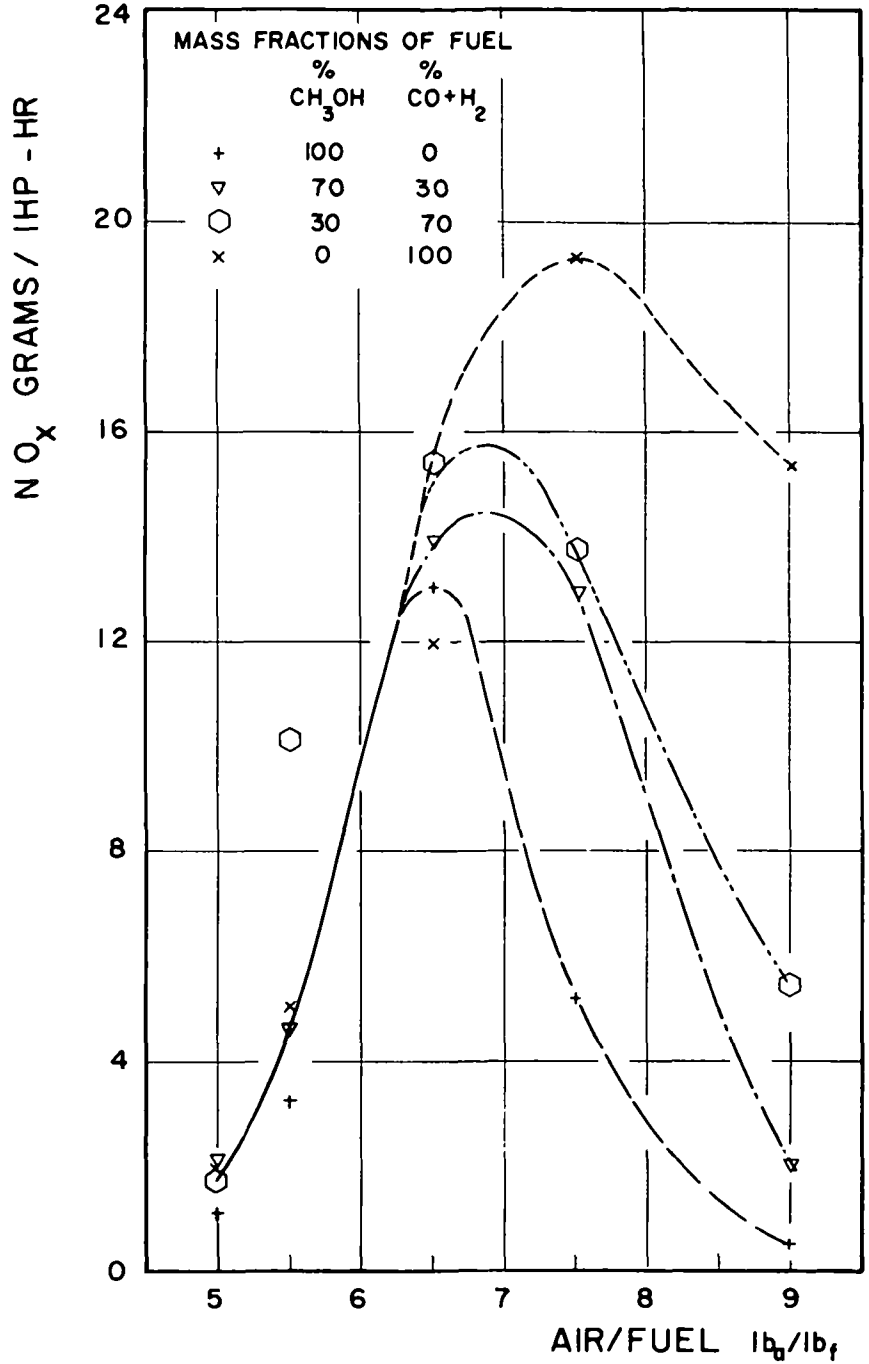

FIG. VII-12a: OXIDES OF NITROGEN EMISSIONS, GRAMS / IHP-HR

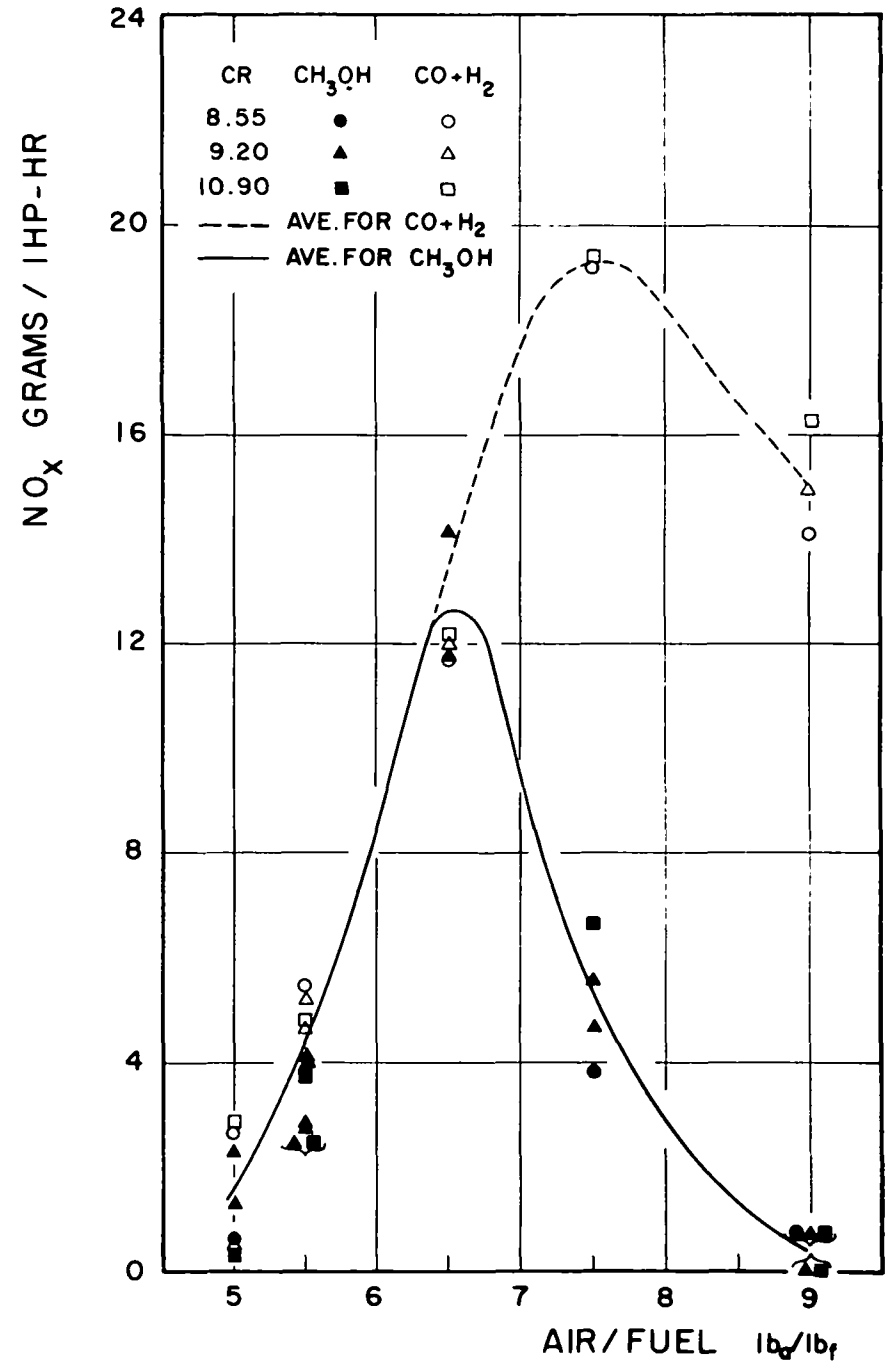

FIG. VII-12b: OXIDES OF NITROGEN EMISSIONS, GRAMS/IHP-HR

was little observable difference between the blends and liquid fuel. However, on the lean side there is a pronounced effect--100% dissociated methanol produced far more NO_X per unit of energy delivered than did pure methanol. Since the dissociated methanol has 20% more energy per pound of fuel, the rise in NO_X with dissociation in the lean A/F range is consistent with the expectation of higher cylinder temperature. Why this is not matched by a like gain in isfc requires further inquiry.

Compression ratio effects when contrasted with A/F and fuel dissociation effects on the NO_X emissions were not very significant, as shown in Fig. VII-12b.

(4) Aldehydes. The aldehyde emissions consisted almost exclusively of formaldehyde (HCHO) and acetaldehyde (CH_3CHO). Both were found to be appreciably affected by A/F ratio, per cent dissociation, CR and spark advance. Formaldehyde concentrations varied from a low of 3-4 ppm to a maximum of 170 ppm with the normal range of values being between 20 and 80 ppm. Acetaldehyde exhibited a much greater range of variation--from trace values to almost 500 ppm. The tabular data did not show any evident interdependency of the formaldehyde and acetaldehyde emissions. However, a clear relationship between the acetaldehyde and methanol emissions was sometimes seen. For some conditions when acetaldehyde emissions were high, methanol emissions were low, indicating that methanol emissions are reduced at the expense of increased aldehyde emissions. It should be emphasized that this relationship did not always hold and that under some conditions methanol and aldehyde emissions were both low.

The A/F ratio, compression ratio and spark advance were the principal variables which determined the level of aldehyde emissions. At low A/F (from 5.0 to 5.5) the total aldehyde emissions were low regardless of compression ratio or spark advance, the worst case being slightly greater than 100 ppm. At stoichiometric or higher A/F ratios, the compression ratio and spark advance significantly affected aldehyde emissions. Moderate to high spark advances (14-25°BTDC) were in general associated with increased aldehyde emissions, particularly at

high A/F and CR ratios. Although some large aldehyde emissions were noted at low spark advances (0-10°BTDC), they were on the average lower than for large spark advances and generally appeared in conjunction with significant decreases in the methanol and hydrocarbon emission levels. The increased emissions at high A/F ratios and spark advances are seen to be in agreement with aldehyde emission trends in gasoline [10]. The effect of CR on aldehyde emissions was not clear.

Fuel dissociation was found to promote aldehyde formation. The worst aldehyde emissions for pure methanol fuel was 205 ppm for test 57 (A/F = 7.5, CR = 10.5, spark advance = 20.0). Worst case emissions for 30, 70, and 100 per cent dissociated fuel were 455 ppm, 425 and 428, respectively. These emissions were also obtained at A/F = 7.5 and CR = 10.5.

Because of data scatter and lack of emission data at some test conditions it was difficult by graphical methods to assess the exact effect of various engine variables on formaldehyde and acetaldehyde emissions. Figure VII-13 presents formaldehyde emission data for maximum power spark advance for various CR and per cent dissociation as a function of A/F ratio. The only clear trends are an apparent reduction of emissions for the dissociated fuel and a tendency of increased data scatter for liquid methanol emissions at increasing A/F ratios. Also, the average formaldehyde emissions for dissociated fuel appear to be higher than for the liquid fuel at low A/F, while just the opposite is seen to be the case at high A/F ratios. Selected acetaldehyde emission data are shown in Fig. VII-14, as a function of spark advance and compression ratio. For 30 per cent dissociation at compression ratios of 8.4 and 10.9, the acetaldehyde emissions are seen to be significantly affected only at an A/F ratio of 7.5. For A/F = 7.5, the aldehydes increase rapidly with increased spark advance. At other A/F ratios, the effects of spark advance appears minimal. In Fig. VII-14 no clear trend is seen with compression ratio except that the variation with compression rates is highly dependent upon A/F ratio.

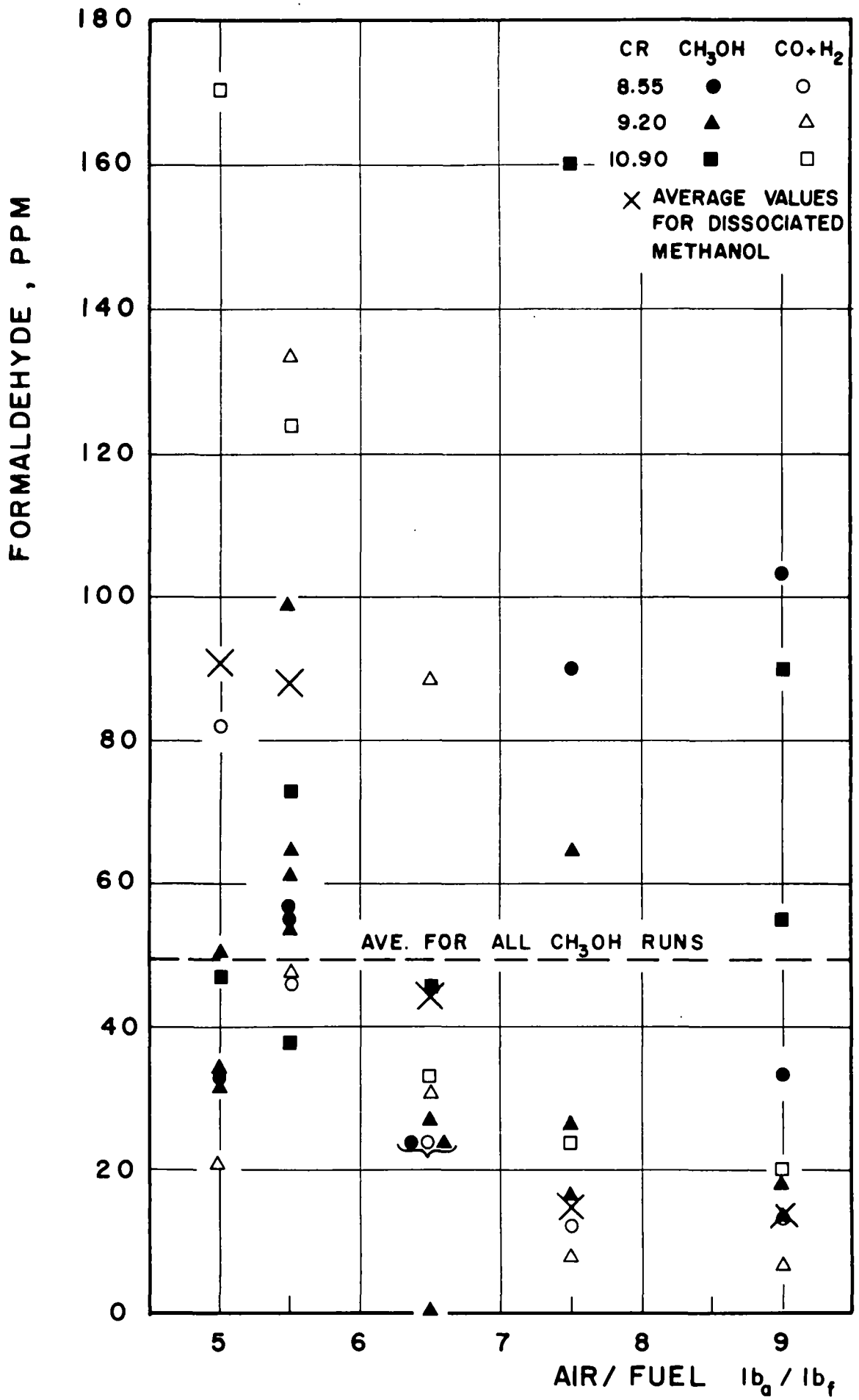

FIG. VIII-13: FORMALDEHYDE EMISSIONS

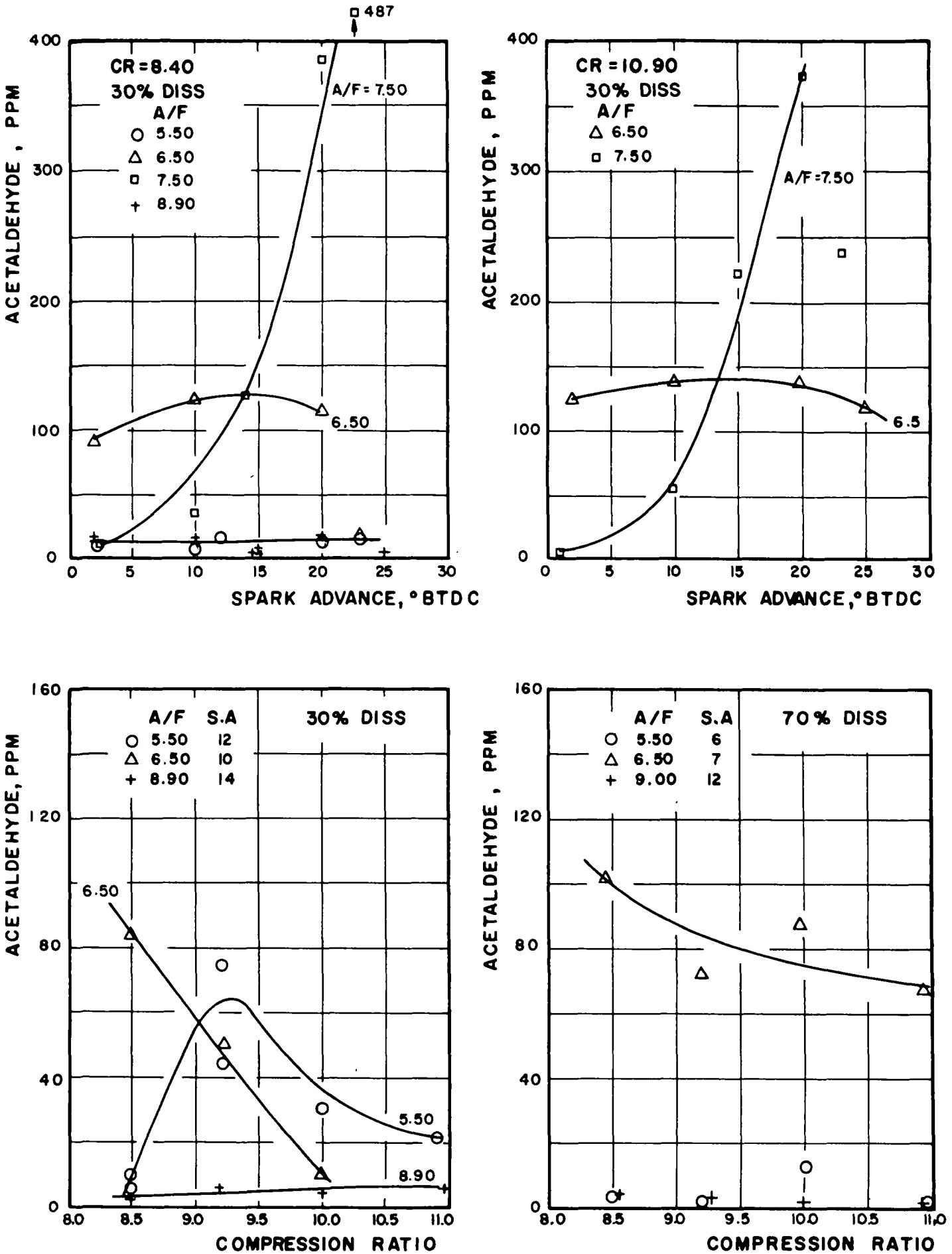

FIG. VII-14: ACETALDEHYDE DATA

(5) Oxygen and Carbon Dioxide. The values of O_2 and CO_2 in the exhaust vary with A/F ratio, as expected, and are similar to those observed for gasoline when stoichiometric mixture is used as a reference point (see Figs. VII-15 and VII-16). It is of some interest to note that in the lean mixture region the dissociated methanol shows a more complete combustion capability in that there is more CO_2 and less O_2 present. This is probably a partial explanation for the relatively higher NO_X values observed previously to be produced by the dissociated methanol in this region.

D. Comparative Gasoline and Methanol Emissions:

Only tentative comparison of gasoline and methanol emissions can be made because of the limited gasoline emission data acquired during the test program. Also, the GC emission data for gasoline were not broken down into individual species but were reported as grams carbon per grams of exhaust. Thus, the relative portions of aldehydes and hydrocarbons in the methanol and gasoline CFR engine tests cannot be compared.

Gasoline and methanol emission data at stoichiometric A/F ratios and at otherwise comparable test conditions are presented in Table VII-3. The CO and total grams carbon per ihp-hr are seen to be in general almost an order of magnitude higher for gasoline than for methanol. The NO_X data are seen to be approximately equivalent. Comparative CO and NO_X data for gasoline and methanol at other than stoichiometric conditions are shown in Fig. VII-17, plotted against the inverse of the fuel equivalence ratio (actual A/F per stoichiometric A/F). This data indicates that the methanol NO_X emissions for liquid methanol are less than those for gasoline for all ϕ, while the fully dissociated methanol NO_X are higher than gasoline NO_X for lean A/F ratios. The methanol CO emissions for both liquid and dissociated fuel are reduced to trace values at much lower equivalence ratios than the gasoline CO emissions. This latter factor seems to indicate a higher combustion efficiency at equal equivalence ratios than gasoline.

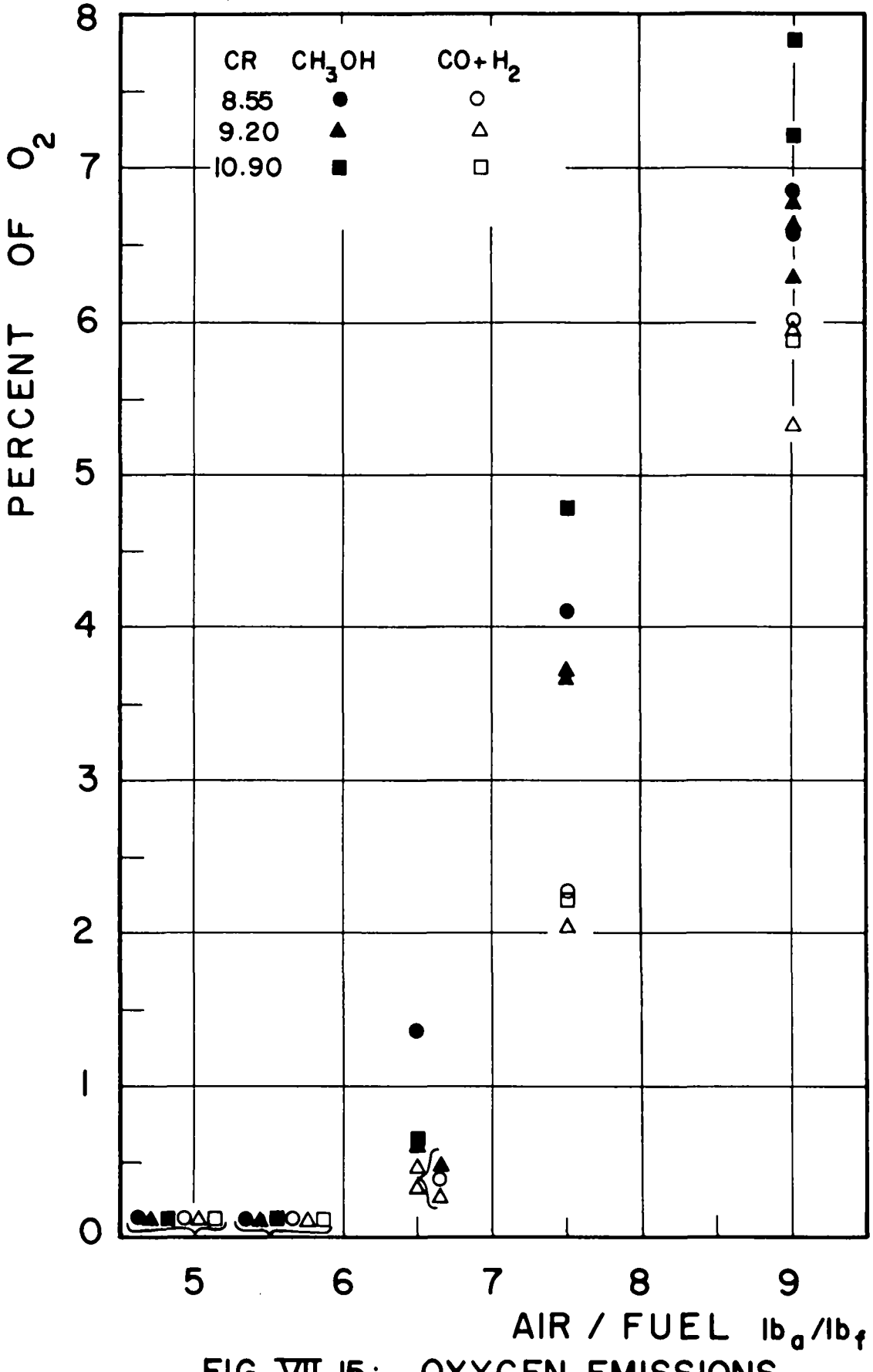

FIG. VII-15: OXYGEN EMISSIONS

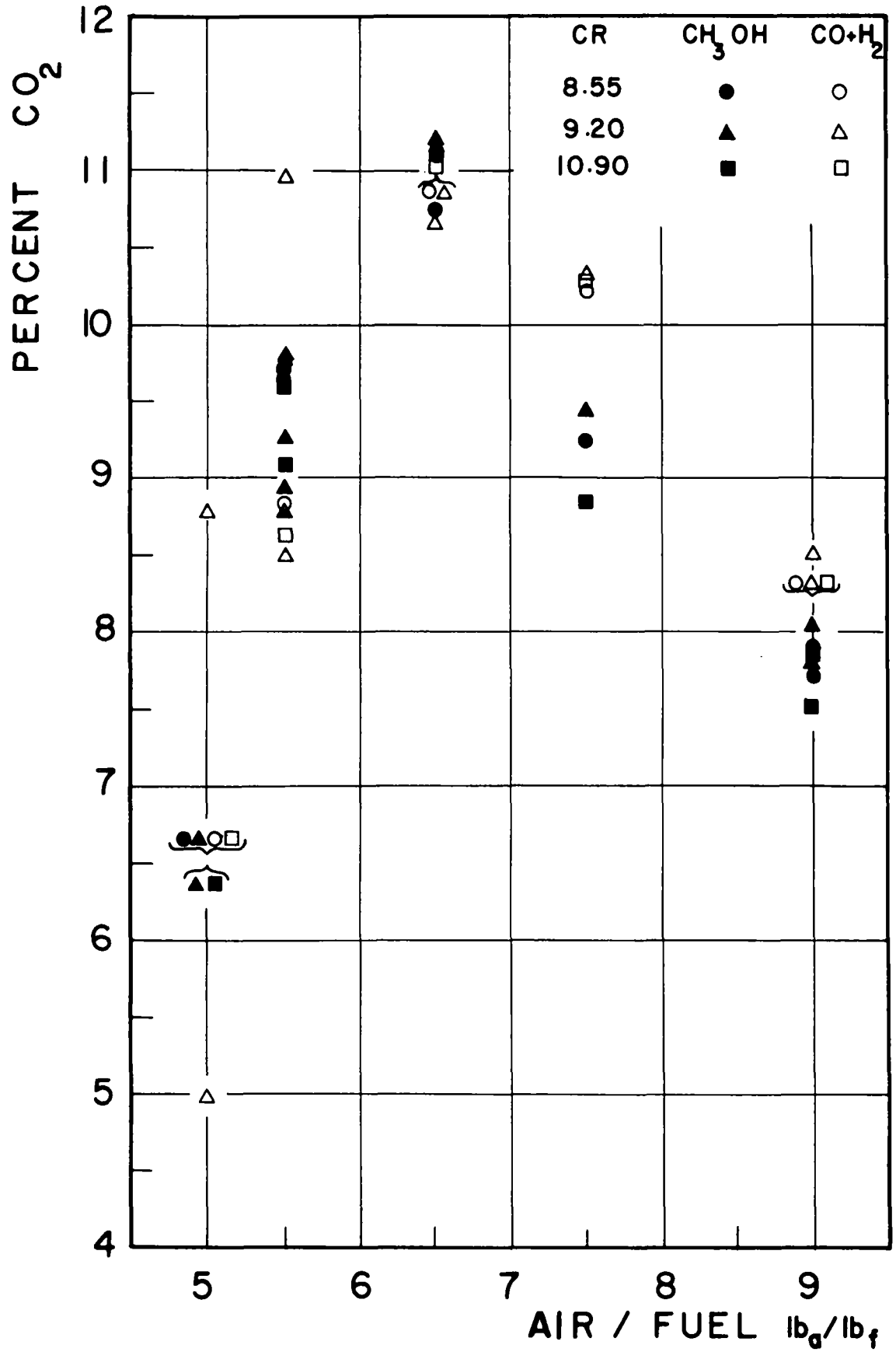

FIG. VII-16 CARBON DIOXIDE EMISSIONS

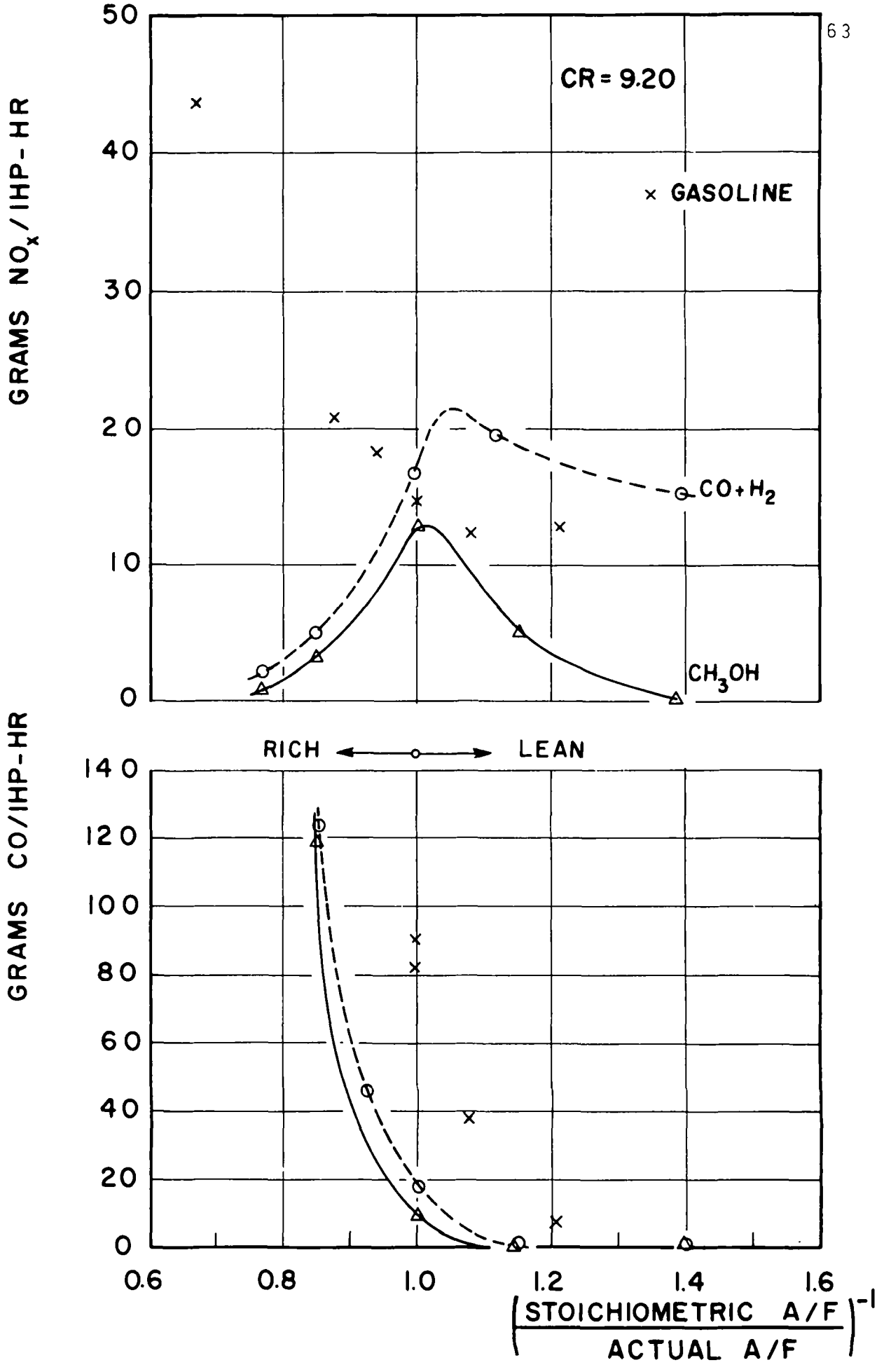

FIG. VII-17: COMPARATIVE METHANOL AND GASOLINE EMISSIONS

TABLE VII-3

Run	% Diss	A/F	ϕ*	CR	SA	In Tem °F	ihp	isfc (lb/hp-hr)	CO (%)	NO_X (%)	Total Exhaust Carbon (gm/ihp-hr)
Gasoline:											
185	NA	14.9	1.01	9.2	18	86	3.90	.461	2.51	.306	3.32
188	NA	14.0	1.07	9.2	18	56	3.90	.492	--	.527	3.74
191	NA	14.9	1.01	9.2	18	88	3.90	.461	2.76	.427	--
Methanol:											
7	0	6.5	1.00	9.2	14	70	3.65	.98	0.08	0.391	.213
13	0	6.5	1.00	9.2	14	73	3.79	.97	0.17	0.372	.316
22	30	6.5	1.00	9.2	14	70	3.58	.99	0.08	0.471	--
24	30	6.5	1.00	9.2	14	70	3.58	.99	0.12	.390	.198
120	30	6.5	1.00	9.2	10	110	3.36	0.99	0.08	0.302	.500
32	70	6.4	0.99	9.2	9	70	3.45	1.02	0.53	ND	.356
123	70	6.5	1.00	9.2	7	110	3.22	1.00	0.17	0.395	.460
158	100	6.5	1.00	9.2	6	110	3.15	1.01	0.48	0.320	.617

*ϕ - equivalence ratio

A rough comparison of these emissions with federal and California state standards is possible if the assumption is made that the basis for generating these standards is equivalent to steady-state operation of a vehicle at 50 mph while developing 50 ihp. With this assumption, the emissions in gm/ihp-hr can be converted to gm/mile on a one to one basis. Then, from Fig. VII-17, it is seen that at an equivalence ratio of 1.0 the CFR engine CO emissions for gasoline (82 gm/mile) are about twice the 1972 federal standard of 39 gm/mile. At the same equivalence ratio the methanol CO emissions are less than half the 1972 federal standard. For NO_X, both the gasoline and methanol are seen to exceed by a considerable amount the tentative range for the 1975 federal standards of 0.3 to 0.4 gm/mile. The total carbon in the gasoline exhaust at stoichiometric A/F ratio, as given in Table VII-3, includes hydrocarbons and aldehydes. Hence, the CFR engine hydrocarbon emissions are seen to be less than the 1972 federal standard of 3.4 gm/mile.

This is as expected considering that the federal standard is based upon a cycle average while the CFR engine data are for steady-state operation at stoichiometric A/F ratio. In comparison, the total methanol carbon emissions including hydrocarbon, methanol and aldehydes are significantly less than the 1972 federal standards. These limited data indicate that the methanol fuel at stoichiometric and leaner A/F ratios has inherently less CO and hydrocarbons in the exhaust than gasoline.

VIII. DECOMPOSITION FUELED ENGINE DESIGN

The following section presents preliminary studies of possible methanol decomposition methods, the related engine control, and exhaust energy requirements needed for automotive engine operation on partially or fully decomposed methanol fuel.

A. Engine Energy Analysis:

It is proposed that methanol decomposition for engine consumption utilizes engine exhaust energy for fuel preheating, vaporizing, superheating and decomposing. At atmospheric pressure approximately 2438 BTU are required to heat one pound of liquid methanol from 68°F to 554°F (405° superheat) and decompose it to CO and H_2. The decomposition energy (1720 BTU/lb) is 70.7% of this heat requirement (see Table VIII.1).

Total exhaust energy recycle requirements are defined by the fuel consumption and desired percentage of methanol decomposition at given engine operating conditions. An estimate of total recycle heat requirements for various operating conditions may be obtained by examining methanol fuel consumption over a range of engine loads and speeds. Comparative engine performance characteristics at one-third full load for gasoline and methanol fueled engines were calculated using gasoline engine performance mappings [11] and assuming that the methanol isfc was twice that of gasoline (see Fig. VIII-1). The relative gasoline to methanol isfc value was obtained from tests on the CFR engine. Methanol consumption for these speed and load conditions is presented in Fig. VIII-2, along with energy rate requirements for 30 per cent methanol decomposition. Energy rate requirements for other decomposition percentages would be proportional.

The significance of these heat requirements is clarified by comparing them with the available exhaust energy. The available exhaust energy is a function of engine load, fuel consumption, speed and other variables and cannot be rigorously predicted by analytical methods alone. However, an estimate of

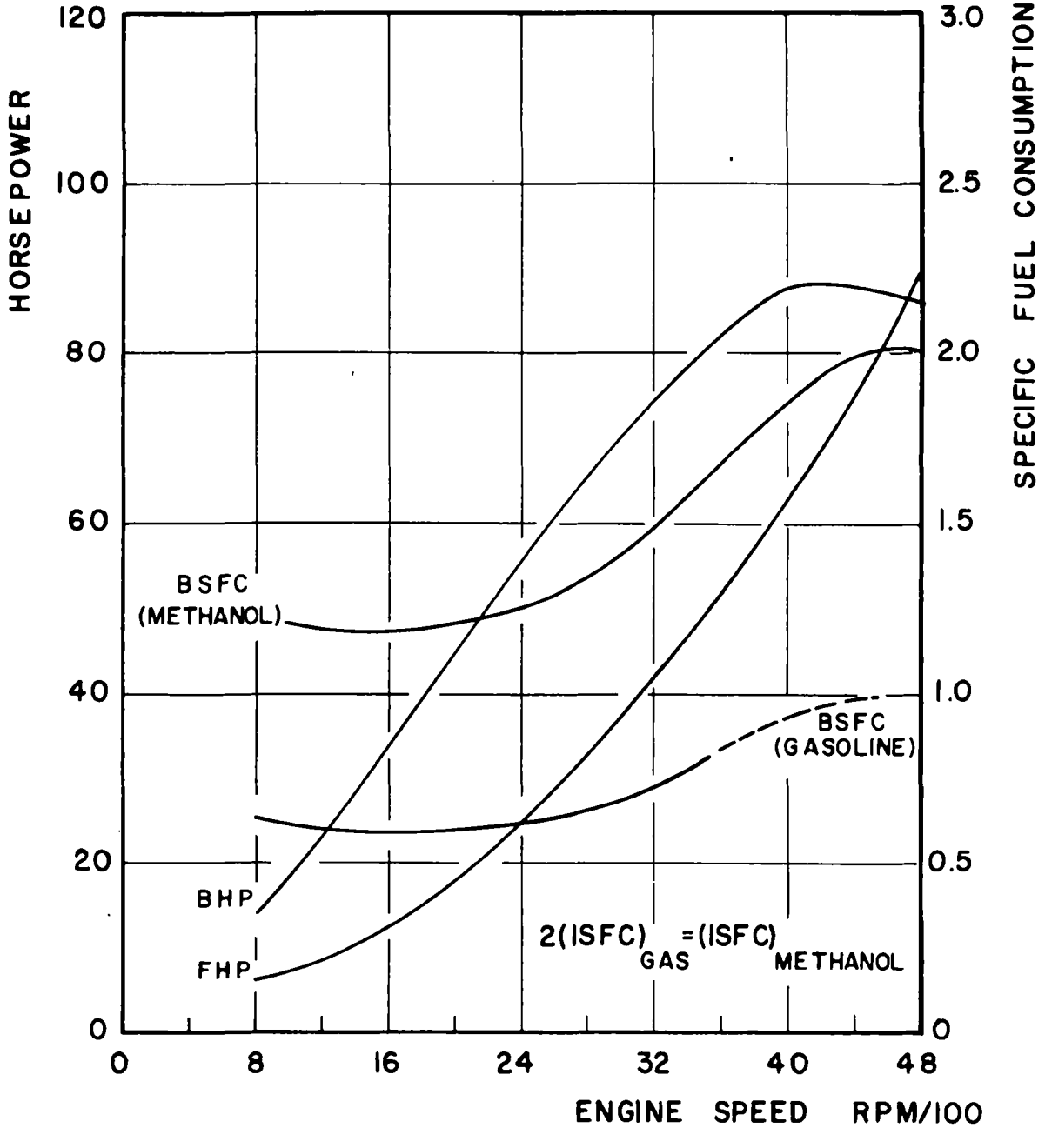

FIG. VIII-1: ENGINE PERFORMANCE CHARACTERISTICS
1/3 FULL LOAD

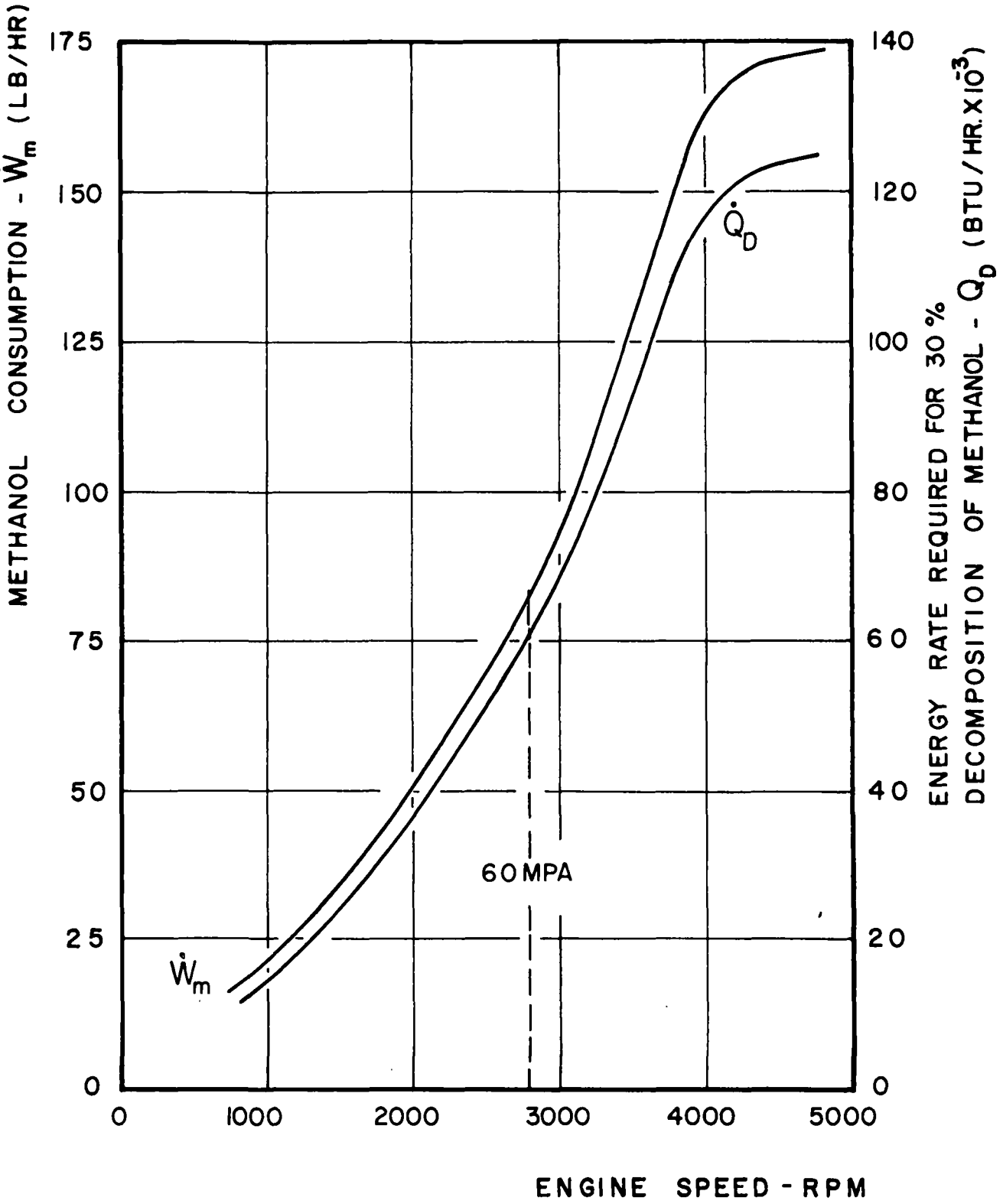

FIG. VIII - 2 : METHANOL FUEL CONSUMPTION AND DECOMPOSITION ENERGY RATE AS A FUNCTION OF ENGINE SPEED

TABLE VIII-1

	Energy Requirement (BTU/lb)	Per cent of total
Preheating 68° to 148°F	48	1.9
Vaporization 1480 @ 1 atm	482	19.7
Superheating 148° to 554°F	188	7.7
Decomposition	1720	70.7
Total:	2438	

the required percentage of exhaust energy as a function of decomposition can be made by using published engine data to establish base line conditions and by assuming that the exhaust energy will vary with engine performance in accordance with simple analytical expressions. Using this approach a computer program was written and results were obtained for a limited range of engine operating conditions. Assumptions and method of calculation used in this computer program are discussed in Appendix C. Basic variables were RPM, per cent dissociation, inlet temperature and isfc. The A/F ratio was held constant at 6.5:1. An energy and mass flow diagram showing the counterflow heat exchange cycle used in the program is shown in Fig. VIII-3. For this cycle, the decomposed and undecomposed energy circuits are separated. Calculations indicate that at normal conditions sufficient exhaust energy is available to decompose 30 and 100% of the methanol (see Figs. VIII-4 and VIII-5). This data indicates that the exhaust contains sufficient energy to perform its decomposition and vaporization fuctions; however,

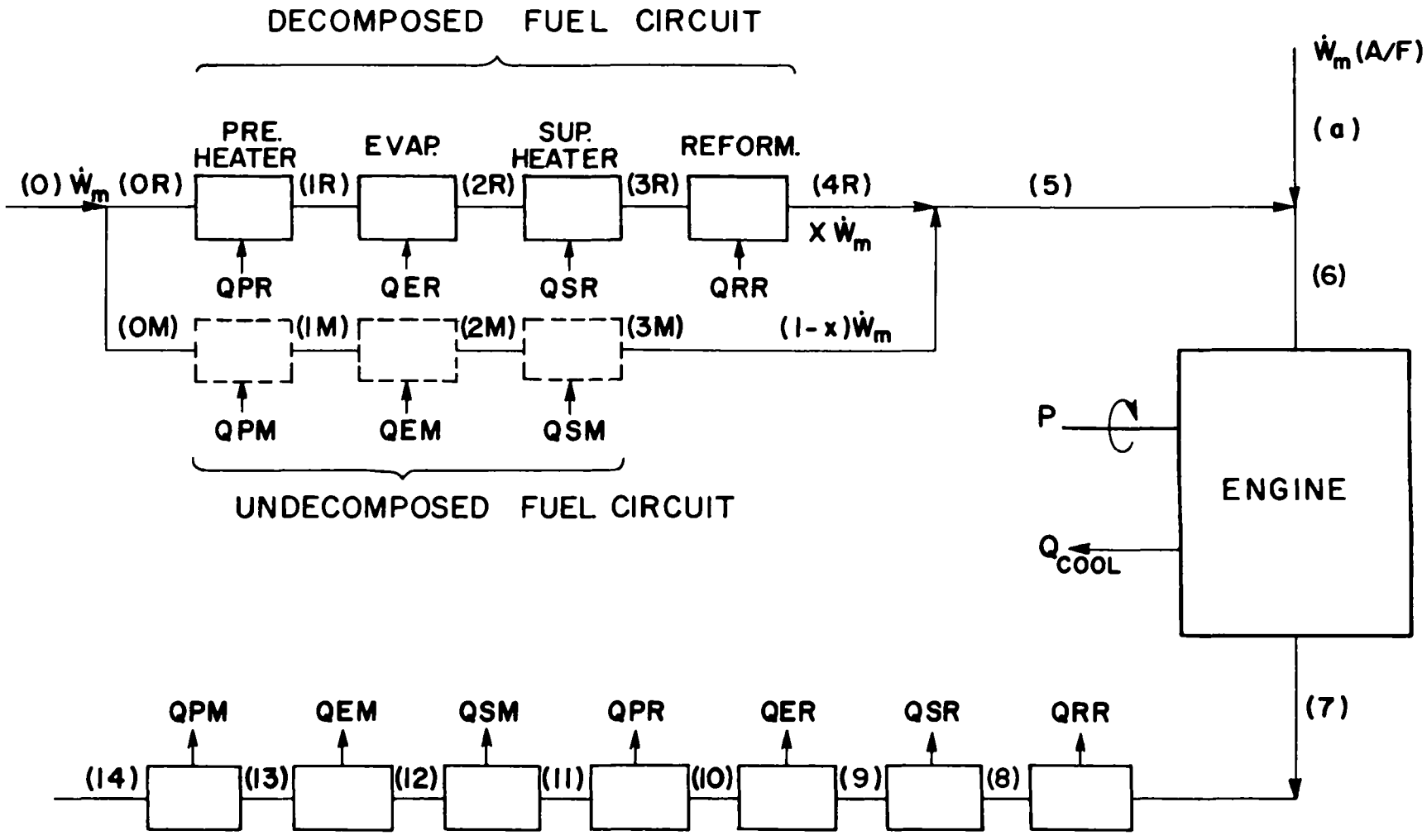

FIG. VIII-3 : ENGINE ENERGY SCHEMATIC

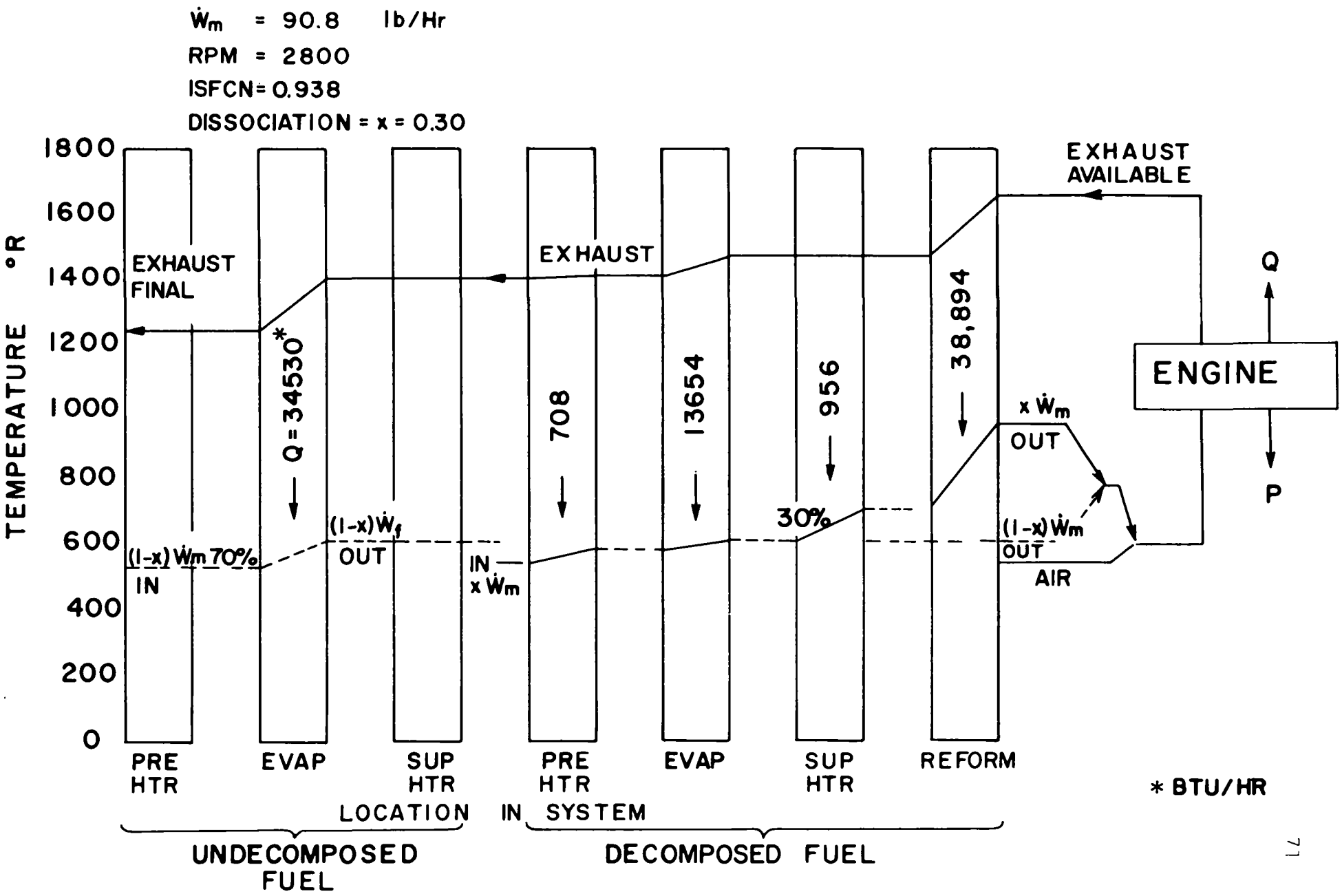

FIG. VIII-4: TYPICAL TEMPERATURE PROFILE 30 % DISSOCIATION

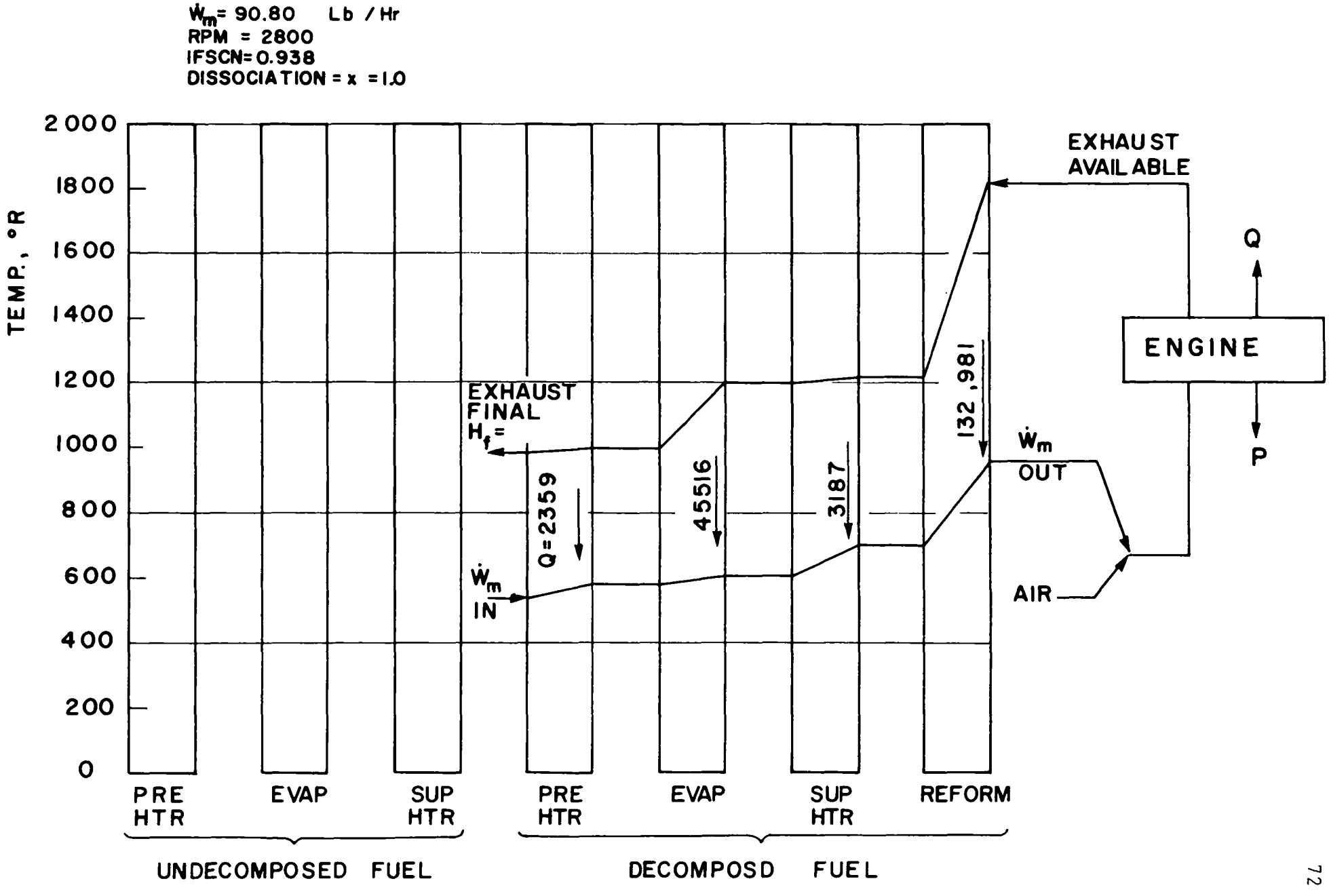

FIG. VIII-5: TYPICAL TEMPERATURE PROFILE 100% DISSOCIATION

at 100 per cent decomposition, the exit temperature difference between the exhaust and decomposition streams drops to 400°F. This low temperature difference would require large heat exchange elements.

B. Decomposition Chamber Design Analysis:

(1) Design Considerations. Catalytic decomposition is essentially an empirical art. However, a decomposition chamber design analysis with data from the literature will provide information on the probable size, performance, operating characteristics and problem areas.

A survey was conducted of catalytic decomposition and synthesis. Performance data was found for synthesis of methanol with currently used catalysts. In addition, decomposition data was acquired in the open literature from basic research for a number of catalysts tested over a limited range of variables [12, 13].

Methanol is synthesized or decomposed according to the reaction:

$$CH_3OH \underset{\text{synthesis}}{\overset{\text{decomposition}}{\rightleftharpoons}} CO + 2H_2$$

Decomposition is endothermic with an energy requirement of 1720 BTU/lb. Other reactions involving decomposition to formaldehyde, methylformate, methane, H_2, and O_2 are also possible but low in probability and are not of major consequence. Catalysts for methanol decomposition and synthesis contain ZnO, CuO, Al_2O_3, or Cr_2O_3, as the primary constituents [12,13,14,15,16]. The exact composition for commercial catalysts is proprietary. A catalyst used for synthesis may also be used for decomposition, although one optimized for synthesis will not necessarily be optimized for decomposition. With a given catalyst the optimum reaction (decomposition or synthesis) is determined primarily by the catalytic bed pressure. High

pressures (1000 to 5000 psia) promote synthesis while low pressures favor decomposition.

Methanol catalysts are generally made up into small porous pellets and are packed into a catalytic bed into which the gaseous feed stock is introduced. Because of their porosity the catalytic pellets have low thermal conductivity and compressive strength. Their effective surface to volume ratio is high and their heat capacity is low.

Prior to initial use, methanol catalysts are generally in an oxidized state for ease of handling. After installation in the catalyst bed they are reduced by heating in a hydrogen atmosphere. In the reduced state, although not pyrophoric, they react readily with oxygen. Since oxygen reduces the catalytic effectiveness, air must be excluded from the decomposition chamber. A partially oxidized catalyst can be regenerated by reduction. Sulfur and chlorides are permanent poisons and should be excluded from the methanol feed stock.

Severe pressure and temperature cycling during continuous methanol synthesis can reduce catalyst effectiveness after 30 days by about 10 per cent [14]. A similar degradation might be expected for continuous decomposition cycling. The effects of cyclic on-off operation of the type expected in an automotive engine decomposition chamber have not been assessed. It has been reported that condensation of methanol in the catalyst bed should be avoided since reheating and vaporization of saturated pellets will destroy some types of pellets. However, this can probably be avoided by reducing thermal shock through gradual heating of the bed and by use of a low initial feed of superheated methanol during start up.

The rate of decomposition or synthesis in a given catalyst bed is determined by the space velocity, the pressure and the temperature. Optimum temperatures, which are pressure dependent, range from approximately 450 to 750°F [12,14]. The rate of synthesis increases with pressure with a higher yield at

pressures of 2000 psig and above. Figure VIII-6a illustrates the effect of pressure and temperature on methanol synthesis and Fig. VIII-6b shows the variation of decomposition with temperature. Although no data was found on the effect of pressure on decomposition, it is believed that pressures of one atmosphere or less are best for decomposition. This is concluded from the facts that all reported data on decomposition were at one atmosphere and the synthesis rates show an increase with pressure.

The catalyst bed space velocity is defined as the ratio of the gaseous feed stock volumetric flow rate at standard conditions to the effective catalyst volume. The space velocity is an empirical sizing parameter which defines the relative volume of catalyst to react a given volumetric flow rate. Data for the Catalysts and Chemicals, Inc. (CCI) C-79 catalyst (CuO, ZnO, Al_2O_3) indicates that methanol yields at a given temperature and pressure increases linearly for space velocities between 10,000 and 40,000 hr^{-1} (see Fig. VIII-7). No decomposition data showing the effects of space velocity on percentage decomposition was found. From data for a zinc-copper-chromium oxide catalyst at a space velocity of 25 hr^{-1}, it is estimated that decomposition percentages above 90 per cent can be expected (see Fig. VIII-6b). As will become evident later, the space velocities of interest here are of the order of 10^3 hr^{-1}. While it is not rigorous to assume that decomposition percentages will increase linearly in an inverse manner when compared with the synthesis yield, it seems reasonable to assume, based on Fig. VIII-7, that the decomposition space velocity can be increased over a considerable range without a drastic reduction in decomposition percentages. However, it is not possible to predict with confidence from the data available if the dissociation yield for the desired space velocity will be satisfactory. This question can only be determined by further exploration.

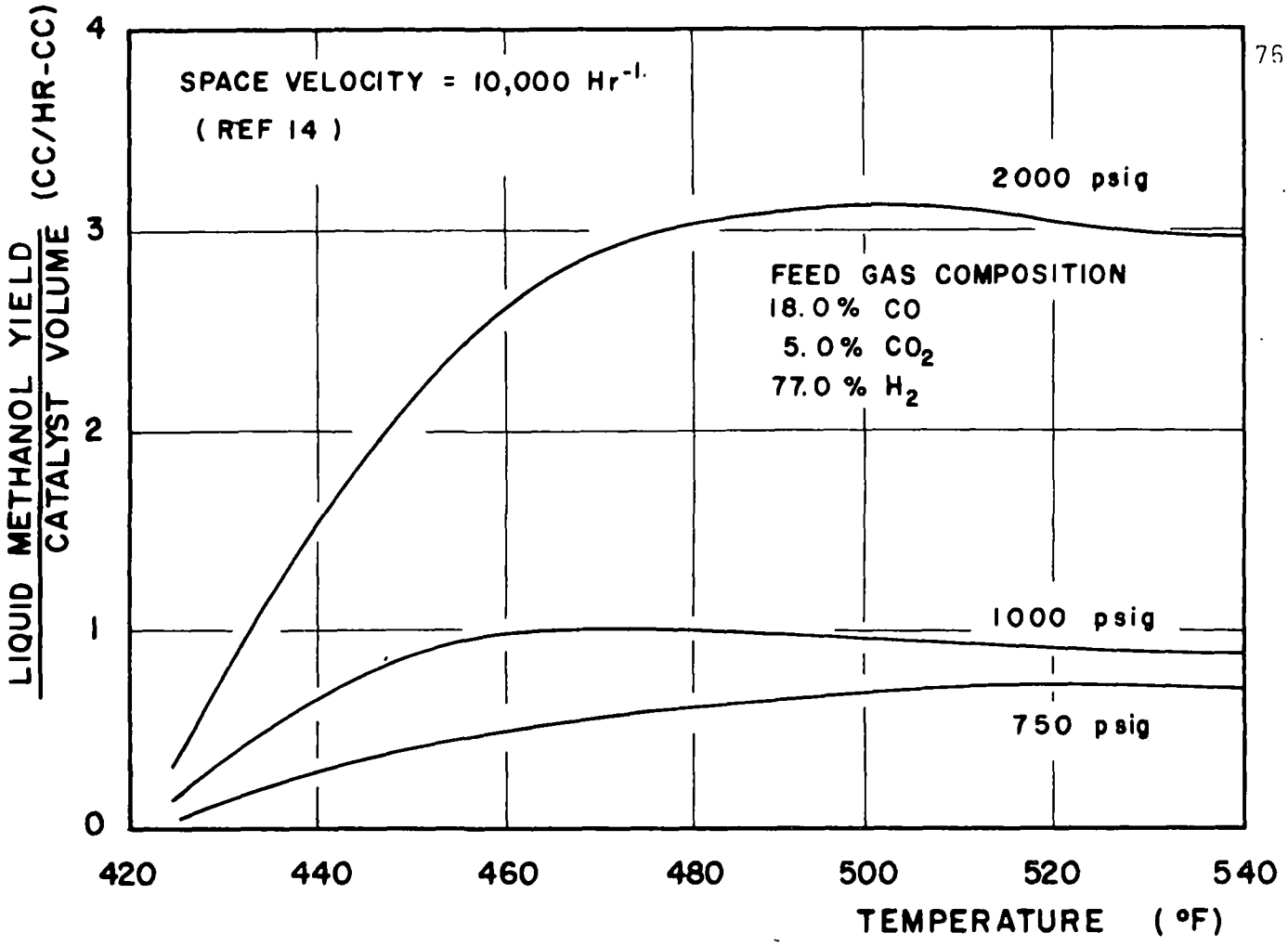

FIG. VIII-6a : EFFECT OF TEMPERATURE AND PRESSURE ON SYNTHESIS YIELD

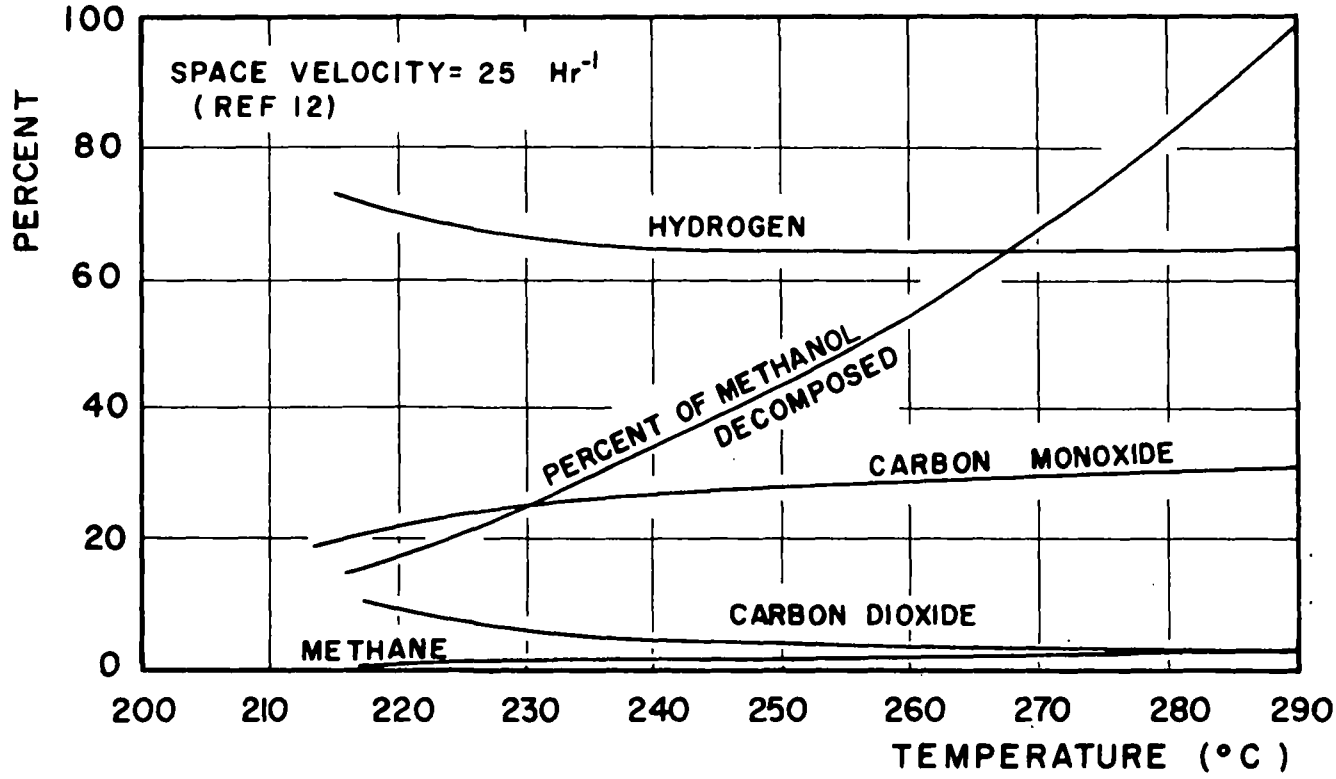

FIG VIII-6b : EFFECT OF TEMPERATURE ON DECOMPOSITION (P= 1 ATM)

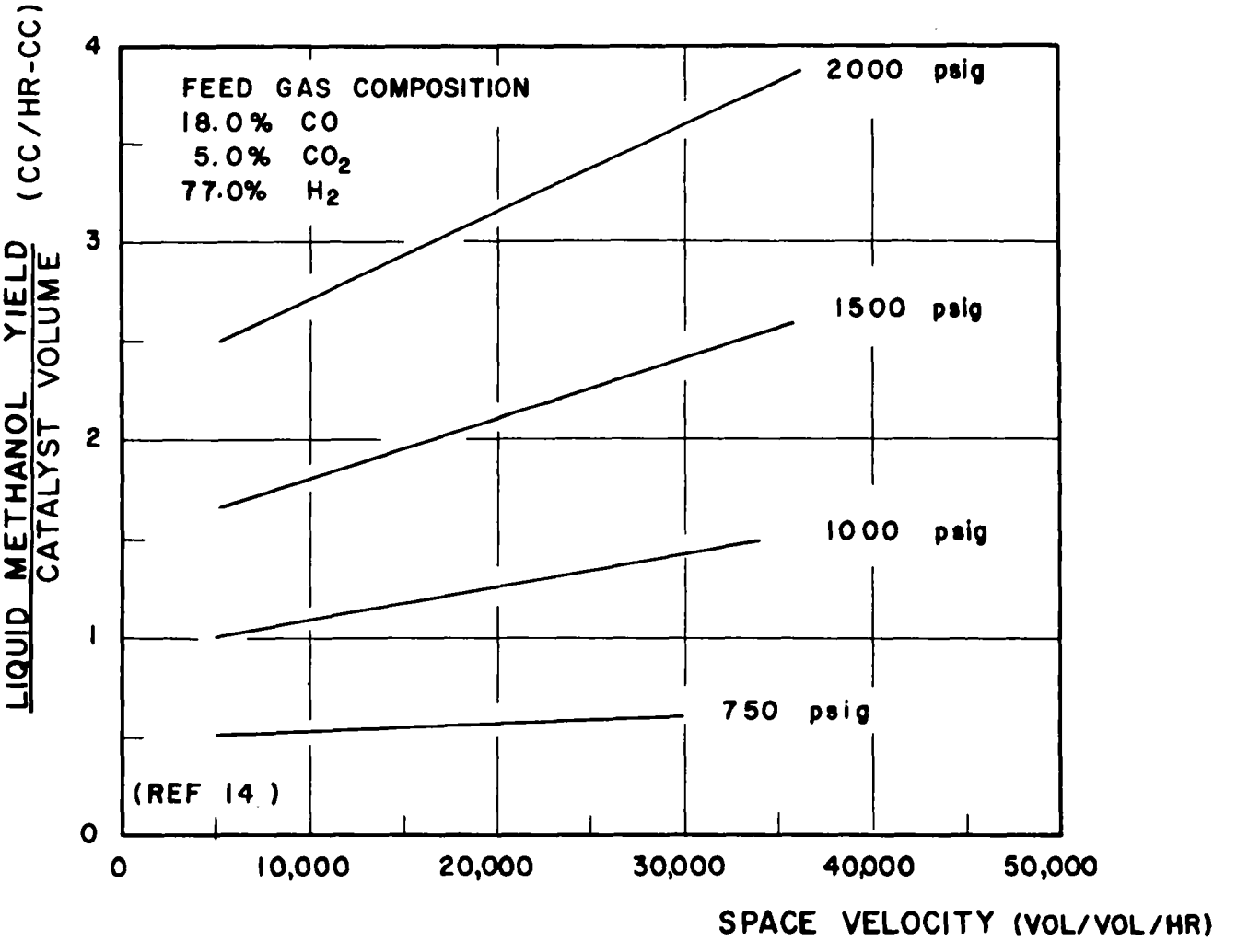

FIG. VIII-7 : EFFECT OF SPACE VELOCITY ON METHANOL SYNTHESIS (T=475° F)

A primary design objective for a decomposition chamber and associated equipment is to supply the high endothermic heat of decomposition (1720 BTU/lb). Also, acceptable decomposition rates are achievable only at temperatures in excess of 400°F. These temperature and energy requirements can be met by superheating the methanol feed stock above 400°F prior to contact with the catalyst, direct heat transfer to the catalytic bed, or by both.

If pure methanol is superheated then the amount of energy available for decomposition (assuming no methanol condensation) is limited to superheat energy. To completely decompose one pound of methanol requires energy approximately equivalent to 2300°F of superheat. Thirty per cent decomposition requires almost 1000°F of superheat (see Fig. VIII-8). Since most catalysts are not capable of withstanding temperatures above 600°F, and since the rate of decomposition falls off drastically below approximately 460°F, the available range of superheat is limited to approximately 140°F. With this constraint, only 3.69 per cent of the methanol can be decomposed during a single pass.

Possible alternate designs which can be used to provide the necessary decomposition energy are: a recycle separator system, a series heating and decomposition system or a system combining catalyst bed heating with recycling or series heating (see Fig. VIII-9). In the recycle separator system, undecomposed methanol exiting from the catalyst bed would be separated from the CO and H_2 and would be recycled (see Fig. VIII-9a). The separator process would be involved in terms of energy exchange and efficient separator design. Heating of the catalyst bed by itself does not appear to present a reasonable method of providing the required decomposition energy. Combined methanol and catalyst bed heating is more feasible (see Fig. VIII-9b). However, the percentage of total energy supplied via catalyst bed heating would be limited by the low catalyst thermal conductivity and heat capacity, especially

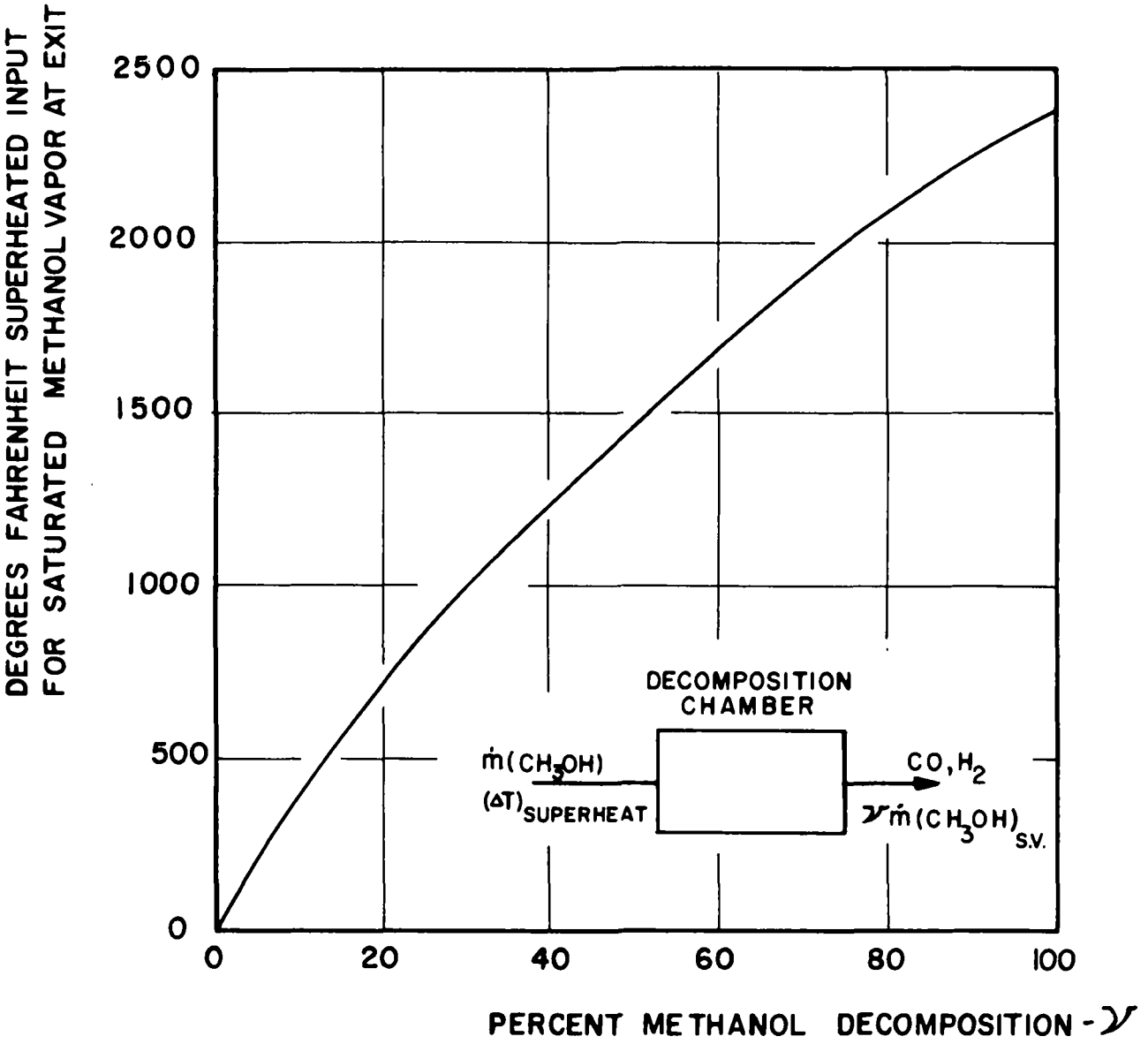

FIG. VIII-8 : REQUIRED SUPERHEAT TEMPERATURE AS A FUNCTION OF METHANOL DECOMPOSITION

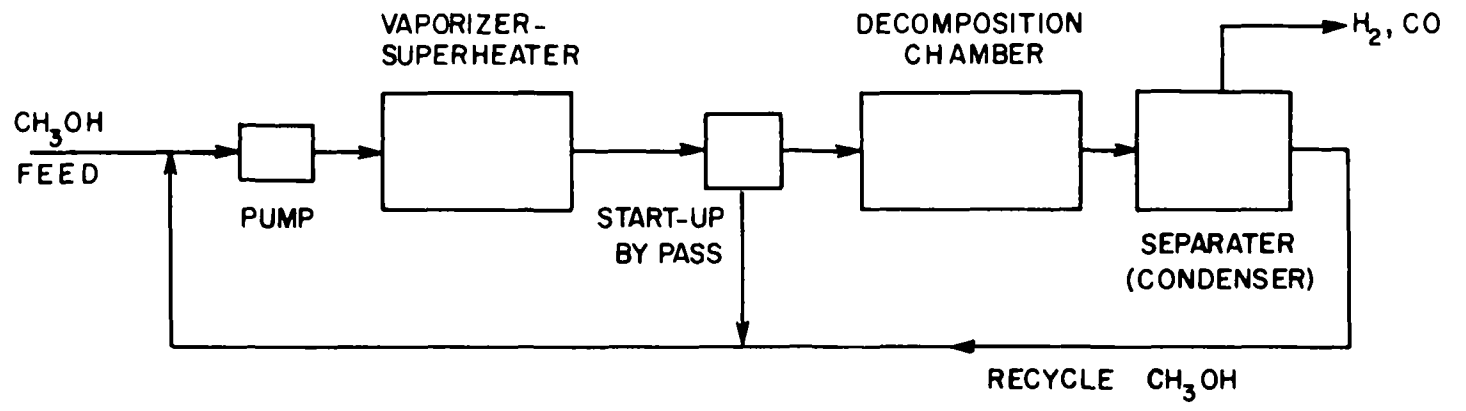

a. RECYCLE SEPARATOR SYSTEM

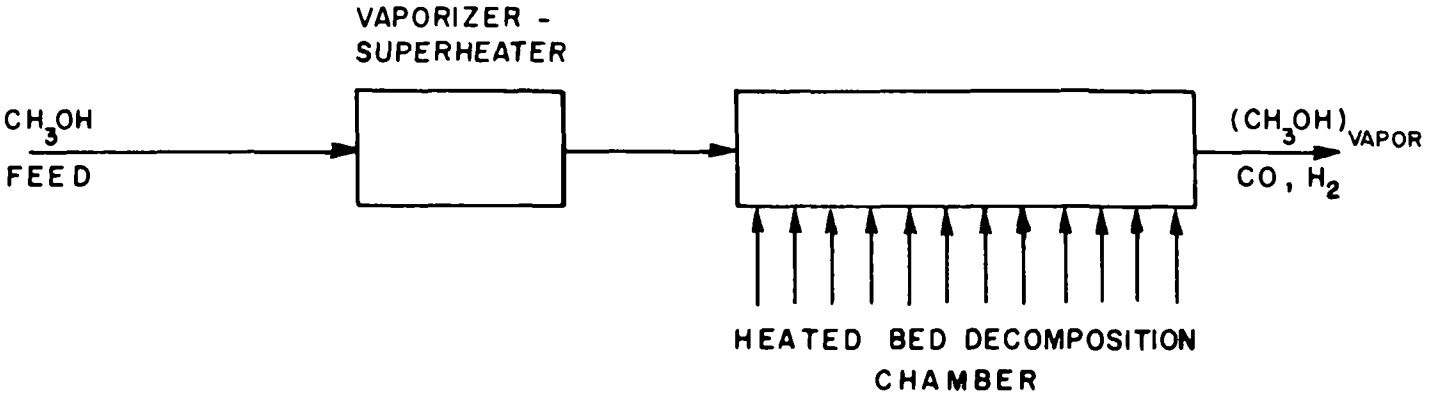

b. HEATED BED DECOMPOSITION

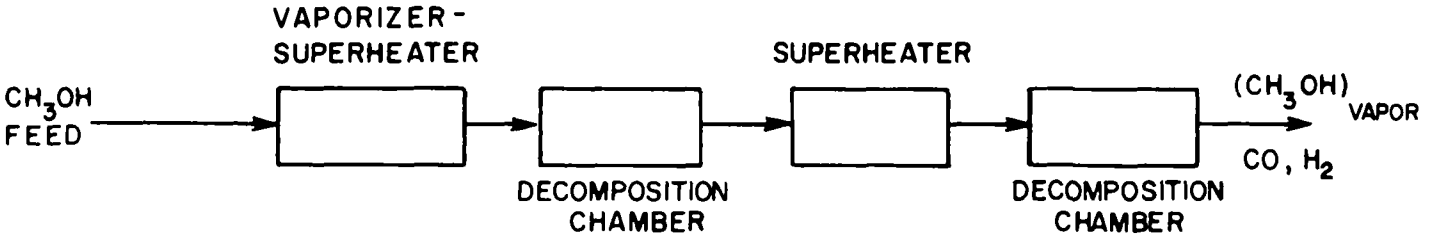

c. SERIES HEATING AND DECOMPOSITION

FIG VIII-9: DECOMPOSITION CHAMBER SCHEMES

during transient start up periods. The best system for the current application is believed to be an alternate series of heating and decomposition chambers, as shown in Fig. VIII-9c. In this system each of the decomposition and heating stages would be designed to operate over the optimum superheat decomposition temperatures ranging between 460° and 600°F. Some heating of the catalyst bed could also be expected because of the anticipated sandwich type structure of the alternating decomposition and heating sections.

(2) Decomposition-Chamber Design. Based upon the design considerations in the previous section, a series heating decomposition bed with limited catalyst heating is believed to be the most feasible design configuration. Figure VIII-10 shows a schematic of a compact series decomposition-heating chamber. Calculations based upon 620°F superheated methanol inlet into the decomposition stages and 460°F inlet into the heating stages indicate that 10 states will be required for 30 per cent methanol dissociation (any heat transfer to the catalyst is neglected).

Sizing of the decomposition chamber is not possible in a rigorous manner because of the lack of catalyst decomposition performance data. However, verbal information from a catalyst manufacturer indicates that a catalyst volume of 0.25 cu ft should be adequate for decomposition of 42 lb/hr. The heat transfer stages could reasonably add an additional .12 cu ft. This total is about that required by a muffler on a current automotive engine. In fact, the baffled heat transfer surfaces in the exhaust side of the decomposition chamber would obviate the need for a muffler.

C. Engine Performance Control:

Decomposition chamber design studies and engine energy exhaust analyses indicate a methanol decomposition limit of approximately 30 per cent at a total fuel flow rate of 120 lb/hr. Assuming that a practical decomposition device can be provided,

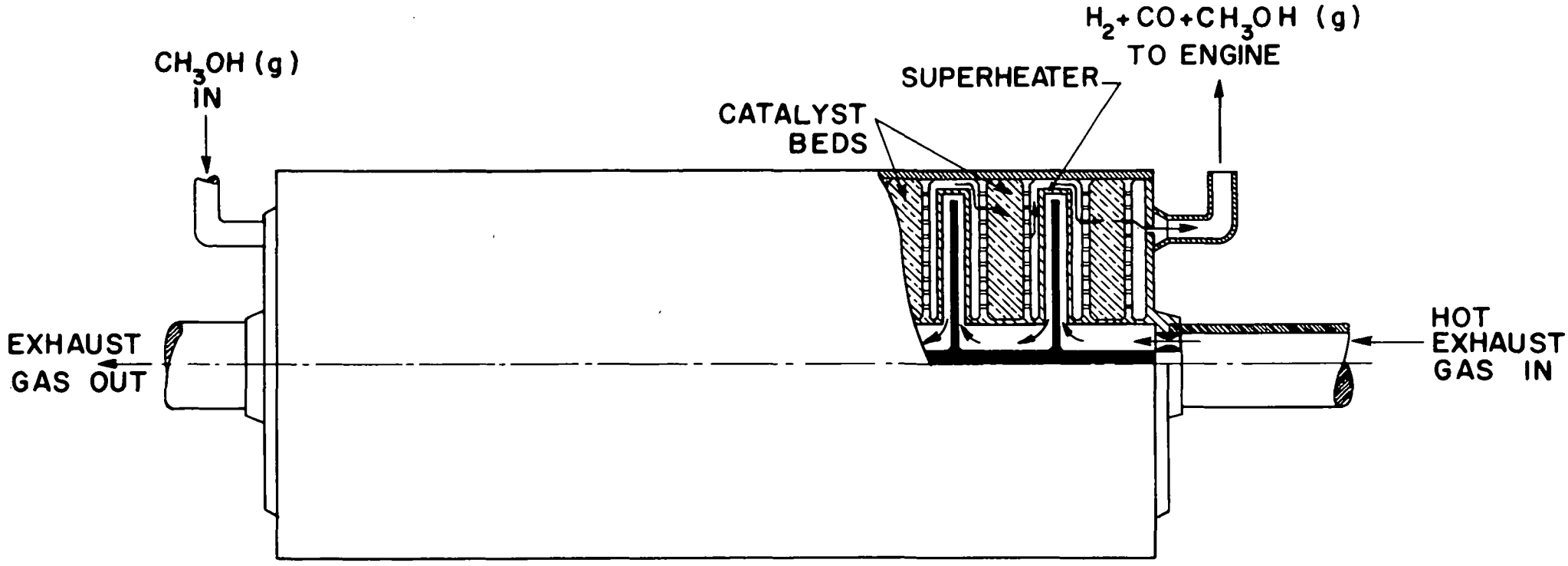

FIG. VIII-10: DECOMPOSITION CHAMBER DESIGN CONCEPT

it is important to consider methods of A/F ratio control during engine warm up and during transient load and speed conditions. Although definition of exact control components is beyond the scope of this study, control problems and general methods of solution will be reviewed.

In order to gain enough energy for methanol decomposition, the total methanol flow must be superheated and routed through the decomposition chamber. The characteristics of the decomposition chamber will probably be such that for quasi steady-state conditions (slowly varying speed and load) the per cent decomposition will increase with engine speed, i.e., available exhaust energy. A/F ratio control under these conditions would be relatively simple with perhaps some fuel temperature compensation to account for density effects in the superheated methanol.

Fuel demands resulting from transient increases in the load or RPM can be met by by-passing superheated or liquid methanol around the decomposition chamber. Transient demands probably could not be met by the decomposition chamber since a probable time lag of 5-10 seconds through the decomposition chamber would not be acceptable. If superheated methanol is used in conjunction with a base flow of 30 per cent dissociated methanol then changes in A/F ratio resulting from variations in fuel mixture gas properties should not be significant. Use of liquid methanol would require gaseous and liquid fuel metering elements with some type of sensing and control elements. These factors tend to favor a single phase system; however, during warm up vaporized methanol would not be available unless an auxiliary vaporization system is provided. Consequently, design conditions necessary to satisfy both transient and warm up operation may favor liquid methanol augmentation.

It is probable that the decomposition chamber start up transient will last at least five minutes. However, it is estimated that exhaust heated,vaporized methanol would be

available after one minute. During this first minute of operation either a liquid metering system must be used or the methanol must be vaporized by an electric heater, a small combustor, by chemical reaction or by other suitable means. The highest start-up fuel consumption should not exceed 2 lb/min with a required heat energy input of 600 BTU/lb or 1200 BTU/min. This rate of energy expenditure would require a 21 kw electrical heater (100 per cent conversion efficiency) or combustion of 0.25 lb (142 cc) of methanol in a combustion heater (50 per cent energy conversion efficiency). Chemical reaction of methanol with a reactive chemical would probably require at least an order of magnitude more total methanol than a combustor and would present greater design, maintenance and servicing problems than a combustor. A final approach would be compression and atomization (pseudo-vaporization) of the methanol to the extent that it could be metered in the same fashion as fully vaporized methanol.

Major components for a dual liquid and gas fuel metering system are shown in Fig. VIII-11. Fuel is pumped to a flow divider which meters fuel to decomposition and liquid fuel flow paths. Metering in the flow divider is controlled by a small A/F ratio control computer which determines appropriate flow divider valve settings by temperature and pressure signals from sensor locations in the air intake and fuel flow lines, and by throttle position and rate of movement. During start up the primary fuel flow is through the liquid line. A start up heater is used to prevent cold start problems (the methanol need not be completely vaporized). While the decomposition chamber is warming up, superheated methanol is by-passed into the gaseous fuel metering leg. As the decomposition chamber is heated and residual methanol from the previous operation cycle is vaporized, superheated methanol is gradually emitted into the chamber until steady-state conditions are reached and the by-pass vale is closed. Transient acceleration fuel demands

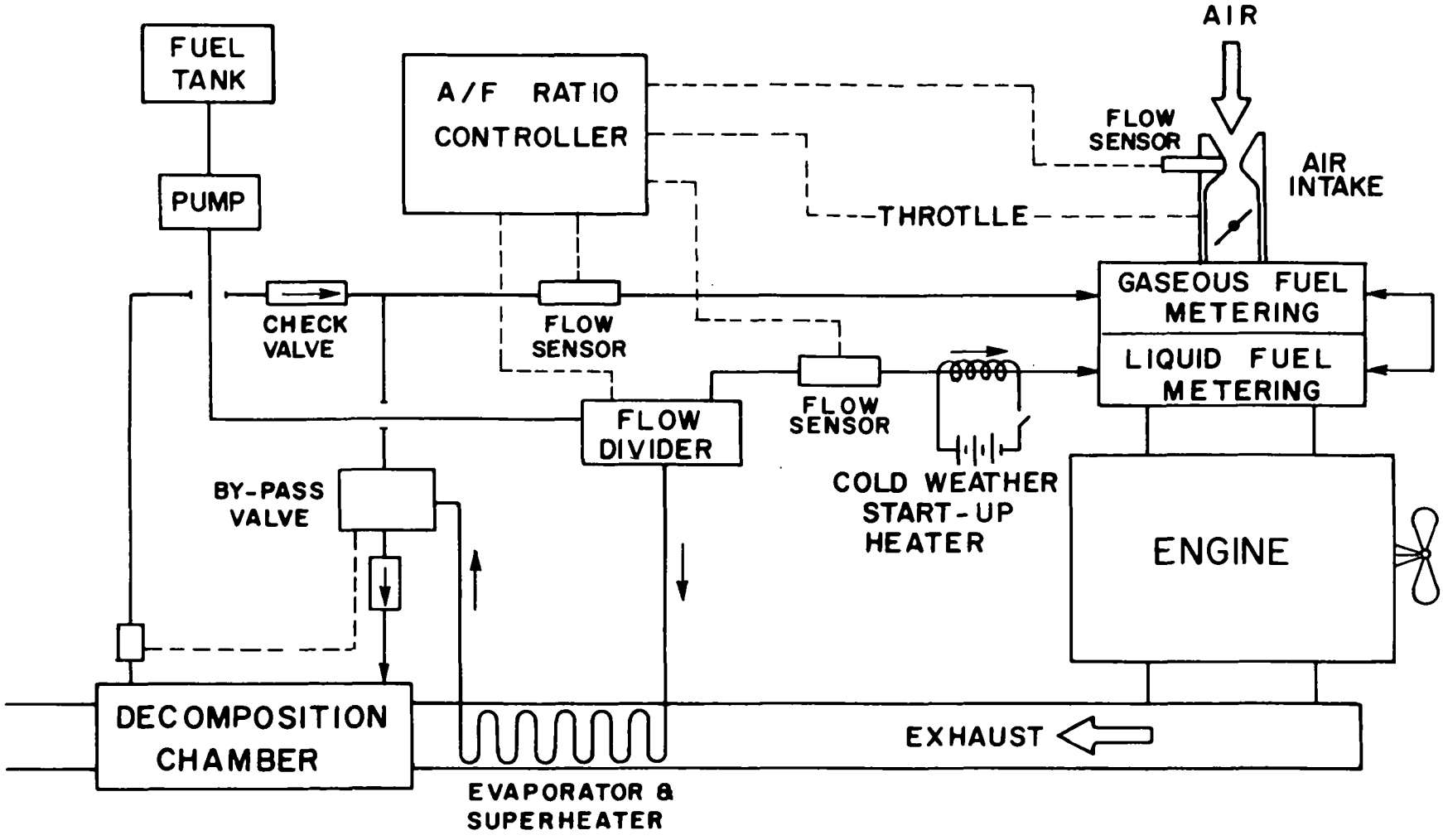

FIG. VIII-II : LIQUID-GAS FUEL METERING SYSTEM

are met during warm up and steady-state operation by proper increases in the liquid fuel flow rate. A schematic showing the arrangement of components in a gaseous fuel system is shown in Fig. VIII-12. Operation of the system is similar to that of the dual system except that an auxiliary fuel vaporizer is used during the initial engine warm up. Transient acceleration fuel demands are met with superheated methanol which by-passes the decomposition chamber.

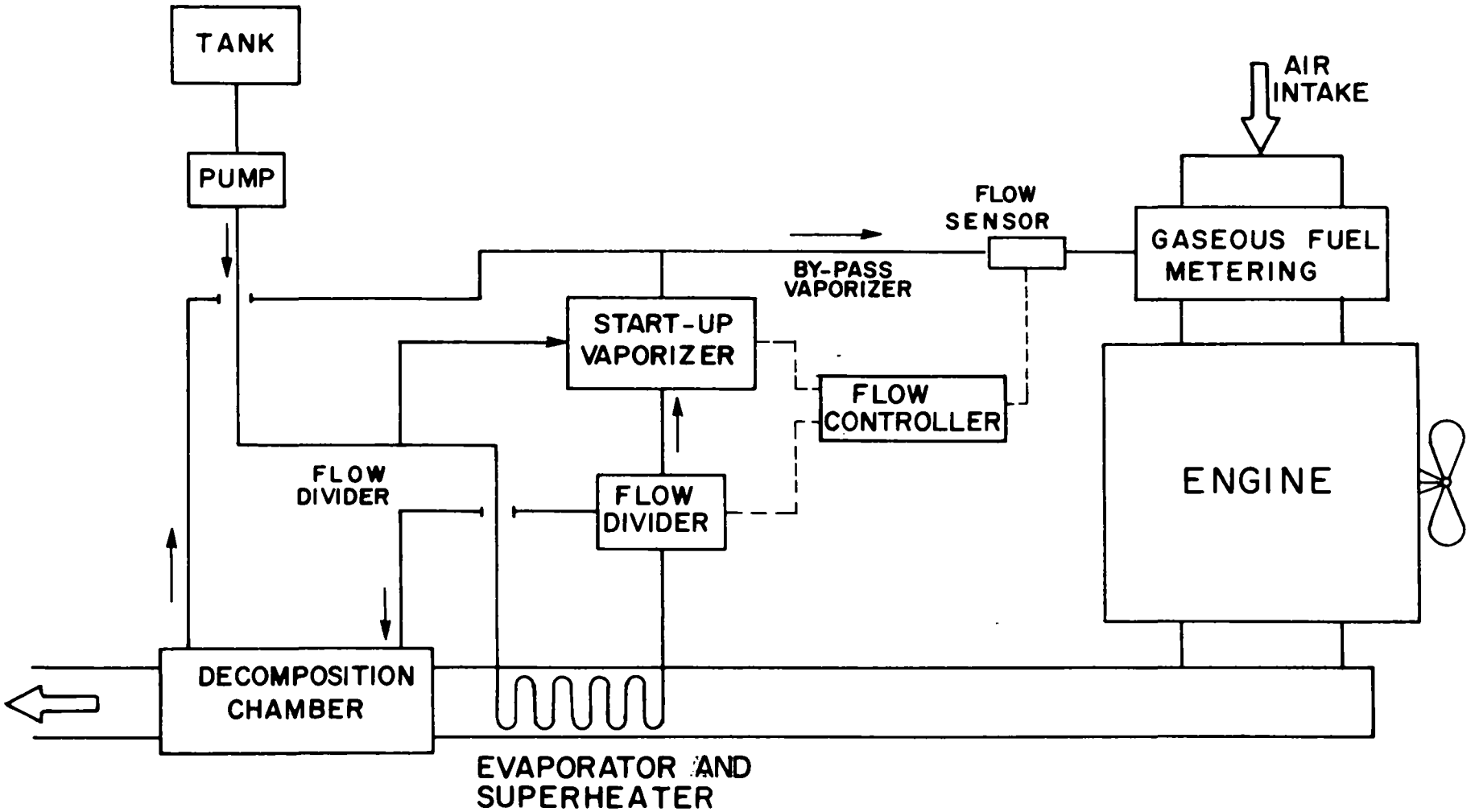

FIG. VIII-12: GASEOUS FUEL METERING SYSTEM

REFERENCES

[1] "Air Pollution Control in California--1970 Annual Report", State of California Resources Agency, Air Resources Board.

[2] Fitch, R. E., Kilgroe, J. D., "Investigation of a Substitute Fuel to Control Automotive Air Pollution--Final Report", prepared for the Division of Motor Vehicle Research and Development, National Air Pollution Control Administration, Contract No. CPA 22-69-70, CETEC Corp., Mountain View, Calif., February 1970.

[3] American Standards Association, "Allowable Concentrations of Formaldehyde", New York, American Standards Association, 1944.

[4] Malmberg, E. W., J. Am. Chem., Sec. 76, 980 (1954).

[5] Walker, J. F., Formaldehyde, 2nd Ed., ACS Monograph 120, Reinhold, New York, 1953.

[6] Satterfield, C. W., et al., Anal. Chem., 26, 1792 (1954).

[7] Lappin, G. L., and Clark, L. D., Anal. Chem., 23, 541 (1951).

[8] Bolt, J. A., "A Survey of Alcohol as a Motor Fuel", ASME Conference Paper, SP 254.

[8a] Starkman, E. S., Newhall, H. K., and Sutton, R. D., "Comparative Performance of Alcohol and Hydrocarbon Fuels", ASME Conference Paper, SP 254.

[9] Fisher, F., and Tropsch, Chm. Ber., 68A, 169 (1935).

[10] Oberdorfer, P. E., "Determination of Aldehydes in Automobile Exhaust Gas", SAE Paper 670123, 1967.

[11] Obert, E. F., Internal Combustion Engines, 3rd Ed., International Textbook Co., Scranton, Pa.

[12] Fenske, M. R., and Frolich, P. K., Ind. Eng. Chem., 21, 1052 (1929).

[13] Huffman, J. R., and Dodge, B. F., Ind. Eng. Chem., 21, 1056 (1929)

[14] "C79 Methanol Synthesis Catalyst Summary of Laboratory Studies and Commercial Experience", Catalysts and Chemicals, Inc., Louisville, Ky., June 1970.

[15] Emmett, P. H., Catalysis, Vol. III - Hydrogeneration and Dehydrogeneration, Reinhold, New York, 1955.

[16] "Catalytic Production of Mixtures of Carbon Dioxide and Hydrogen from Aqueous Methanol", U. S. Patent No. 3,393,979, July 1968.

[17] "Low Pressure Catalyst Operating Instructions", Catalysts and Chemicals, Inc., Louisville, Ky.

A P P E N D I C E S

APPENDIX A
CALCULATION METHODS

The mass flow rate of air to the engine is calculated from:

$$\dot{m}_{air} = \frac{\pi}{4} d^2 C_d \sqrt{2 g_c \Delta p \rho}$$

where

$\dot{m}_{air}$ = mass flow rate of air
d = diameter of nozzle
C_d = coefficient of flow
Δp = pressure difference across nozzle
ρ = density of air

A Fisher Porter Tri Flat Meter (FP-$\frac{1}{8}$-12-G-5) was used to measure the fuel flow rate. Formulas used are

$$\dot{m}_f = CB \sqrt{(\rho_f - \rho_{meth})\rho_{meth}} \quad \frac{1 \text{ lbm}}{453.6 \text{ g}}$$

and

$$N = \frac{A}{\mu} \sqrt{(\rho_f - \rho_{meth})\rho_{meth}}$$

where

N = viscous influence number
A = size factor (Table 7)*
μ = methanol viscosity, centipoise
ρ_f = float density
ρ_{meth} = methanol density, g/cc
B = size factor #2(table 7)*
C = flow coefficient (table 104 - function of N)*
$\dot{m}_f$ = flow rate, lbm/min

The A/F was obtained by dividing $\dot{m}_{air}$ by $\dot{m}_f$.

The brake horsepower is:

$$BHP = \frac{w}{\varepsilon} \times 1.341 \left(\frac{\text{watt}}{\text{hp}}\right) + \frac{F \times N}{6000}$$

---

*Fisher & Porter Co., Tri-Flat Variable Area of Flow Meter Handbook (#10A9010).

where

w = synchronous motor output to wattmeter, watts

ε = synchronous motor efficiency

F = dynamometer force, lbf

N = speed of engine, rpm

The indicated horsepower is:

$$IHP = BHP + FHP$$

The indicated specific fuel consumption is:

$$ISFC = \frac{\dot{m}_f}{IHP}$$

The sensitivity of the chromatograph to different compounds was established by injection of standards and measurement of peak areas as a function of sample size. The calculations for individual compounds are described here.

Methane: Pure CH_4, in the loop at 105°C, gives an average peak of 1.62×10^7 units so that,

$$\text{fraction of } CH_4 \text{ in exhaust} = \frac{\text{units in } CH_4 \text{ peak}}{1.62 \times 10^7}$$

and

$$\text{ppm } CH_4 \text{ in exhaust} = (10^6)\frac{\text{units in } CH_4 \text{ peak}}{1.62 \times 10^7}$$

To convert to g carbon/g exhaust, using the ideal gas equation,

$$PV = \frac{g_{CH_4}}{16} RT = \frac{g_C}{12} RT$$ for methane and carbon ($V = V_{CH_4}$ or V_{carbon}, respectively).

The molecular weight of the exhaust averaged 27 during these runs, and

$$PV = \frac{g_{exhaust}}{27} RT$$ for the exhaust ($V = V_{exhaust}$)

Dividing,

$$\frac{g_{carbon}}{g_{exhaust}} = \frac{12(\text{vol } CH_4)}{27\ (\text{vol exhaust})}$$

$$= 0.444\ (\text{fraction of } CH_4 \text{ in exhaust})$$

$$= 0.444\ (\text{ppm} \times 10^{-6})$$

$$\frac{mg_{carbon}}{g_{exhaust}} = 0.444 \times 10^{-3}\ (\text{ppm})$$

Methanol: Liquid samples of methanol ranging from microliters down to 0.2 microliters (injected as 2 microliters of a 10% solution of methanol in acetone) averaged 1.04×10^7 units per microliter. As the density of methanol is 0.79 g/ml, this represents 1.3×10^4 units per microgram. One microgram is $1/32 \times 10^{-6}$ moles, or 31 nanomoles. Assuming methanol vapor to follow ideal gas behavior and occupy 22.4 liters at 1 atm and 0°C, 1 mole will occupy 3.18×10^4 ml at 115°C, and 31 nanomoles will occupy 31 (3.2×10^{-5}) ml. The total sample volume is 2.9 ml, so

$$\text{ppm} = (31)\left(\frac{3.2 \times 10^{-5}}{2.9}\right)(10^6)\left(\frac{\text{units}}{1.3 \times 10^4}\right)$$

$$\text{ppm} = (2.6 \times 10^{-2} \times \text{units})$$

Hydrocarbons: For methane, a 1.0 ml gaseous sample at 1 atm and 20°C gives a peak of area 1.58×10^7 units. Assuming an ideal gas, this 1 ml sample contains 6.68×10^{-4} g CH_4, or 5.0×10^{-4} g carbon.

$$\text{Sensitivity} = \frac{1.58 \times 10^7 \text{ units}}{5.0 \times 10^{-4} \text{ g carbon}} = 3.4 \times 10^{10} \text{ units/g C}$$

For 3-methyl hexane, 1 microliter = 0.686 mg C_7H_{16}, and the peak area from 1 microliter is 2.6×10^7 units. 0.686 mg C_7H_{16} contains $(0.686)\frac{84.1}{100.2}$ mg carbon = 0.573 mg carbon.

$$\text{Sensitivity} = \frac{2.6 \times 10^7 \text{ units}}{0.573 \times 10^{-3} \text{ g carbon}} = 4.5 \times 10^{10} \text{ units/g C}$$

Similar calculations for other hydrocarbons give an average of 4×10^{10} units/g C. This figure was used for all the hydrocarbons in runs 185 and 188, and for ethane, propane, and the unknown peak in the methanol-fueled runs. This gives grams of carbon, and the calculation of grams of exhaust is given above, under methanol.

Formaldehyde: Sensitivity was 1.02×10^5 units per microliter. A calculation exactly the same as given above for methanol except for the figure 1.02×10^5 gives the concentration in ppm.

Acetaldehyde: Sensitivity was 8×10^6 units per microliter. Again, the usual calculation gives ppm. Note that the sensitivity of the instrument for aldehydes, and especially formaldehyde, is much less than for hydrocarbons.

APPENDIX B

TABLE 1

Test	A/F	CR	% Diss	SA	T_{im}	ihp	isfc	CO_2 (%)	O_2 (%)	CO (%)	NO_X (%)	CH_3OH (ppm)	CH_4 (ppm)	C_2H_6+U (ppm)	C_3H_6 (ppm)	HCOH (ppm)	CH_3CHO (ppm)
4	13.7	9.2	0	12	100	3.91	.474	12.07	0.14	0.81	0.410	--	--	--	--	--	--
5	4.9	9.2	0	14	70	3.72	1.24	6.60	0.03	--	0.060	565	292	10	1	51	--
6	5.5	9.2	0	14	70	3.73	1.11	9.26	0.05	2.90	0.113	441	174	12	2	79	--
7	6.5	9.2	0	14	70	3.65	.98	11.17	0.60	0.08	0.391	107	20	5	--	Tr	--
8	7.5	9.2	0	14	70	3.22	.965	9.45	3.71	0.08	0.117	138	13	3	Tr	65	--
10	8.9	9.2	0	20	70	2.81	.965	8.05	6.31	0.04	0.007	424	13	2	--	18	--
11	5.0	9.2	0	14	70	3.81	1.21	6.56	0.03	--	0.036	736	184	8	1	33	--
12	5.4	9.2	0	14	71	3.78	1.14	8.79	0.03	3.52	0.078	655	150	10	1	57	--
13	6.5	9.2	0	14	73	3.79	.97	11.20	0.41	0.17	0.327	167	17	4	Tr	25	--
14	7.5	9.2	0	14	68	3.37	.94	9.44	3.74	0.09	0.142	140	8	4	Tr	21	--
15	9.0	9.2	0	20	71	2.75	.98	7.82	6.67	0.09	0.012	394	94	2	Tr	13	--
21	5.5	9.2	30	14	70	3.64	1.10	9.50	0.06	2.59	0.107	222	525	10	1	75	--
22	6.5	9.2	30	14	70	3.58	.99	11.22	0.50	0.08	0.471	--	--	--	--	--	--
23	5.5	9.2	30	14	69	3.64	1.15	8.87	0.21	3.30	0.072	221	435	8	--	44	--
24	6.5	9.2	30	14	70	3.58	.99	11.20	0.49	0.12	0.390	72	32	8	Tr	13	--
25	7.5	9.2	30	14	71	3.31	.94	9.96	2.78	0.08	0.357	62	32	5	--	5	--
26	9.0	9.2	30	20	69	2.99	.91	8.57	5.31	0.08	0.111	155	13	4	--	3	--
27	5.0	9.2	30	14	70	3.57	1.44	6.66	0.14	--	0.030	131	236	2	Tr	12	--
29	6.4	9.2	70	9	70	3.38	.98	11.00	0.90	0.08	--	23	44	4	1	19	--
30	7.6	9.2	70	9	70	3.11	.94	9.62	3.42	0.07	--	43	53	2	Tr	9	--
31	9.0	9.2	70	12	78	2.81	.90	7.89	6.55	0.08	0.207	77	51	1	--	6	--
32	6.4	9.2	70	9	70	3.45	1.02	11.02	0.23	0.53	--	71	88	8	Tr	57	--
33	5.5	9.2	70	6	78	3.49	1.13	9.13	0.07	3.06	0.128	201	586	6	Tr	55	--

A/F - air-fuel ratio
CR - compression ratio
% Diss - per cent of methanol in dissociated form
SA - spark advance
T_{im} - intake manifold temperature
ihp - indicated horsepower
isfc - indicated specific fuel consumption, lb/hp-hr
-- - indicates no data were recorded for this point
Tr - indicates only trace elements of the compound less than .5 ppm

Test	A/F	CR	% Diss	SA	T_{im}	ihp	isfc	CO_2 (%)	O_2 (%)	CO (%)	NO_X (%)	CH_3OH (ppm)	CH_4 (ppm)	C_2H_6+U (ppm)	C_3H_6 (ppm)	HCOH (ppm)	CH_3CHO (ppm)
34	5.1	9.2	70	6	65	3.43	1.22	6.67	0.05	--	0.045	176	660	12	Tr	74	--
35	9.0	9.2	100	12	105	2.68	.91	8.53	5.38	0.08	--	39	45	Tr	--	7	--
36	7.4	9.2	100	12	108	2.93	.97	10.38	2.06	0.06	--	77	55	6	--	8	1
37	6.5	9.2	100	12	107	3.06	1.04	10.67	0.46	0.81	--	2	78	5	Tr	89	--
38	6.0	9.2	100	12	108	3.03	1.21	8.51	0.05	--	0.116	5	808	22	1	133	--
39	4.9	9.2	100	12	105	2.66	1.43	5.00	0.06	--	0.011	1	950	4	--	20	--
40	5.0	8.5	0	15	69	3.96	1.18	6.60	0.03	--	0.015	646	746	4	--	33	Tr
41	5.5	8.5	0	15	68	3.97	1.06	9.65	0.06	2.40	0.097	319	498	3	Tr	57	8
42	6.5	8.5	0	14	68	3.80	.95	10.75	1.35	0.08	--	107	2	7	Tr	22	12
43	7.5	8.5	0	14	69	3.36	.95	9.25	4.09	0.08	0.096	158	9	1	--	90	29
44	9.0	8.5	0	15	67	2.80	.98	7.71	6.88	0.09	0.009	440	8	3	--	103	Tr
47	6.5	8.5	0	12	109	3.58	.98	10.88	1.12	0.08	--	102	36	10	1	55	3
48	6.5	8.5	0	12	44	3.93	.95	10.80	1.22	0.12	--	199	46	10	1	87	6
49	7.5	8.5	0	20	44	3.58	.93	9.55	3.54	0.08	0.178	246	38	6	Tr	101	8
50	7.5	8.5	0	20	109	3.31	.94	9.73	3.21	0.08	0.237	195	33	6	Tr	109	42
51	5.0	10.9	0	12	70	4.08	1.17	6.50	0.06	--	0.009	810	1420	Tr	--	47	6
52	5.5	10.9	0	12	69	4.13	1.03	9.11	0.07	3.09	0.066	500	675	5	--	38	21
53	6.5	10.9	0	12	70	4.05	.91	11.11	0.64	0.12	--	162	42	10	Tr	46	Tr
54	6.5	10.9	0	12	110	3.87	.93	11.20	0.48	0.12	--	228	51	10	1	54	21
55	6.2	10.9	0	12	43	4.15	.95	10.90	1.02	0.12	--	425	47	10	1	114	21
56	7.5	10.9	0	20	42	3.69	.90	9.03	4.41	0.13	0.185	413	33	5	Tr	122	10
57	7.5	10.9	0	20	110	3.48	.90	9.43	3.69	0.13	--	376	50	6	Tr	164	41
58	7.5	10.9	0	20	71	3.34	.95	8.86	4.78	0.08	0.165	--	28	7	--	135	41
59	9.0	10.9	0	20	76	2.99	.91	7.52	7.22	0.08	0.009	--	26	4	--	89	10
60	5.0	8.5	30	8	70	3.73	1.16	9.00	0.07	3.22	0.077	252	673	11	1	77	15
61	5.4	8.5	30	2	73	3.80	1.07	9.87	0.07	2.12	0.142	219	483	11	Tr	62	12
62	5.5	8.5	30	10	72	3.73	1.09	9.97	0.09	1.97	0.173	227	476	16	Tr	71	8
63	5.5	8.5	30	12	71	3.77	1.07	10.06	0.09	1.85	0.187	207	431	16	Tr	77	17
64	5.5	8.5	30	20	71	3.61	1.12	9.79	0.11	2.18	0.167	249	654	17	1	64	12
65	5.5	8.5	30	23	72	3.57	1.14	9.74	0.11	2.26	0.166	223	548	16	1	61	15
66	8.9	8.5	30	23	80	2.72	.965	7.86	6.59	0.09	0.089	370	50	6	Tr	72	6
67	8.9	8.5	30	20	77	2.69	.975	7.79	6.73	0.08	0.048	334	31	6	Tr	103	17
68	8.9	8.5	30	14	70	2.64	.995	7.73	6.84	0.08	0.028	334	25	5	Tr	218	4
69	8.9	8.5	30	10	67	2.67	.98	7.85	6.63	0.08	0.023	356	31	7	Tr	74	15
70	8.9	8.5	30	2	68	2.47	1.06	7.79	6.73	0.08	0.014	286	23	8	Tr	79	13

Test	A/F	CR	% Diss	SA	T_{im}	ihp	isfc	CO_2 (%)	O_2 (%)	CO (%)	NO_X (%)	CH_3OH (ppm)	CH_4 (ppm)	C_2H_6+U (ppm)	C_3H_6 (ppm)	HCOH (ppm)	CH_3CHO (ppm)
71	7.5	8.5	30	2	70	3.01	1.01	9.02	4.49	0.08	0.101	101	9	4	Tr	68	10
72	7.5	8.5	30	10	70	3.14	.96	9.02	4.49	0.08	0.206	130	18	8	Tr	47	36
73	7.5	8.5	30	14	70	3.25	.93	9.18	4.20	0.08	--	162	35	10	Tr	60	128
74	7.4	8.5	30	20	70	3.22	.94	9.22	4.14	0.08	--	106	40	12	Tr	62	382
75	7.4	8.5	30	23	70	3.11	.97	9.19	4.19	0.08	--	--	40	11	Tr	61	487
76	7.4	8.5	30	14	110	3.22	.94	9.60	3.44	0.08	--	114	30	11	Tr	41	335
77	7.5	8.5	30	14	44	3.39	.89	9.19	4.19	0.08	--	118	40	13	Tr	67	324
78	9.1	10.9	30	18	71	2.86	.895	7.61	7.06	0.08	0.044	365	35	5	Tr	87	6
79	9.5	10.9	30	10	70	2.69	.95	7.28	7.65	0.08	0.012	456	38	6	Tr	61	--
80	9.5	10.9	30	20	70	2.84	.90	7.41	7.41	0.08	0.030	398	50	6	Tr	39	--
81	9.5	10.9	30	23	70	2.80	.91	7.43	7.39	0.08	0.035	416	41	6	Tr	61	--
82	5.5	8.5	0	15	70	3.66	1.12	9.71	0.03	2.34	0.104	410	496	7	1	55	3
83	5.5	9.1	0	15	70	3.70	1.11	9.74	0.03	2.30	0.109	439	629	20	1	65	41
84	5.5	10.0	0	12	70	3.77	1.09	9.72	0.07	2.30	0.106	467	520	20	1	78	30
85	5.5	10.9	0	16	70	3.81	1.08	9.60	0.11	2.43	0.106	690	809	21	2	73	20
86	9.0	10.9	0	20	70	2.86	.945	7.86	6.60	0.09	0.013	713	45	7	Tr	55	20
87	9.0	10.0	0	20	70	2.77	.975	7.79	6.72	0.09	0.009	780	37	5	--	45	41
88	9.0	9.2	0	20	70	2.73	.99	7.76	6.78	0.08	0.007	785	34	7	Tr	30	10
89	9.0	8.5	0	20	70	2.69	1.01	7.88	6.55	0.09	0.007	585	30	6	--	33	--
90	5.5	8.5	30	12	70	3.49	1.15	9.73	0.13	2.25	0.142	321	563	12	Tr	63	6
91	5.5	9.2	30	12	70	3.56	1.13	9.84	0.15	2.10	0.152	240	480	18	1	53	21
92	5.5	10.0	30	12	70	3.60	1.12	9.57	0.17	2.43	0.127	206	685	17	Tr	68	13
93	5.5	10.9	30	12	70	3.62	1.11	9.70	0.19	2.24	0.146	311	613	21	1	71	21
94	9.0	10.9	30	16	70	2.94	.895	7.98	6.37	0.08	0.057	287	26	6	--	75	17
95	9.0	10.0	30	18	70	2.90	.905	8.08	6.21	0.08	0.057	311	31	7	--	86	6
96	9.0	9.2	30	16	70	2.80	.94	7.98	6.37	0.08	0.043	304	31	7	Tr	76	6
97	9.0	8.5	30	16	70	2.69	.98	7.78	6.75	0.09	0.024	510	32	6	Tr	88	2
98	9.0	8.5	30	16	70	2.60	.96	7.37	7.49	0.08	0.010	479	69	6	--	35	Tr
99	5.5	8.5	70	5	72	3.35	1.09	10.73	0.23	0.90	0.336	856	241	17	Tr	49	4
100	5.5	9.2	70	6	70	3.39	1.09	10.71	0.25	0.91	0.352	88	280	20	Tr	48	2
101	5.5	10.0	70	6	70	3.43	1.07	10.62	0.25	1.03	0.342	134	333	25	1	83	14
102	5.5	10.9	70	4	70	3.49	1.06	10.63	0.29	0.99	0.346	102	299	25	1	73	8
103	9.0	10.9	70	12	76	2.80	.87	7.79	6.66	0.13	0.122	117	50	10	--	21	2
104	9.0	10.0	70	12	75	2.77	.88	7.70	6.83	0.13	0.104	121	44	10	Tr	26	2
105	9.0	9.2	70	12	76	2.69	.905	7.75	6.80	0.08	0.094	86	44	8	Tr	15	2

Test	A/F	CR	% Diss	SA	T_{im}	ihp	isfc	CO_2 (%)	O_2 (%)	CO (%)	NO_X (%)	CH_3OH (ppm)	CH_4 (ppm)	C_2H_6+U (ppm)	C_3H_6 (ppm)	HCOH (ppm)	CH_3CHO (ppm)
106	9.0	8.5	70	12	76	2.64	.92	7.70	6.89	0.08	0.082	96	36	8	Tr	19	--
107	9.0	8.5	100	10	102	2.64	.93	8.26	6.01	0.00	0.315	13	72	7	Tr	13	82
108	9.0	9.2	100	10	105	2.68	.915	8.21	5.97	0.08	0.337	2	46	10	Tr	16	303
109	9.0	10.0	100	10	107	2.71	.895	8.27	5.85	0.09	0.369	1	38	9	Tr	20	397
110	9.0	10.9	100	10	106	2.72	.885	8.21	5.89	0.13	0.386	1	43	10	Tr	20	405
111	9.0	10.0	70	12	75	2.81	.905	8.03	6.30	0.08	0.351	387	43	10	Tr	31	74
112	9.6	10.0	70	6	75	2.77	.86	7.49	6.79	0.43	0.130	--	--	--	--	--	--
113	5.5	9.2	0	15	70	3.68	1.11	9.76	0.14	2.21	0.074	508	672	14	1	55	4
114	6.5	8.5	0	16	108	3.41	1.015	10.95	1.00	0.08	0.254	--	--	--	--	--	--
115	6.5	9.2	0	16	110	3.45	1.005	10.86	1.15	0.08	0.257	--	--	--	--	--	--
116	6.5	10.0	0	16	108	3.50	.99	10.95	1.00	0.08	0.273	--	--	--	--	--	--
117	6.5	10.9	0	16	110	3.56	.975	11.02	0.88	0.08	0.284	--	--	--	--	--	--
118	6.5	10.9	30	10	110	3.45	.96	11.03	0.84	0.08	0.329	--	--	--	--	--	--
119	6.5	10.0	30	10	110	3.41	.97	11.03	0.84	0.08	0.325	85	57	37	1	29	10
120	6.5	9.2	30	10	110	3.36	.99	10.84	1.19	0.08	0.302	77	54	38	Tr	33	52
121	6.5	8.5	30	10	109	3.31	1.00	10.98	0.94	0.08	0.294	65	--	31	1	29	63
122	6.5	8.5	70	7	110	3.17	1.015	10.98	0.77	0.21	0.385	23	84	27	1	26	13
123	6.5	9.2	70	7	110	3.22	1.00	10.96	0.86	0.17	0.395	30	73	30	1	21	72
124	6.5	10.0	70	7	110	3.29	.98	10.92	0.92	0.17	0.405	34	55	29	1	29	88
125	6.5	10.9	70	7	109	3.31	.97	10.92	0.73	0.31	0.405	--	116	26	1	29	68
126	5.5	10.9	30	2	70	3.63	1.09	10.38	0.04	1.48	0.152	--	--	--	--	--	--
127	5.5	8.5	30	2	70	3.50	1.13	10.53	0.03	1.30	0.146	--	--	--	--	--	--
128	5.5	8.5	30	5	70	3.58	1.10	10.49	0.03	1.36	0.148	--	--	--	--	--	--
129	5.5	10.9	30	5	70	3.73	1.06	10.37	0.05	1.49	0.149	--	--	--	--	--	--
130	5.5	10.9	30	10	68	3.74	1.08	9.78	0.05	2.24	0.116	--	--	--	--	--	--
131	5.5	8.5	30	10	73	3.59	1.12	9.69	0.03	2.37	0.100	--	--	--	--	--	--
132	5.5	8.5	30	20	70	3.52	1.145	9.65	0.03	2.42	0.105	--	--	--	--	--	--
133	5.5	10.9	30	20	70	3.66	1.10	9.64	0.05	2.42	0.111	284	741	14	Tr	35	5
134	5.5	10.9	30	23	70	3.55	1.14	9.70	0.07	2.33	0.120	288	716	17	Tr	40	4
135	5.5	8.5	30	23	70	3.44	1.17	9.64	0.06	2.42	0.111	318	1210	75	--	25	6
136	6.5	8.5	30	23	70	3.33	1.04	11.00	0.91	0.09	0.358	86	44	20	Tr	47	21
137	6.5	10.9	30	23	70	3.49	.995	10.97	0.95	0.09	0.406	114	48	17	Tr	60	139
138	6.5	10.9	30	23	70	3.55	.98	10.93	1.03	0.09	0.404	115	50	17	Tr	52	139
139	6.5	8.5	30	20	70	3.42	1.01	10.99	0.92	0.08	0.364	62	48	21	Tr	52	118
140	6.5	8.5	30	10	70	3.47	1.00	10.93	1.03	0.08	0.322	51	44	15	Tr	44	125

Test	A/F	CR	% Diss	SA	T_{im}	ihp	isfc	CO_2 (%)	O_2 (%)	CO (%)	NO_X (%)	CH_3OH (ppm)	CH_4 (ppm)	C_2H_6+U (ppm)	C_3H_6 (ppm)	HCOH (ppm)	CH_3CHO (ppm)
141	6.5	10.9	30	10	70	3.58	.97	10.93	1.04	0.08	0.347	83	47	17	1	44	138
142	6.5	10.9	30	2	70	3.52	.985	10.82	1.24	0.08	0.299	40	42	16	1	37	127
143	6.5	8.5	30	2	70	3.38	1.03	10.89	1.10	0.08	0.277	23	36	16	Tr	26	92
144	6.5	8.5	30	10	46	3.49	.995	10.69	1.47	0.08	0.305	39	41	17	Tr	25	151
145	6.5	10.9	30	10	45	3.65	.95	10.66	1.53	0.08	0.342	67	38	16	Tr	50	221
146	7.5	10.9	30	13	45	3.38	.915	9.46	3.69	0.08	0.244	109	38	13	Tr	91	364
147	7.5	10.9	70	2	70	3.12	.955	9.40	3.80	0.08	0.302	--	--	--	--	--	--
148	7.5	10.9	70	10	70	3.17	.94	9.51	3.61	0.08	0.398	36	25	14	Tr	45	395
149	7.5	10.9	70	6	70	3.20	.93	9.44	3.73	0.08	0.369	28	28	14	Tr	45	288
150	7.5	8.5	70	6	70	3.05	.975	9.39	3.82	0.08	0.331	23	30	16	Tr	46	277
151	5.7	8.5	100	5	110	3.10	1.185	8.83	0.07	3.44	0.136	7	1675	15	Tr	45	20
152	5.6	9.2	100	5	110	3.12	1.18	8.82	0.07	3.46	0.128	5	1500	17	1	47	Tr
153	5.6	10.0	100	5	110	3.17	1.16	8.89	0.08	3.36	0.128	8	1370	36	1	65	6
154	5.7	10.9	100	5	110	3.18	1.155	8.62	0.07	--	0.122	46	1713	30	5	124	58
155	5.0	10.9	100	5	110	3.08	1.285	6.55	0.05	--	0.074	20	2350	38	6	170	180
156	6.5	10.9	100	6	110	3.24	.98	11.03	0.39	0.41	0.335	8	396	23	--	33	55
157	6.5	10.0	100	6	110	3.18	1.00	10.98	0.38	0.48	0.329	14	304	28	Tr	44	21
158	6.5	9.2	100	6	110	3.15	1.01	10.98	0.39	0.48	0.320	3	349	26	Tr	30	6
159	6.5	8.5	100	6	110	3.10	1.025	10.98	0.38	0.47	0.307	2	386	24	--	22	2
160	5.5	9.2	0	15	70	3.70	1.14	8.96	0.03	3.31	0.058	411	754	19	Tr	74	7
161	7.5	10.9	30	1	70	3.10	1.005	9.54	3.55	0.08	0.142	59	12	9	Tr	26	4
162	7.5	10.9	30	10	70	3.27	.955	9.55	3.53	0.08	0.252	114	16	10	--	47	55
163	7.5	10.9	30	15	70	3.31	.94	9.53	3.56	0.09	0.295	159	24	12	Tr	53	221
164	7.5	10.9	30	20	70	3.26	.955	9.53	3.57	0.09	0.357	134	21	11	Tr	46	374
165	7.5	10.9	30	23	70	3.22	.97	9.61	3.42	0.09	0.407	133	21	11	Tr	36	232
166	7.5	10.9	100	10	113	3.03	.95	10.29	2.19	0.08	0.489	1	28	14	Tr	24	227
167	7.5	8.5	100	10	113	2.94	.98	10.24	2.28	0.08	0.471	Tr	28	12	--	12	134
168	5.1	8.5	100	5	111	3.00	1.345	6.57	0.06	--	0.064	2	1030	25	2	81	18
169	5.0	8.5	70	6	70	3.32	1.24	6.91	0.02	--	0.047	70	490	15	1	59	Tr
170	5.0	10.9	70	6	71	3.45	1.195	6.93	0.03	--	0.051	143	957	30	3	66	Tr
171	6.5	10.9	70	6	71	3.41	.90	10.86	1.17	0.08	0.440	25	46	20	1	17	48
172	6.5	8.5	70	6	70	3.29	.935	10.83	1.22	0.08	0.406	12	37	17	Tr	5	013
173	7.5	10.9	70	10	110	3.16	.93	10.15	2.46	0.08	0.442	50	45	21	Tr	18	410
174	7.5	8.5	70	10	110	3.01	.975	10.07	2.60	0.08	0.408	18	55	17	Tr	17	2154
175	7.5	10.9	30	12	110	3.28	.93	9.69	3.28	0.08	0.300	228	38	16	Tr	--	2108

Test	A/F	CR	% Diss	SA	T_{im}	ihp	sfc	CO_2 (%)	O_2 (%)	CO (%)	NO_X (%)	CH_3OH (ppm)	CH_4 (ppm)	C_2H_6+U (ppm)	C_3H_6 (ppm)	HCOH (ppm)	CH_3CHO (ppm)
176	5.0	10.9	30	10	70	3.65	1.205	6.80	0.08	--	0.066	441	1191	23	--	75	2
177	5.5	9.2	30	16	70	3.78	1.13	9.29	0.04	2.88	0.054	341	679	13	Tr	28	Tr
178	5.5	9.2	30	10	70	3.61	1.11	9.86	0.04	2.15	0.106	216	444	12	--	30	52
179	5.5	8.5	30	10	70	3.59	1.115	9.91	0.04	2.08	0.107	189	401	10	--	18	--
180	9.0	8.5	30	16	70	2.61	.955	7.32	7.69	0.00	0.005	299	29	9	Tr	38	53
181	9.0	9.2	0	20	70	2.70	1.00	7.65	7.09	0.00	0.004	508	27	9	Tr	44	65
182	5.0	10.9	0	5	110	2.83	1.42	6.56	0.03	--	0.027	56	--	13	Tr	41	62
183	6.5	8.5	100	14	69	3.65	1.01	11.16	0.62	0.08	0.278						
184	6.5	10.9	0	14	71	3.86	.955	11.16	0.62	0.08	0.314						
185	14.9	9.2	0	18	86	3.90	.461	10.82	0.08	2.51	0.306						
Tests 186 through 191 were conducted with gasoline; all previous tests were with methanol.																	
186	10.0	9.2		18	80	3.67	.735	5.71	0.08	--	1.080						
187	13.1	9.2		20	84	3.84	.535	7.21	0.06	--	0.566						
188	14.0	9.2		18	87	3.90	.492	9.66	0.08	--	0.527						
189	16.1	9.2		18	90	3.87	.431	11.39	0.84	1.15	0.350						
190	17.9	9.2		18	91	3.72	.404	12.06	0.88	0.23	0.358						
191	14.9	9.2		18	88	3.90	.461	10.63	0.08	2.76	0.427						

APPENDIX C

REFORMING CYCLE
ENERGY BALANCE ANALYSIS

A. Reforming Cycle:

A reforming cycle is one in which exhaust energy from a heat engine is used to dissociate some or all of the fuel before injection into the engine. Associated with reforming are preheating, evaporation and superheating of the fuel. There are several sequences in which energy can be withdrawn from the exhaust to accomplish these processes, especially if the reformed and non-reformed portions of the fuel are treated separately.

For the reasons described in the body of the report, the cycle was set up, as shown in Fig. VIII- . This arrangement is one of counterflow in which the reforming of the fuel is accomplished by energy extracted from the exhaust first, at the most elevated temperature. The schedule of heat transfer events is as shown.

The significant assumptions which were made in setting up the energy balance are as follows:

(1) Fuel in pure methanol (CH_3OH)

(2) A/F = 6.43

(3) The fuel dissociates into the components $CO + 2\ H_2$

(4) All mixing processes are perfect

(5) No energy is lost from the system except for engine cooling

(6) The fuel is completely reacted with the oxygen in the air so that the exhaust composition (mole fraction) is:

$$CO_2 - 0.115$$

$$H_2O - 0.231$$

$$N_2 - \underline{0.654}$$

$$1.000$$

B. Analysis:

The fuel flow rate is specified along with the fractions of the fuel which pass through the reforming and non-reforming branches; the temperatures at the steps in both branches; the nominal ISFC; the engine RPM; and intake (evaporative) pressure. The calculations pass through the cycle with no iteration or loops (except for iterations to calculate temperature as a function of enthalpy). Engine performance, enthalpy levels, exhaust temperatures are calculated.

(1) Method of Calculating Enthalpy. The enthalpy of a chemical species is taken to be:

$$H_i = \Delta H^o_{f_i} + \int_{T_o}^{T} C_{p_i}\, dT$$

where ΔH^o_f is heat of formation of the species at the reference temperature T_o (298.15°K) and the integral expression is the sensible enthalpy of the species of the temperature T, above or below the reference temperature. The enthalpies of all species except methanol were obtained from the JANAF Thermochemical Tables; the heat of formation of methanol was calculated its heat of combustion and its specific heat (source unknown) curve fitted and integrated to produce the sensible enthalpy as a function of temperature.

Under adiabatic conditions the enthalpy of the reactants in a process is equal to the enthalpy of the products. The enthalpies of the products can then be calculated according to the following relation provided that the product composition is known:

$$\sum_{react} \left(\Delta H^o_f + \int_{T_o}^{T_{react}} C_p\, dT\right) = \sum_{prod} \left(\Delta H^o_f + \int_{T_o}^{T_{prod}} C_p\, dT\right)$$

(2) Effects of Intake Variables and Engine Performance on Exhaust Properties. Little data exists on the performance and operation of a methanol engine; consequently, the treatment of the effects of the intake and engine operating variables on performance and exhaust conditions is highly simplified. This can be easily modified as more data becomes available. At present, the engine ISFC variation with inlet mixture enthalpy is calculated from the expression:

$$ISFC = ISFC_{nom} - .00055\ (H_6 + 461.51)\ ,$$

derived from the experimental data of the previous program, where $ISFC_{nom}$ is input, and - 461.51 BTU/lb is the enthalpy of the nominal intake mixture. The exhaust enthalpy is assumed to vary by 40% as much as the intake enthalpy. The effect of fuel flow rate is calculated by an empirical expression which alters the exhaust temperature from its input nominal value - 1460°R.

C. Computer Program:

The program (Fortran IV) is set up to calculate a broad matrix of data points of the particular engine and nominal operating point selected for this study. There is presently some internal override of the input variables.

(1) Input Variables. The input is contained in two cards:

Card 1 -	5 - 10 column fields
RPM	Engine speed - revs. per minute
PIN	Intake pressure - psia
ISFCN	ISFC at nominal operating condition
XR1	Fraction of fuel through reforming branch
XR2	Fraction of XR1 fuel which is dissociated

Card 2	8 - 10 column fields
TA	Air intake temperature
TO	Fuel intake temperature
T1R	Reform branch temperature after preheating
T3R	Reform branch temperature after superheating
T4R	Reform branch temperature after reforming
T1M	Non-reform temperature after preheating
T2M	Non-reform temperature after evaporation
T3M	Non-reform temperature after superheating

(2) Program Structure. The program is now set up to function through a succession of DO loops in the following order:

ISFCN = .888, .915, .938, .963 (lb/hp-hr)

RPM = 2400, 2800, 3200

T4R = 860, 960, 1060 (°R)

XRL = 0, .3, .7, 1.0

$\dot{w}_{fuel}$ = 80.8, 85.8, 90.8, 95.8, 100.8 (lb/hr)

(3) Output: The output consists of 57 variables for each case: temperatures, flow rates, all input variables except ISFCN, enthalpies, and heat exchange values. Temperatures are in °R, enthalpies in BTU/lb, and heat transfer values (according to the flow diagram) in BTU/hr.

The output format is printed at the top of each page.